Lukas Haider, BSc

Development of a Board for Real Time Audio Processing Using the ADSP-SC589 Digital Signal Processor

MASTER'S THESIS

to achieve the university degree of

Diplom-Ingenieur

Master's degree programme: Electrical Engineering

submitted to

Graz University of Technology

Supervisor

Ass.Prof. Dipl.-Ing. Dr.techn. Gunter Winkler

Institute of Electronics

Graz, March 2020

AFFIDAVIT

I declare that I have authored this thesis independently, that I have not used other than the declared sources/resources, and that I have explicitly indicated all material which has been quoted either literally or by content from the sources used. The text document uploaded to TUGRAZonline is identical to the present master's thesis.

23.03.2020,

Date, Signature

Abstract

Evaluation boards for digital signal processors (DSPs) are rather expensive and do not always provide the needed interface and components for audio applications. This thesis covers the system design of an evaluation board specifically for audio signal processing. It shows the possible input signals and how each of them needs to be processed in order to generate high quality input for the DSP. Moreover, to ensure optimum signal transition, function and usage of modern analog-to-digital and digital-to-analog converters are explained and the best wiring and a high-end layout for increased electromagnetic compatibility are discussed. The goal of this thesis is to offer a guide for the design process of such a board and provide the information on how it can be recreated independently.

Kurzfassung

Evaluation Boards für digitale Signalprozessoren sind meist kostspielig und bieten nicht immer die nötigen Anschlüsse und Komponenten für Audioanwendungen. Diese Arbeit beschreibt die Systementwicklung eines solchen Boards, speziell für die Audiosignalverarbeitung. Mögliche Eingangssignale und deren individuelle Verarbeitung zur Erzeugung hochwertiger Eingangssignale für den Signalprozessor werden beschrieben. Zudem wird die Funktionsweise von modernen Analog-Digital-Umsetzern und Digital-Analog-Umsetzern sowie deren Verwendung erklärt, um optimale Signalwandlung zu gewährleisten. Die ideale Beschaltung und ein hochwertiges Layout zur Verbesserung der elektromagnetischen Vertäglichkeit werden ebenfalls diskutiert. Das Ziel der Arbeit ist es, die LeserInnen durch den Designprozess eines solchen Boards zu führen und Informationen für einen selbstständigen Nachbau bereit zu stellen.

Acknowledgements

I would first like to thank my thesis advisor Ass.Prof. Dipl.-Ing. Dr.techn. Gunter Winkler of the Institute of Electronics at Graz University of Technology for always helping with words and deeds whenever I encountered difficulties or had a question about my research or writing. He consistently allowed this paper to be my own work, but steered me in the right direction whenever I needed it.

I would also like to thank everyone from the Institute of Electronic Music and Acoustics that was involved in this project, especially Dipl.-Ing. Daniel Rudrich who was like a second supervisor and Rüdiger Fasching who created the software part of this project. Without their passionate participation and input, the project could not have been successfully created.

I wish to show my gratitude to Ass.Prof. Dipl.-Ing. Dr.techn. Mario Auer who has supported me through my previous projects and has paved the way for this thesis.

I would like to pay my special regards to my cousin Barbara Reitbauer for correcting the proofs of every paper and thesis I attempted to write in English. I am gratefully indebted to her for her very valuable comments on this thesis.

I must express my very profound gratitude to my family and to my girlfriend Lisa for not only providing me with unfailing support and continuous encouragement throughout my many years of study and through the process of writing this thesis, but also for actively lending me a hand whenever it was needed. This accomplishment would not have been possible without them. Thank you!

Finally, I wish to express my deepest gratitude to you, my dear friend Patrick Ofitsch. I can not count the times how often you helped me out during my studies and were there for me as a friend. You left us way too soon, I miss you.

Contents

List of Figures

List of Tables

List of Acronyms and Symbols

AAF anti-aliasing filter

ADC analog-to-digital converter

BJT bipolar junction transistor

cap capacitor

CFA current feedback amplifier

CMVR common-mode voltage range

DAC digital-to-analog converter

DC direct current

DIL dual in-line

DSP digital signal processor

EMC electromagnetic compatibility

EMI electromagnetic interference

en voltage noise

ESL equivalent series inductance

ESR equivalent series resistance

FET field-effect transistor

I_B bias current

ICs integrated circuits

in current noise

JFET junction gate field-effect transistor

LED light-emitting diode

LSB least significant bit

mic microphone

op-amp operational amplifier

PAD passive attenuation device

PCB printed circuit board

PLL phase-locked loop

preamp preamplifier

QFN quad-flat no-leads

RFI radio frequency interference

RMS root mean square

SINAD signal-to-noise-and-distortion ratio

SMD surface-mounted device

SNR signal-to-noise ratio

SOIC small-outline integrated circuit

SPI serial peripheral interface

SR slew rate

THD+N total harmonic distortion plus noise

THT through-hole technology

TRS tip ring sleeve

TS tip sleeve

V_{OS} offset voltage

1 Introduction

The purpose of this thesis is to design and build an affordable development board for the the ADSP-SC589 Digital Signal Processor for real time audio processing applications. The various chapters follow the signal path of an audio signal from the input to the digital signal processor (DSP) to the output, starting at signal parameters, connectors and cables, followed by the corresponding input impedance and phantom power for condenser microphones. The thesis covers analog signal processing in order to get the best result on the analog-to-digital converter (ADC) by creating a symmetric signal if needed and adjusting the gain. There is also an overview of the important operational amplifier (op-amp) parameters to help select the right one for other projects. The concept of the analog-to-digital and digital-to-analog converters used in this design is explained. It is shown how DC-DC converters can be designed to power the circuit.

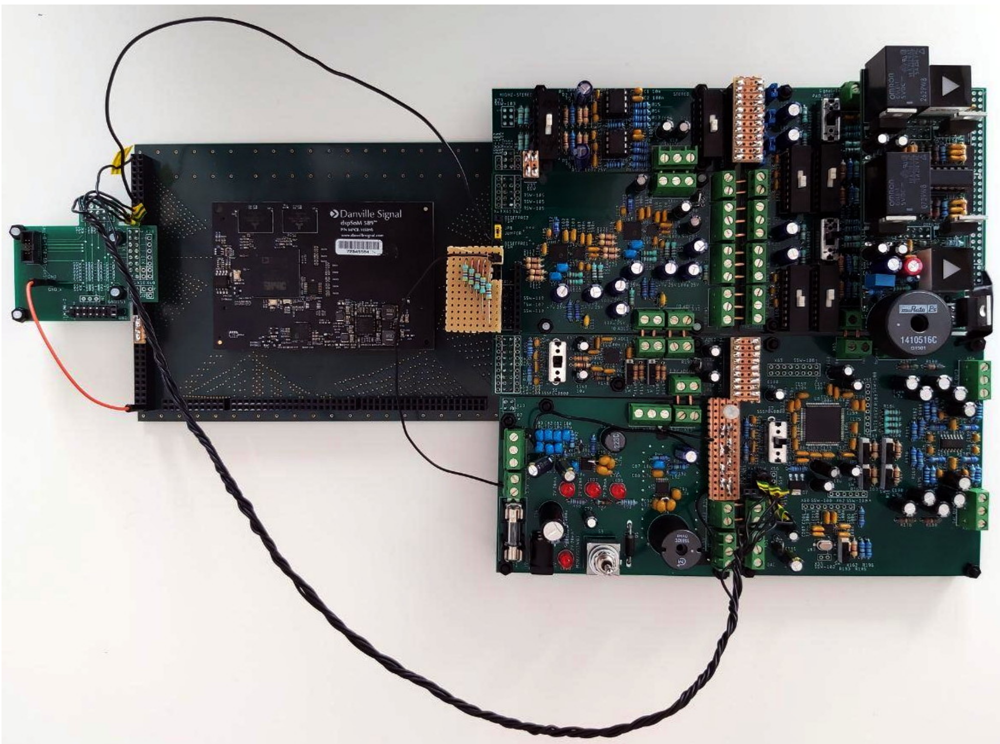

Figure 1.1: This figure shows the final design and all the connections that are needed for the board to work.

The circuit and wiring of the project is explained in great detail. This includes the input conditioning, a programmable op-amp, an ADC, a digital-to-analog converter (DAC) with the corresponding reconstruction filter and clock generation, as well as the power supply. All these circuits are manufactured as single modules. When connected, they form the board that can be seen in figure 1.1. This modular design, allows better testing and debugging while it also allows removing and replacing some parts. Each module is described in the corresponding chapter. Additionally, some circuits that are not manufactured, but created in the design process, are included. The measuring process for the final design is explained in the corresponding chapter where the results are also discussed. In the concluding chapter at the end of this thesis, this board is compared to an evaluation board available for purchase in terms of price and function. It also includes suggestions for improvements. The whole circuit diagram and a list of the components can be found in the appendix at the end of this document.

A similar project was done by Victor Palos in 2017. It is published as his Master's Thesis *Analog and digital interface board for sound processing* [1]. The main difference is, that he uses an Arduino micro-controller as interface between the DSP and his circuit. It is specified to remove this controller, as the DSP can handle the control of the preamplifier, ADC and DAC itself. An new interface is requested as well as a power supply that suits the DSP better. The dspSoM^{TM}589 should be used, it provides a small board carrying the DSP, some memory and other basic components. All this and some complications with the configuration of some components on Victor Palos' board lead to a complete redesign and this distinct project.

1.1 General Information

If not stated differently, all voltages are root mean square (RMS) values. Dimensioning is only described for channel 1, as the values in channel 2 are exactly the same, unless otherwise noted. All 4-layer, except the supply board layouts use the second layer for the supply voltages and the third for analogue and digital ground. Layers one and four are used for signal paths. Usually, all components are mounted on the top. Exceptions can be some error corrections for the prototype. All 0Ω resistors connecting analogue and digital grounds are replaced by ferrite beads in order to reduce noise coupling from one to the other.

Most boards are produced by `www.pcbway.com`. As there is a price jump, if a board is larger than $100mm$ on one side. The size of each board is less than $100mm$ x $100mm$, in order to keep the costs as low as possible. Interconnections of boards are usually screw clamps, if the boards connected are not determined. In a few cases socket strips are used. That means the connections must be between those two boards.

In the description under the section Usage it is always assumed the board is oriented as in the corresponding picture, when stating directions.

2 Audio Signals

When designing an audio input, it is important, to know the parameters of the input signals. The attributes of audio signals are usually in a well-defined range, corresponding to the signal source. In order to provide optimum signal conditioning for the ADC and consequently for the DSP, it is necessary to analyse the signal parameters. There are basically three main input signals: line level, microphone and guitar. Other instruments usually use microphones or already provide a line level signal (e.g. keyboard). The voltage level is usually given in dB und can be calculated from the RMS voltage u as seen in equation (2.1) and vice versa (equation (2.2)).

$$L_u = 20 \cdot log\left(\frac{u}{u_0}\right) dB \tag{2.1}$$

$$u = u_0 \cdot 10^{\frac{L_u}{20}} V \tag{2.2}$$

The reference voltage u_0 used internationally equals $0.775V$ which is the RMS of a signal with an amplitude of $1V$. These levels are labelled dBu. In the USA and Japan the dBV - level, which uses a reference voltage u_0 of $1V$ [2, p. 16], is also rather common.

$$\begin{aligned} L(dBu) - L(dBV) &= 20 \cdot log\left(\frac{u}{0.775}\right) - 20 \cdot log\left(\frac{u}{1}\right) \\ &= 20 \cdot log\left(\frac{1}{0.775}\right) \\ &= 2.2dB \end{aligned} \tag{2.3}$$

As seen in equation (2.3), a voltage level in dBu is always $2.2dB$ larger than the same voltage in dBV [2, p. 16].

2.1 Line Level

Line level is typically used for analogue signals of interconnected audio devices. There are defined levels for professional equipment and home use equipment. Also, the maximum output impedance and thus the corresponding input impedance are defined, as can be seen in section 3.1.

2.1.1 Voltage

The standard nominal level for studio equipment is $+4dBu$, which is about $1.23V$ RMS. For consumers it is typically $-10dBV$ ($316mV$ RMS) [3, p. 973], which is a lot lower than for professional equipment.4, as seen in figure 2.1. However, a large input range to cover both input levels is not needed.

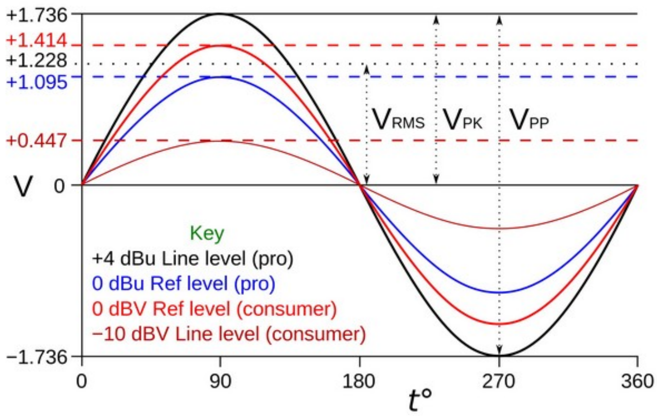

Figure 2.1: For professional equipment, line level is defined as $+4dBu$ and displayed in black. Its reference voltage $0dBu$ is coloured blue. The consumer level with $-10dBV$ is a lot lower and displayed in dark red, while the reference voltage for dBV is coloured light red.
Source: adapted from [4]

2.1.2 Frequency

The frequency range of the signals usually covers human hearing range, which is commonly approximated with $16Hz$ to $16kHz$ [3, p. 24]. As a rule of thumb, usually $20Hz$ to $20kHz$ is used.

2.2 Microphone

The are two types of microphones: condenser microphones, which require an external power source as described in section 3.3, and dynamic microphones.

2.2.1 Voltage

The maximum output voltage for condenser microphones at a sound pressure of $100Pa$, which is the acoustic pain threshold of humans, is $5V$ RMS. Under the same conditions, dynamic microphones can output only $0.2V$ RMS [5, p. 20]. At $1Pa$ microphone signals are between $-50dBu$ and $-30dBu$ [2, p. 135]. Exposure to a sound pressure of $1Pa$ for a longer time can already result in hearing loss.

	Electrodynamic microphones	Condenser microphones
nominal output impedance	200Ω	200Ω
nominal input impedance	$1k\Omega$	$1k\Omega$
nominal output voltage (@ $0.2Pa$)	$0.2mV$	$2mV$
maximum output voltage (@ $100Pa$)	$0.2V$	$5V$

Table 2.1: While the nominal impedance values are the same for dynamic and condenser microphones, the voltage output of a condenser microphone (mic) is at least ten times higher than the output of a dynamic mic.
Source: adapted from [5, p. 20]

2.2.2 Frequency

The ÖVE/ÖNORM EN 61938:2013 states that all the given impedances are valid between $20Hz$ and $20kHz$, basically defining the audio signal range of microphones [5, p. 12]. However, there are measuring microphones with a frequency range from 2Hz up to larger than $100.000Hz$ [3, p. 344], but they are not used for typical audio recording and require an amplifier that suits those frequencies.

2.3 Guitar

Guitar pickups exist in two forms: the single-coil pickup (figure 2.2) and the humbucker(figure 2.3). The humbucker is designed to reduce the effect of external magnetic fields [6, p. 28], it provides a higher signal amplitude but also has a larger source resistance (see section 3.1).

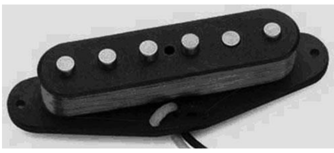

Figure 2.2: The pickup consists of several cylindrical magnetic poles and a coil with a large number of windings wrapped around them. A moving steel string above the magnets causes distortion to the magnetic field, these field-changes are picked up by the coil, which generates the voltage signal.
Source: adapted from [6, p. 26]

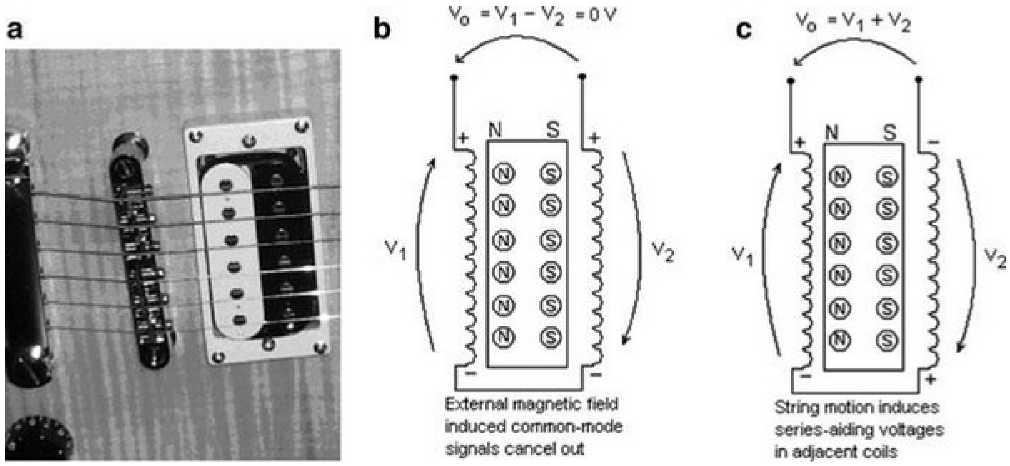

Figure 2.3: The humbucker pickup consists of two coils, instead of one. They are arranged in such a way that common-mode signals from external magnetic fields induced in each coil cancel each other out. The voltages induced by the strings are added and generate a larger output voltage.
Source: adapted from [6, p. 28]

2.3.1 Voltage

The initial peak of a guitar signal varies depending on the pickup. Single coil pickups generate $0.2V$ to $0.5V$, while humbuckers can generate from $0.4V$ to over $1V$ peak voltages [6, p. 30]. The average voltage is typically 20% to 25% lower. The first peak is the interesting part, as the whole signal should reach the ADC without clipping.

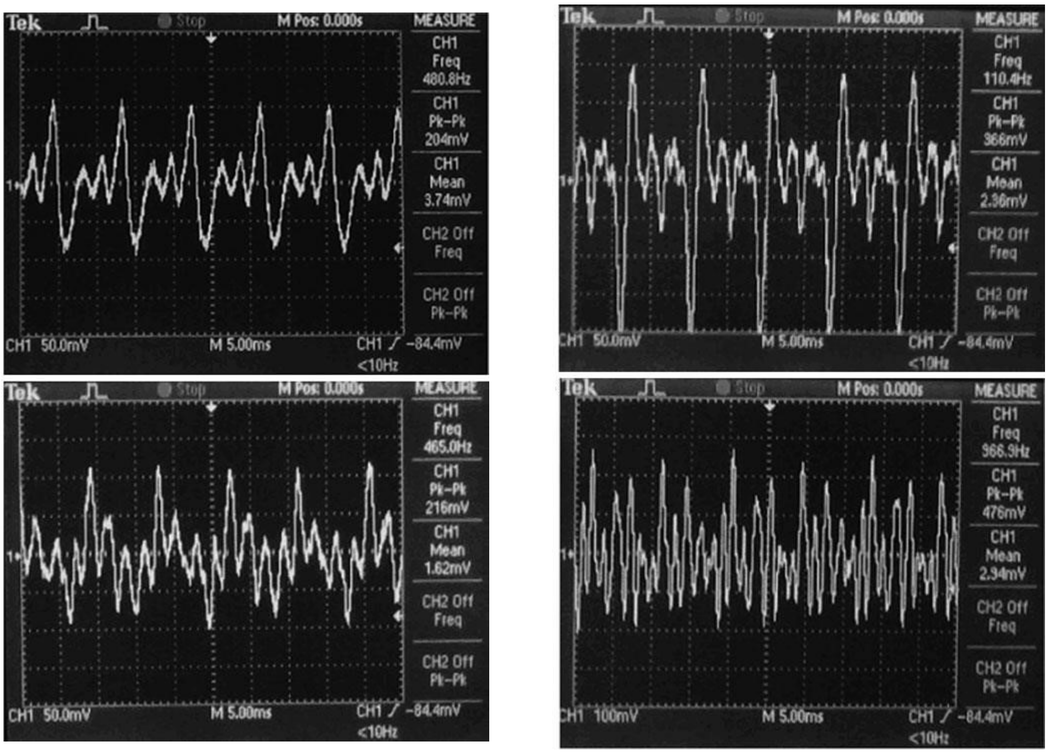

(a) Single coil

(b) Humbucker

Figure 2.4: Both top pictures show the signal of an open A string, 110 Hz. The two pictures on the bottom show a barre chord A. A single-coil pickup was used for the pictures on the left side (a) and a humbucker for the pictures on the right side (b). The humbucker has about twice the signal amplitude of the single-coil pickup. It should be noted that the bottom right picture is set to $100\frac{mV}{division}$ while the rest is set to $50\frac{mV}{division}$
Source: adapted from [6, p. 27] and [6, p. 30]

2.3.2 Frequency

The frequency on a standard tuned 24-fret guitar ranges from $82.4Hz$ to $1318.2Hz$. If five-string bass guitars are included, the total range starts at $30.9Hz$. The frequency of each string and fret can be seen in figure 2.5. It can be seen that the frequency range of a guitar is a lot smaller than the actual hearing range of a human being.

Tabelle der Grundtonfrequenzen für eine Gitarre in Standardstimmung E – A – d – g – h – e' (Frequenzangaben gerundet auf eine Nachkommastelle)

	leer	I.	II.	III.	IV.	V.	VI.	VII.	VIII.	IX.	X.	XI.	XII.	..	XXIV.
Saite	e' (329,6 Hz)	f' (349,2 Hz)	f#' / gb' (370 Hz)	g' (392 Hz)	g#' / ab' (415,3 Hz)	a' (440 Hz)	a#' / b' [bb'] (466,2 Hz)	h' [b'] ()493,9 Hz	c'' (523,3 Hz)	c#'' / db'' (554,4 Hz)	d'' (587,3 Hz)	d#'' / eb'' (622,3 Hz)	e'' (659,3 Hz)	..	e''' (1318,5 Hz)
	h [b] (246,9 Hz)	c' (261,6 Hz)	c#' / db' (277,2 Hz)	d' (293,7 Hz)	d#' / eb' (311,1 Hz)	e' (329,6 Hz)	f' (349,2 Hz)	f#' / gb' (370 Hz)	g' (392 Hz)	g#' / ab' (415,3 Hz)	a' (440 Hz)	a#' / b' [bb'] (466,2 Hz)	h' [b'] (493,9 Hz)	..	h'' [b''] (987,8 Hz)
	g (196 Hz)	g# / ab (207,7 Hz)	a (220 Hz)	a# / b [bb] (233,1 Hz)	h (246,9 Hz)	c' (261,6 Hz)	c#' / db' (277,2 Hz)	d' (293,7 Hz)	d#' / eb' (311,1 Hz)	e' (329,6 Hz)	f' (349,2 Hz)	f#' / gb' (370 Hz)	g' (392 Hz)	..	g'' (748 Hz)
	d (146,8 Hz)	d# / eb (155,6 Hz)	e (164,8 Hz)	f (174,6 Hz)	f# / gb (185 Hz)	g (196 Hz)	g# / ab (207,7 Hz)	a (220 Hz)	a# / b [bb] (233,1 Hz)	h [b] (246,9 Hz)	c' (261,6 Hz)	c#' / db' (277,2 Hz)	d' (293,7 Hz)	..	d'' (587,3 Hz)
	A (110 Hz)	A# / B [Bb] (116,5 Hz)	H [B] (123,5 Hz)	c (130,8 Hz)	c# / db (138,6 Hz)	d (146,8 Hz)	d# / eb (155,6 Hz)	e (164,8 Hz)	f (174,6 Hz)	f# / gb (185 Hz)	g (196 Hz)	g# / ab (207,7 Hz)	a (220 Hz)	..	a' (440 Hz)
	E (82,4 Hz)	F (87,3 Hz)	F# / Gb (92,5 Hz)	G (98 Hz)	G# / Ab (103,8 Hz)	A (110 Hz)	A# / B [Bb] (116,5 Hz)	H [B] (123,5 Hz)	c (130,8 Hz)	c# / db (138,6 Hz)	d (146,8 Hz)	d# / eb (155,6 Hz)	e (164,8 Hz)	..	e' (329,6 Hz)
	,H (61,7 Hz)	C (65,4 Hz)	C# / Db (69,3 Hz)	D (73,4 Hz)	D# / Eb (77,8 Hz)	E (82,4 Hz)	F (87,3 Hz)	F# / Gb (92,5 Hz)	G (98 Hz)	G# / Ab (103,8 Hz)	A (110 Hz)	A# / B [Bb] (116,5 Hz)	H [B] (123,5 Hz)	..	h [b] (246,9 Hz)

Tabelle der Grundtonfrequenzen für eine Bassgitarre in Standardstimmung ,E – ,A – D – G (Frequenzangaben gerundet auf eine Nachkommastelle)

	leer	I.	II.	III.	IV.	V.	VI.	VII.	VIII.	IX.	X.	XI.	XII.	..	XXIV.
Saite	G (98 Hz)	G# / Ab (103,8 Hz)	A (110 Hz)	A# / B [Bb] (116,5 Hz)	H [B] (123,5 Hz)	c (130,8 Hz)	c# / db (138,6 Hz)	d (146,8 Hz)	d# / eb (155,6 Hz)	e (164,8 Hz)	f (174,6 Hz)	f# / gb (185 Hz)	g (196 Hz)	..	g' (382 Hz)
	D (73,4 Hz)	D# / Eb (77,8 Hz)	E (82,4 Hz)	F (87,3 Hz)	F# / Gb (92,5 Hz)	G (98 Hz)	G# / Ab (103,8 Hz)	A (110 Hz)	A# / B [Bb] (116,5 Hz)	H [B] (123,5 Hz)	c (130,8 Hz)	c# / db (138,6 Hz)	d (146,8 Hz)	..	d' (293,7)
	,A (55 Hz)	,A# / ,B [,Bb] (58,3 Hz)	,H [,B] (61,7 Hz)	C (65,4 Hz)	C# / Db (69,3 Hz)	D (73,4 Hz)	D# / Eb (77,8 Hz)	E (82,4 Hz)	F (87,3 Hz)	F# / Gb (92,5 Hz)	G (98 Hz)	G# / Ab (103,8 Hz)	A (110 Hz)	..	a (220 Hz)
	,E (41,2 Hz)	,F (43,7 Hz)	,F# / ,Gb (46,2 Hz)	,G (49 Hz)	,G# / ,Ab (51,9 Hz)	,A (55 Hz)	,A# / ,B [,Bb] (58,3 Hz)	,H [,B] (61,7 Hz)	C (65,4 Hz)	C# / Db (69,3 Hz)	D (73,4 Hz)	D# / Eb (77,8 Hz)	E (82,4 Hz)	..	e (164,8 Hz)
	,,H (30,9 Hz)	,C (32,7 Hz)	,C# / ,Db (34,6 Hz)	,D (36,7 Hz)	,D# / ,Eb (38,9 Hz)	,E (41,2 Hz)	,F (43,7 Hz)	,F# / ,Gb (46,2 Hz)	,G (49 Hz)	,G# / ,Ab (51,9 Hz)	,A (55 Hz)	,A# / ,B [,Bb] (58,3 Hz)	,H [,B] (61,7 Hz)	..	H [B] (123,5 Hz)

Figure 2.5: The table at the top shows the frequency for each string from fret one to twelve and fret 24 for standard tuned six- and seven-string guitars. The bottom table does the same for four- and five-string bass guitars.
Source: adapted from [7]

2.4 Audio Cables

As an American audio company states in one of their user manuals:

> "Regardless of length, balanced lines are best." [8, p. 2]

Balanced lines cancel out ground noise [9, p. 456], because they minimise capacitive coupling into the shield [10, p. 440]. For balanced signals and unbalanced signals above $100mA$ twisted lines should be used while a coaxial cable is recommended for other unbalanced signals [5, p. 32]. Twisting reduces the effect of magnetic EMI, since it reduces the loop area of the cable to zero [11, p. 579]. Shielding is less important than twisting [5, p. 32], as inductive and electromagnetic coupling can pass almost unhindered [3, p. 971]. However, for some applications it is still recommended to use high-quality shielded twisted pair cables [12, p. 2].

2.4.1 Connectors

RCA or jack connectors, as seen in figure 2.6 are usually used on semi-professional equipment [3, p. 967], while professional systems use balanced signals with the XLR connector [3, p. 968].

(a) TS (b) RCA

Figure 2.6: The most common connectors for unbalanced input are the 6.3*mm* jack plug (a) and the RCA connector (b). The mono jack plug is also called TS. T stands for tip and S for sleeve. The RCA connector is also called cinch connector in other languages.
Source: adapted from [13]

Microphones also use XLR or the less reliable 6.3*mm* stereo jack [2, p. 133], depicted in figure 2.7. Guitar signals are transferred via instrument cables, which typically use the 6.3*mm* tip sleeve (TS) jack. Jack plugs can have up to five conductors, for each additional conductor a ring is added between tip and sleeve, which is also represented in the name, as a five-conductor jack is called TRRRS. Portable devices usually use a 3.5*mm* jack plug, whereas mobile phones typically use a four-conductor TRRS configuration.

(a) TRS (b) XLR

Figure 2.7: It is standard to use the XLR connector for balanced input on professional equipment, as it is more reliable than the stereo jack plug. The stereo jack plug is often called TRS, whereby the additional R means ring.
Source: adapted from [13]

3 Audio Input

The audio input board prepares the audio signals for the preamplifier board. In theory, the whole preamplifier also includes the audio input board, however, it was designed separately because a modular design has been chosen. Its purpose is to provide an input according to the parameters in section 3.1 and adjust the signal for the preamplifier (preamp).

3.1 Input Impedance

The main reason why the input impedance is not always as high as possible, is that higher impedance usually means more noise. Thermal noise results from random motion of electrons and has its energy uniformly distributed over the frequency spectrum [11, p. 573]. Different impedance is required for each input signal in order to to keep a good balance between signal strength and noise. Guitar pickups have quite a high output impedance from $5k\Omega$ to $7k\Omega$ for single coils and $6k\Omega$ to $20k\Omega$ for humbuckers [6, p. 33], which is why they require high input impedance. Typical impedance is between $250k\Omega$ and $1M\Omega$. While the latter one would be ideal [6, p. 43], it is hard to reach such values. Line and microphone outputs should also be connected to a matching input impedance, which would be higher than $1k\Omega$ for microphones [5, p. 20] and higher than $10k\Omega$ for line level connections [5, p. 17].

	Source impedance	**Input impedance**
Line-In	$\leq 1k\Omega$	$\geq 10k\Omega$
Microphone	$\leq 200\Omega$	$\geq 1k\Omega(-5k\Omega)$
Guitar		
single-coil	$5-7k\Omega$	$250k\Omega - 1M\Omega$
humbucker	$6-20k\Omega$	

Table 3.1: The input impedance for line-input should be $10k\Omega$ or slightly larger. For microphones it should be somewhere between $1k\Omega$ and $5k\Omega$. For guitar input $1M\Omega$ would be ideal, but the actual inputs are somewhere between $250k\Omega$ and $1M\Omega$.

3.1.1 Impedance Bridging

While impedance matching is used to transfer as much power as possible to the source, in audio applications the voltage signal should be transferred as strongly as possible. Commonly used phrases like "8 ohm output" and "150 ohm input" make it seem as if impedance matching is used [14], which was the case with early microphones in the USA, when actually impedance bridging is used in modern audio technology [3, p. 376]. The ratio between source and receiver impedance should at least be 1:5 [3, p. 376] [2, p. 134], however, in real applications this ratio lies more between 1:10 and 1:1000 [3, p. 962].

3.2 Passive Attenuation Devices

A passive attenuation device (PAD) is used to reduce the input signal to a certain level. These PADs are usually placed before an amplifier to avoid clipping. Unfortunately doing so increases the noise level [15, p. 7], as thermal noise from the resistors (equation (3.1)) is added at the input.

$$U_R = \sqrt{4 \cdot k \cdot T \cdot R \cdot B} \tag{3.1}$$

This noise is independent from the frequency and proportional to the resistance value [16, p. 57]. It can be calculated with the Boltzmann constant $k = 1.38 \cdot 10^{-23} JK^{-1}$, the temperature T in Kelvin, the bandwidth B in Hz and the resistance R in Ω. This noise is then also amplified in the the following amplifier.

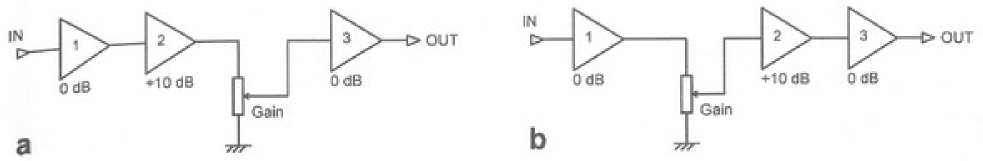

Figure 3.1: In graphic (a) the signal is amplified before it is attenuated. This means that if the signal has a high amplitude, it could be outside the common-mode voltage range. It is more likely that the signal clips at the output of the amplifier, as the amplifier output is limited by the supply voltage. In graphic (b) this is avoided by attenuating the signal first. Unfortunately, the added thermal noise from the voltage divider gets amplified as well.
Source: adapted from [15, p. 7]

Advantages of PADs are that they protect the input of the following device, as they reduce the input-voltage and allow attenuation for amplification circuits that cannot provide this function by themselves, such as the non-inverting amplifier. There are three and four resistor versions (figure 2.7). The four resistor version is recommended because it also attenuates common mode signals, which otherwise pass unattenuated [15, p. 476]. PADs should not be placed at the source of the signal but at the input of the receiver [17, p. 6]. As stated before, the main disadvantage is that they reduce the signal while adding noise and therefore make the signal-to-noise ratio (SNR) worse. Power PADs can be used after overdriven amps to get the distortion effect while keeping the volume low.

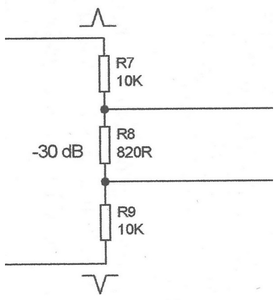

(a) three resistor version

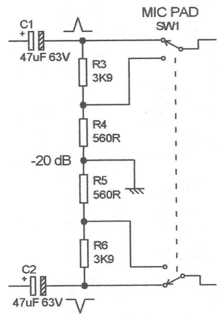

(b) four resistor version

Figure 3.2: PADs can be implemented with three or four resistors. While the three resistor version (a) requires less space on the board, it does not reduce common mode input. Version (b) is recommended, for better common mode rejection. Source: adapted from [15, p. 475]

3.3 Phantom Power

Condenser microphones cannot generate electricity in response to an impinging soundwave, but have to be powered by an external source [8, p. 2]. The most common powering method is the phantom powering system [18, p. 3]. The power travels on both audio lines simultaneously in respective to ground. Therefore, microphones that do not use power simply ignore it. Measuring between both signal lines reads $0V$ direct current (DC) [8, p. 3]. Before reaching the amplifier, the phantom voltage is then blocked by a transformer or a DC blocking capacitor (cap) [16, p. 361]. While $12V$ and $24V$ systems are still in use, 48V should be used for newly designed systems [5, p. 22]. The maximum supply current is $10mA$ [5, p. 25].

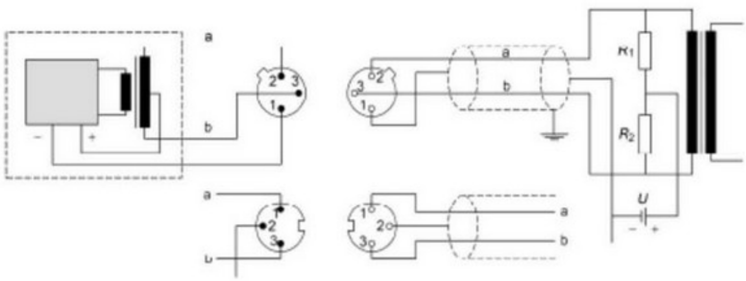

Figure 3.3: The same voltage U is applied to the signal lines a and b, over the resistors R_1 and R_2 with respect to ground potential. On the right-hand side, this voltage is removed by a transformer. Source: adapted from [5, p. 24]

3.3.1 Protection Circuit

Phantom power should be turned off, when not used, especially when using an unbalanced device, or else it will see the $48V$ at its output [17, p. 1]. A break-before-make switch should be used, as otherwise the supply will be shorted, when switching [19, p. 1].

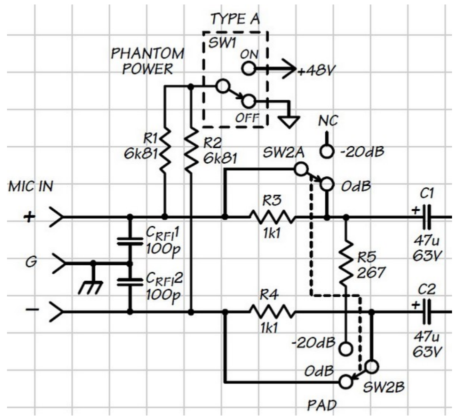

Figure 3.4: The switch has to be a break-before-make configuration, otherwise the $48V$ supply will be shorted when switching. The resistors R_1 and R_2 should match each other and the nominal value closely.
Source: adapted from [19, p. 2]

Another important thing is that the supply resistors are in between 10% of their nominal value and in between 0.4% of each other [5, p. 22]. They each dissipate $0.338W$ so at least a $\frac{1}{2}W$ resistor should be used [19, p. 1]. To protect the following input from phantom power fault, a diode bridge clamps the input to the regulated supply [19, p. 4] [15, p. 728].

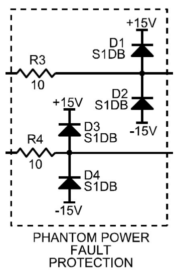

Figure 3.5: The protection circuit consists of a diode bridge, connected to the supply rails and 10Ω resistors to limit the current. In case of a fault, the current will flow from the phantom voltage supply to the positive supply rail over the diode D_1.
Source: adapted from [20, p. 9]

3.3.2 DC Blocking

There are two ways to block the DC from the signal. The one that can be seen in figure 3.3 is accomplished by a transformer. The second option is a DC blocking cap. Transformers can provide gain if they are winded accordingly. They are usually larger, heavier and more expensive, but still have a large fan-base among audiophiles, as they provide galvanic isolation and essentially perfect symmetry [17, p. 4]. The reason why capacitors are used in this application, is due to the high price of the transformers and the limited space on the board.

3.4 Unbalanced Input

Most modern ADCs use differential input. Although they can handle single-ended input, balanced signals should be used for optimum performance [21, p. 1].

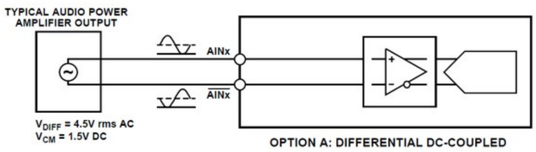

Figure 3.6: The inputs of the ADAU1979 can handle 4.5V RMS differential input with up to 1.5V common mode DC.
Source: adapted from [22, p. 15]

Guitar outputs generally provide unbalanced signals. Such signals can be easily converted into balanced ones. There are specifically designed integrated circuits (ICs) for this purpose, as for example the LT6350, or it can be accomplished by a simple buffer followed by an inverter for the inverted line as in figure 3.7 [15, p. 544].

3.5 Requirements

The board should be able to handle two input channels. The signals can be of any source mentioned in chapter 2. It should also be able to convert unbalanced into balanced input in order to provide ideal output impedance for the gain control. The cost should also be kept as low as possible. It should be easy and intuitive to use.

The input board provides an interface to various inputs and prepares the signal for the preamplifier. One input for each possible signal, would result in three inputs per channel. Even though this would be ideal for the signal, it increases the size of the device and reduces usability for the end user. Switches to select the input are also required in order to avoid noise from the unused inputs. However, if each input had its own PAD-switch, it would quickly result in a confusing number of switches. Generally, adding more functions increases the complexity of the circuit, which adds to costs and size. Furthermore, the more components are added, the higher is the chance of a fault. It also makes it easier to catch unwanted electromagnetic interference (EMI).

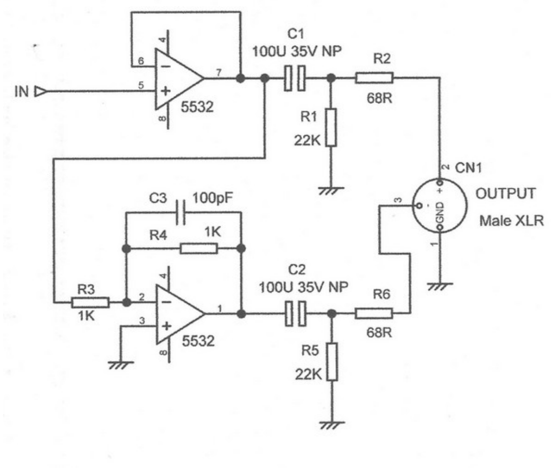

Figure 3.7: For the cold output, the signal is inverted by a inverting-amplifier after a buffer, where the hot output is created. DC blocking capacitors are used, before reaching the output connector.
Source: adapted from [15, p. 545]

"Combo" connectors that combine XLR and tip ring sleeve (TRS) jack plug inputs (see figure 3.8), can be used for each channel [19, p. 10]. This reduces the connectors per channel to one. It also avoids plugging in more than one device per channel.

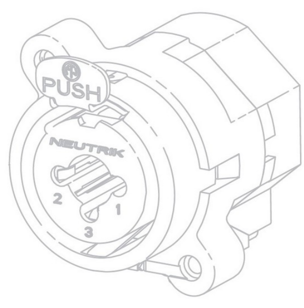

Figure 3.8: XLR as well as TRS jacks con be plugged into this connector.
Source: adapted from [23, p. 1]

As really wide gain range is only required for microphones, only their PAD can be switched off. Line level and guitar input always use a PAD to allow attenuation along with amplification together with the preamp. These inputs range from $-15dB$ to $+40dB$, while microphone input ranges from $-6.4dB$ to $+68.6dB$ in combination with the PAD. In the end, more functions almost always make usage more complicated. The best thing to do, therefore, is to present a logical and well arranged user interface, which should be kept as simple as possible while still fulfilling the requirements.

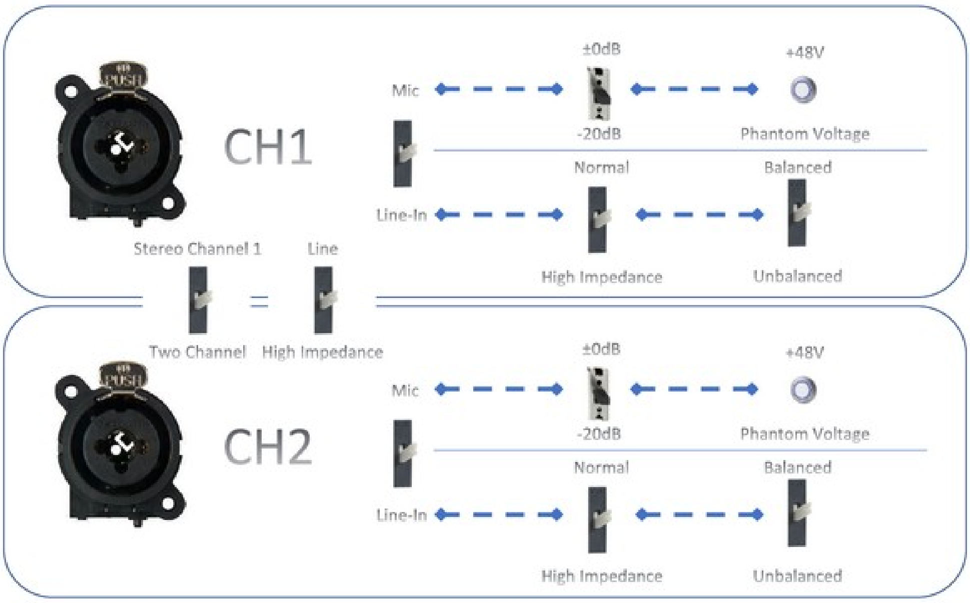

Figure 3.9: This is a draft of what the interface should look like. The first switch allows to select stereo input on channel one or to use channel one and channel two separately. The next switch defines the input impedance if channel one is used as stereo input. Otherwise, the input device (mic- or line-in) can be selected for each channel. Depending on this selection, there are two additional options for the selected input.

A possible implementation of this concept can be seen in figure 3.9. Because of size limitations of the boards, the stereo/mono input selection has been fitted onto a separate board. This also enhances the idea of a modular design, as this board can be removed if not needed. Figure 3.10 shows the selectable signal paths. Everything outside the green boarder is on the main audio input board.

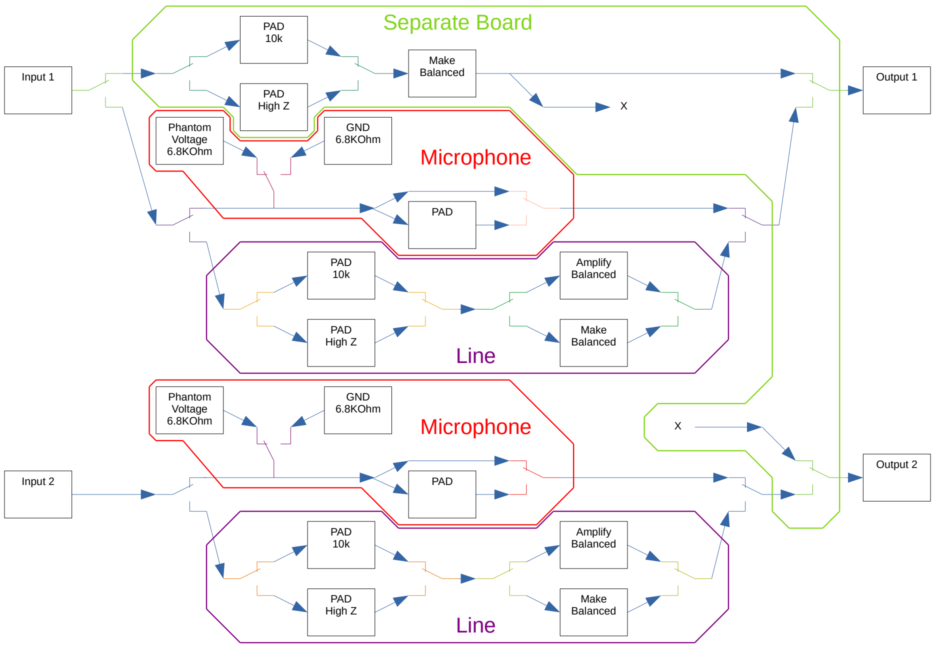

Figure 3.10: The option to use both ADC inputs for one single stereo input, is designed as an attachable separate board. For each channel one can choose between microphone or line input. Moreover, for each input further options are available Actual switches are depicted as multiple switches using the same colour in the block diagram.

3.6 Circuit

3.6.1 Main Audio Input Board

At the DC supply input a decoupling capacitor with $10\mu F$ is used for the positive (C59) and negative rail (C60). The Resistors R57 and R76 are each selected for a $2V$ and $20mA$ light-emitting diode (LED). The two LEDs LED1 and LED2 indicate the supply voltage. X72 allows interconnection to X71 (figure 3.17). If this is not the case, JP9 to JP12 can be used. C43, C44 and C55 are used for radio frequency interference (RFI) protection.

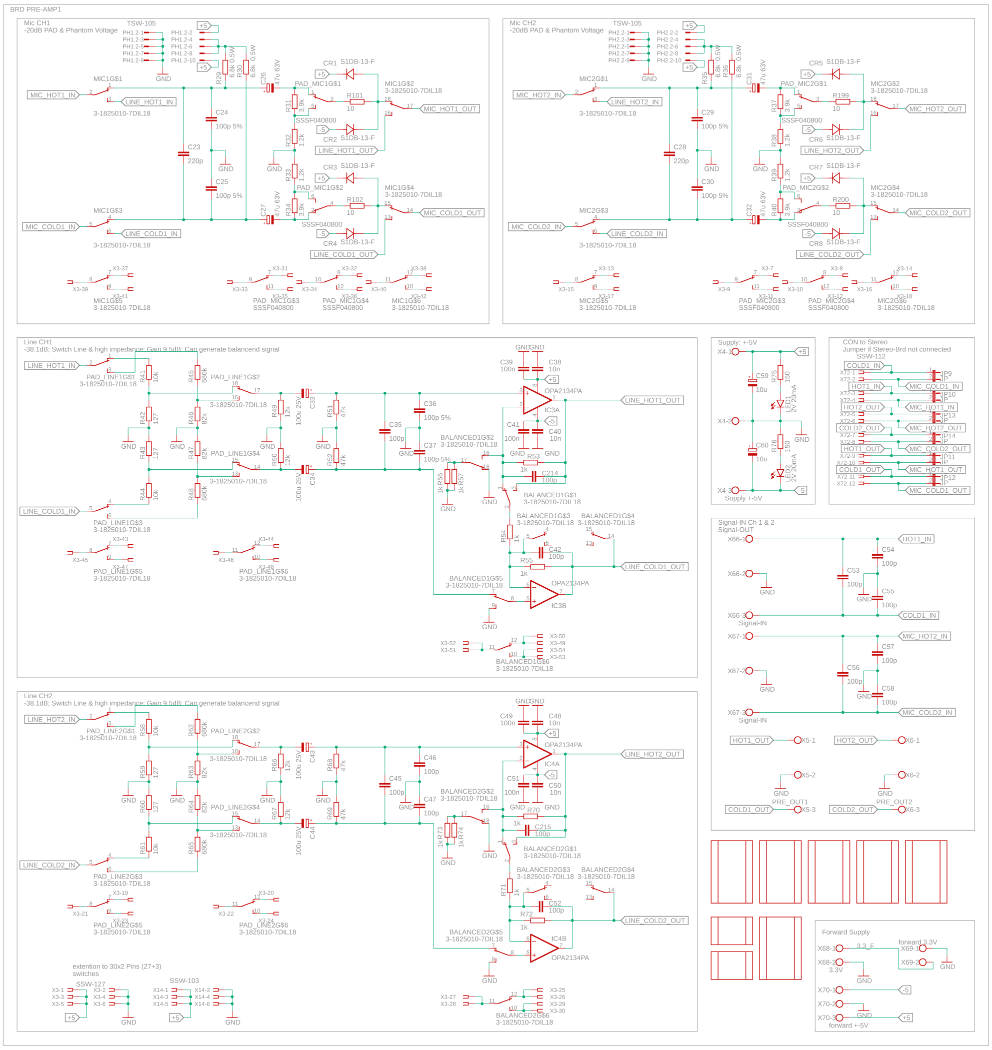

Figure 3.11: This figure shows the schematics of the main input board. The switches allow to select between microphone and line input as well as further configurations such as the microphone PAD switch, the input impedance and differential input switches for line input.

Microphone input

The microphone input uses additional RFI protection, because the typically low voltage of a microphone signal is more vulnerable to interference. This is done by C23, C24 and C25. R29 and R30 are given with $6.8k\Omega$. The parameters are described in subsection 3.3.1. C26 and C27 are used to remove the phantom voltage from the signal lines and generally for DC blocking. It is important that they can sustain more than $48V$. The preamp described in chapter 4 has an input impedance of about $1.4k\Omega$. When the

PAD is used, R32 and R33 are in parallel to this impedance as shown in equation (3.2), otherwise all four resistors are in parallel to the preamp resistance as in equation (3.3).

$$R_{in} = R31 + R34 + (R32 + R33)//R_{preamp} = R31 + R34 + 0.88k\Omega = 8.68k\Omega \quad (3.2)$$

$$R_{in} = (R31 + R34 + R32 + R33)//R_{preamp} = 10.2k\Omega//1.4k\Omega \approx 1.2k\Omega \quad (3.3)$$

The attenuation equals the ratio of R_{out} to R_{in}.

$$20 \cdot log(R_{out}/R_{in}) = 20 \cdot log(0.88/8.68) = -19.88dB \approx -20dB \quad (3.4)$$

The diode bridge CR1 to CR4 forms the phantom fault protection. R101 and R102 should limit the current slightly in case of a fault.

Line input

By using a buffer at the output, the input of the preamp does not effect the input impedance of the line input. R51 and R52 are used to allow input bias current and R49 and R50 prevent the input to be open circuit while switching the PAD switches. Those four resistors do effect the input impedance. Single-ended input impedance should be about $10k\Omega$ for regular line input and above $680k\Omega$ for high impedance input. The PADs should have an attenuation of about $-38.1dB$, as the op-amp configurations provide $+9.5dB$ and the preamp ranges from $+13.6dB$ to $68.6dB$. Therefore, the total gain for line input ranges from $-15dB$ to $+40dB$. The input impedance is mainly defined by R41 and R44 or R45 and R48. R42, R43, R46 and R47 are calculated to provide the wanted attenuation, while in parallel with R49, R50 and R51 and R52. The input impedance and attenuation for regular line input are calculated in equation (3.5) and equation (3.6).

$$\begin{aligned} R_{in} &= R41 + R44 + (R42 + R43)//(R49 + R50)//(R51 + R52) \\ &= R41 + R44 + 250\Omega \\ &= 20.25k\Omega \end{aligned} \quad (3.5)$$

$$20 \cdot log(R_{out}/R_{in}) = 20 \cdot log(0.25/20.25) = -38.16dB \quad (3.6)$$

The impedance is for differential input. For single-ended input the value has to be devided by two in order that the impedance for regular single-ended line input equals the wanted $10.125k\Omega$. The calculations for high-impedance input are shown in (3.7) and equation (3.8)

$$\begin{aligned} R_{in} &= R45 + R48 + (R46 + R47)//(R49 + R50)//(R51 + R52) \\ &= R45 + R48 + 17.12k\Omega \\ &= 1377.12k\Omega \end{aligned} \quad (3.7)$$

$$20 \cdot log(R_{out}/R_{in}) = 20 \cdot log(17.12/1377.12) = -38.11dB \quad (3.8)$$

Again, the input impedance for single-ended signals has to be divided by two, which leads to the required $688.56k\Omega$.

The capacitors C33 and C43 are for DC blocking and C35, C36 and C37 provide again RFI protection for the op-amp configuration. The op-amp configuration can be used as a differential amplifier or as an amplifier for a single-ended signal and an inverter that creates the second signal. So either way, a differential output signal is produced as can be seen in figure 3.12 and figure 3.13.

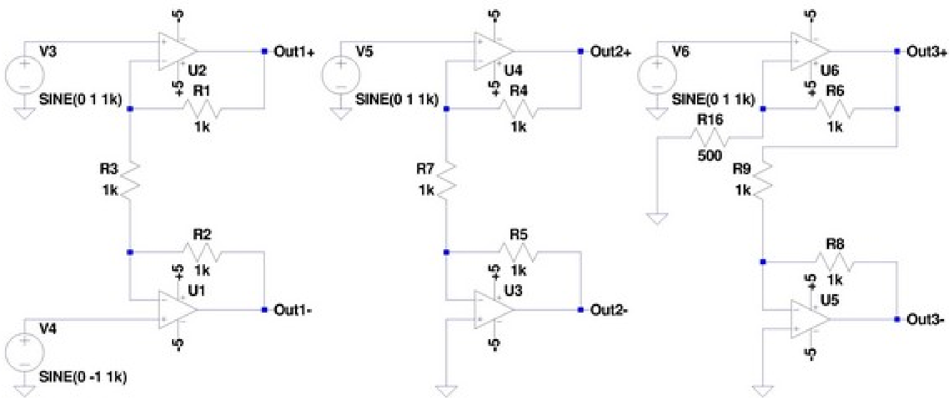

Figure 3.12: The first circuit is a differential amplifier that uses a differential signal as input. The second circuit is the same as the first, but with a single-ended input. The input on the third circuit is also single-ended, but the inverted output signal is generated separately.

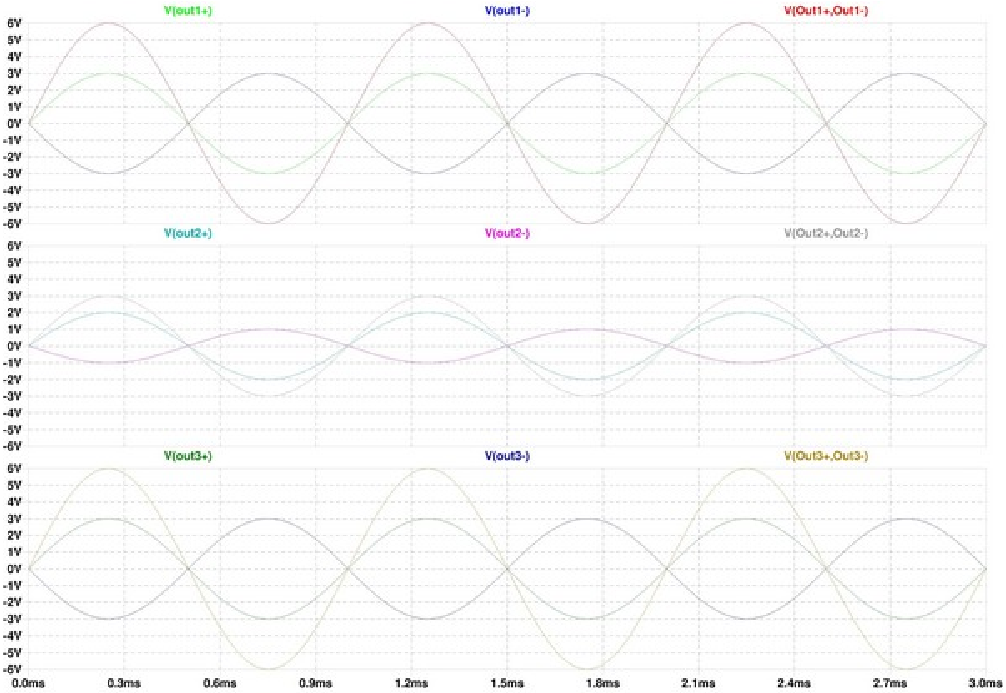

Figure 3.13: The first circuit creates an output signal with a gain of three times. The positive and negative output signals have the same amplitude, as can be observed in the first plot plane. When the same circuit is used with single-ended input, it is evident that the output signal has only half the amplitude of the differential signal. Furthermore, the amplitude of the two outputs is different, which can be seen in the second plot plane. This might cause problems under certain conditions. In order to use the whole dynamic range of the ADC with a single-ended signal, a differential signal is created using an amplifier with a gain of three times and an inverter to create the differential signal, as seen in the third plot plane.

For a gain of three times for the differential amplifier, R53, R54 and R55 have to be equal, thus $1k\Omega$ was used (equation 3.9). R45 and R55 being equal also allows the inverter to have an amplification of one (equation 3.11). In order to create the same output for single-ended input and differential input, the gain of the non-inverting amplifier has to be three times. This is achieved by putting two $1k\Omega$ (R56, R57) resistors in parallel (equation 3.10).

$$A_{differential} = 1 + \frac{R53 + R55}{R54} = 1 + \frac{1+1}{1} = 3 \tag{3.9}$$

$$A_{non-inverting} = 1 + \frac{R53}{R56//R57} = 1 + \frac{1}{1//1} = 3 \tag{3.10}$$

$$A_{inverting} = \frac{R55}{R54} = \frac{1}{1} = 1 \quad (3.11)$$

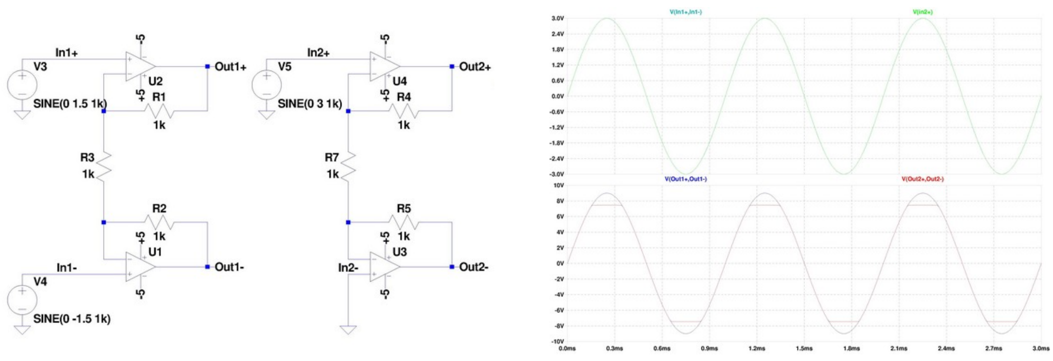

(a) Circuit

(b) Output

Figure 3.14: It is not advised to increase a single-ended input signal to match the differential signal, as this might cause clipping on the output on either op-amp configuration.

To prevent the op-amps from oscillating, capacitors are added in parallel in the feedback loop.

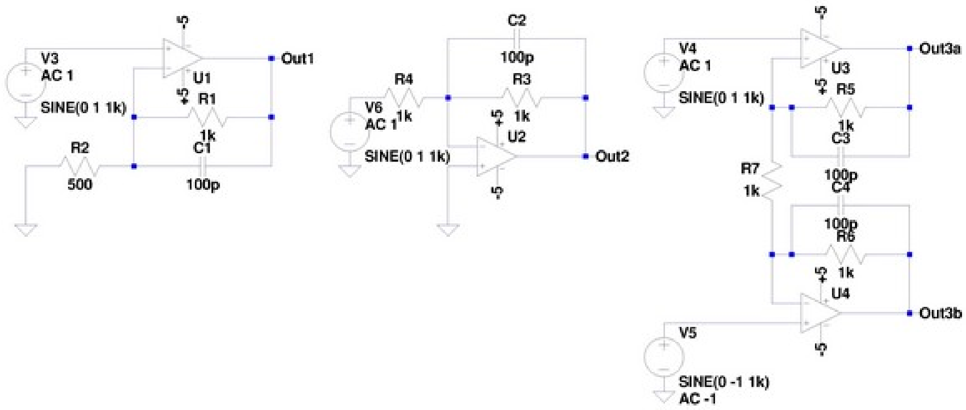

Figure 3.15: Adding a capacitor in parallel to the feedback loop, can avoid oscillation. The $3dB$ cutoff frequency has to be lower than the oscillation frequency.

Frequency behavior can be calculated by using the typical gain calculation and replacing the feedback resister by a feedback impedance Z_n.

$$Z_n = R_n // \frac{1}{s \cdot C_m} = \frac{\frac{R_n}{s \cdot C_m}}{R_n + \frac{1}{s \cdot C_m}} = \frac{R_n}{1 + s \cdot R_n \cdot C_m} \quad (3.12)$$

The following calculations relate to figure 3.15.
The gain of the non-inverting amplifier:

$$A_{non-inv} = 1 + \frac{Z1}{R2} = 1 + \frac{\frac{R1}{1+s\cdot R1\cdot C1}}{R2} = 1 + \frac{R1}{R2} \cdot \frac{1}{1 + s \cdot R1 \cdot C1} \tag{3.13}$$

For the inverting amplifier the gain is calculated as:

$$A_{inv} = \frac{Z3}{R4} = \frac{\frac{R3}{1+s\cdot R3\cdot C2}}{R4} = \frac{R3}{R4} \cdot \frac{1}{1 + s \cdot R3 \cdot C2} \tag{3.14}$$

For the differential amplifier R5 equals R6 and C3 equals C4, thus Z5 equals Z6:

$$A_{dif} = 1 + \frac{2 \cdot Z5}{R7} = 1 + \frac{2 \cdot \frac{R5}{1+s\cdot R5\cdot C3}}{R7} = 1 + \frac{2 \cdot R5}{R7} \cdot \frac{1}{1 + s \cdot R5 \cdot C3} \tag{3.15}$$

It can be observed that there is always low-pass behaviour with the cutoff frequency defined by R_n and C_m. As $R_n = 1k\Omega$ and $C_m = 100pF$, the cutoff frequency is the same for all three configurations:

$$F_c = \frac{1}{2 \cdot \pi \cdot R_n \cdot C_m} = \frac{1}{2 \cdot \pi \cdot 1000k\Omega \cdot 100pF} = 1.59MHz \tag{3.16}$$

This is why C42 and C214 in figure 3.11 are $100pF$ capacitors.

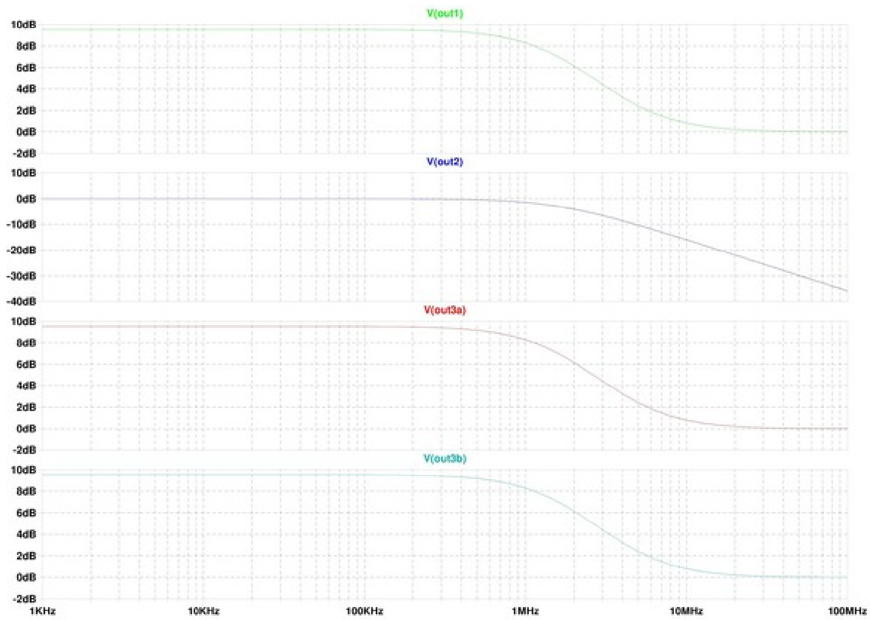

Figure 3.16: This plot is created without taking the transition frequency into consideration. It can be observed that the gain of the non-inverting amplifier and the differential amplifier will at least be one ($0dB$).

3.6.2 Stereo Input Board

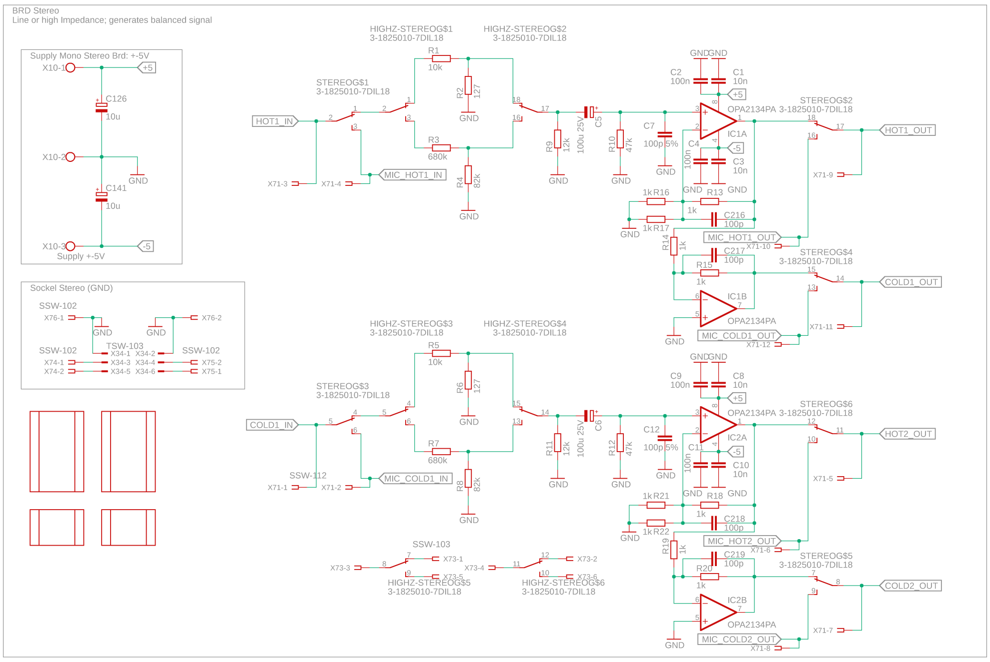

Figure 3.17: The stereo input board allows to separate a stereo input on channel one. Both signals are converted into differential signals. Each signal is then sent to one channel of the gain control.

The stereo input board uses the same input configuration as the line input on the main audio input board, as shown through equation 3.17 to equation 3.20. First for normal line input:

$$\begin{aligned} R_{in} &= R1 + R2//R9//R10 \\ &= R1 + 125\Omega \\ &= 10.125k\Omega \end{aligned} \tag{3.17}$$

$$20 \cdot log(R_{out}/R_{in}) = 20 \cdot log(0.125/10.125) = -38.16dB \tag{3.18}$$

Then for high impedance input:

$$\begin{aligned} R_{in} &= R3 + R4//R9//R10 \\ &= R3 + 8.56k\Omega \\ &= 688.56k\Omega \end{aligned} \tag{3.19}$$

$$20 \cdot log(R_{out}/R_{in}) = 20 \cdot log(8.56/688.56) = -38.11dB \tag{3.20}$$

The resistor R9 that avoids an open input while switching the PAD has $12k\Omega$ and the resistor for input bias current R10 has $47k\Omega$, just like R51 on the main board. The non-inverting amplifier and the inverter also use the same configuration, only without the ability to switch into a differential configuration (equation 3.21 and equation 3.22).

$$A_{non-inverting} = 1 + \frac{R13}{R16//R17} = 1 + \frac{1}{1//1} = 3 \tag{3.21}$$

$$A_{inverting} = \frac{R15}{R14} = \frac{1}{1} = 1 \tag{3.22}$$

The capacitors C216 and 217 are also used to prevent oscillation. The behavior is described in equation 3.13 and equation 3.14. The cutoff frequency is calculated in equation 3.16

3.6.3 Phantom Power Board

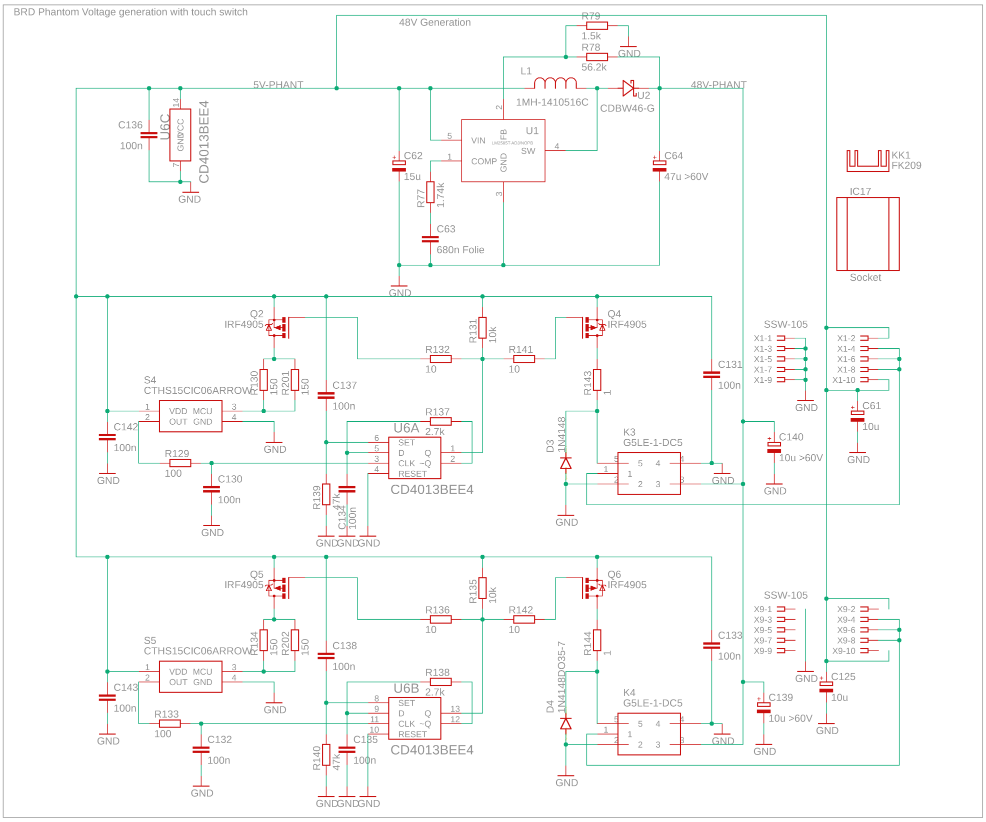

Figure 3.18: On this board, the 48V phantom power is produced. There are two touch switches that toggle the relays for each channel in order to provide the voltage to the main input board.

The phantom power generation circuit has been created by the WEBENCH®Power Designer [24]. The parameters are $5V$ input voltage, $48V$ output voltage and $20mA$ output current. The design was selected based on the simplicity of the circuit and the package of the regulator component in order to make soldering as easy as possible. It is available under the following link: `https://webench.ti.com/appinfo/webench/scripts/SDP.cgi?ID=A61C8908008F49E3`

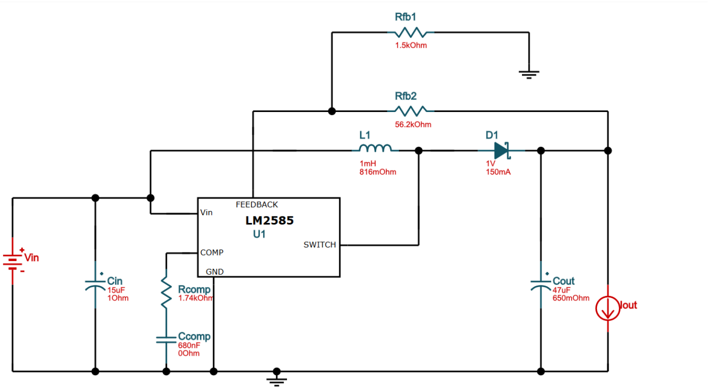

Figure 3.19: The circuit is provided by the WEBENCH®Power Designer [24]. It uses the LM2585 as a boost regulator. For Ccomp a film capacitor should be used.
Source: adapted from [24]

For some circuits the Power Designer allows simulation. The results for switching the load and for steady output can be seen in figure 3.20.

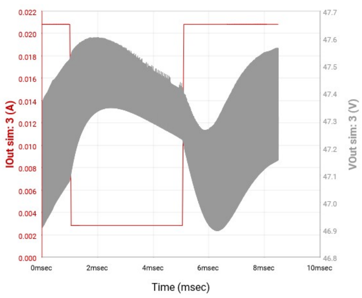

(a) Load Transient

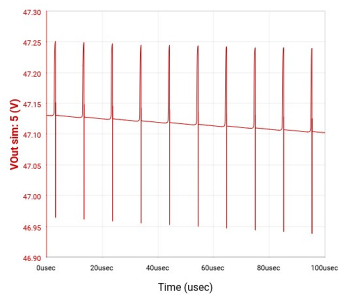

(b) Steady State

Figure 3.20: These two simulation results are provided by the WEBENCH®Power Designer [24]. Figure (a) shows the voltage behaviour when the load is switched off and on again. In figure (b) a steady behaviour can be observed.
Source: adapted from [24]

The toggle switch is a modified version of the circuit shown in figure 3.21. The advantage of this toggle switch, compared to a physical switch, is that after powering down, the toggle switch will be turned off. This prevents the user from accidentally leaving the phantom power switched on.

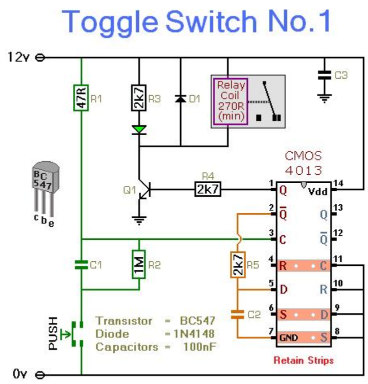

Figure 3.21: This circuit shows how to use a push button to switch a relay and a LED. It uses the CMOS4013 D flip-flop, where the data input is connected to the inverted output. This makes the output toggle, whenever the clock input detects a rising flank.
Source: adapted from [25]

The low-pass between data input and inverted output is the same, defining the values of R137 and C134. The incorporated LEDs of the touch-switch are connected to ground, therefore it is required to use a high-side switching component. For this reason a P-channel MOSFET has been used instead of the bipolar junction transistor (BJT). It has to be able to sustain the current needed by the relay while the on resistance has to be small enough to not affect the needed voltage. The IRF4905 meets these requirements. A $10k\Omega$ pullup resistor (R131) has been used at the output as well. R137 and R141 form a low-pass with the gate capacitance and are placed there to avoid ringing. Because this is not a critical value, 10Ω has been used. As a P-channel MOSFET has been used, logic high is needed at the gate in order to turn it off. C137 and R139 make sure to set the output, and thus turn off the transistor when the whole circuit is switched on. This is done in order to prevent accidental application of phantom voltage. The values are determined by simulation. As the clock rise time for the CD4013 must be lower than $15\mu s$ [26, p. 4], the maximum values for R129 and C130 are limited.

$$\tau = R \cdot C = 100\Omega \cdot 100nF = 10\mu s \tag{3.23}$$

However, the time constant still has to be as large as possible to avoid accidentally turning on of the phantom power and to avoid ringing. As the touch switch has two internal LEDs [27, p. 4], a resistor with about 75Ω should be used. This can be accomplished by putting R130 and R201 in parallel. As a $5V$ relay is used, R143 has only 1Ω. D3 is used as free-wheeling diode, when the coil is switched off. C136 and C142 are used to stabilise the supply voltage for the flip-flop and the switch.

3.7 Layout

Key-goals for all layouts are to keep production cost as low as possible and provide good electromagnetic compatibility (EMC).

3.7.1 Main Audio Input Board

The main audio input board should provide an arrangement of the switches that fits the interface concept.

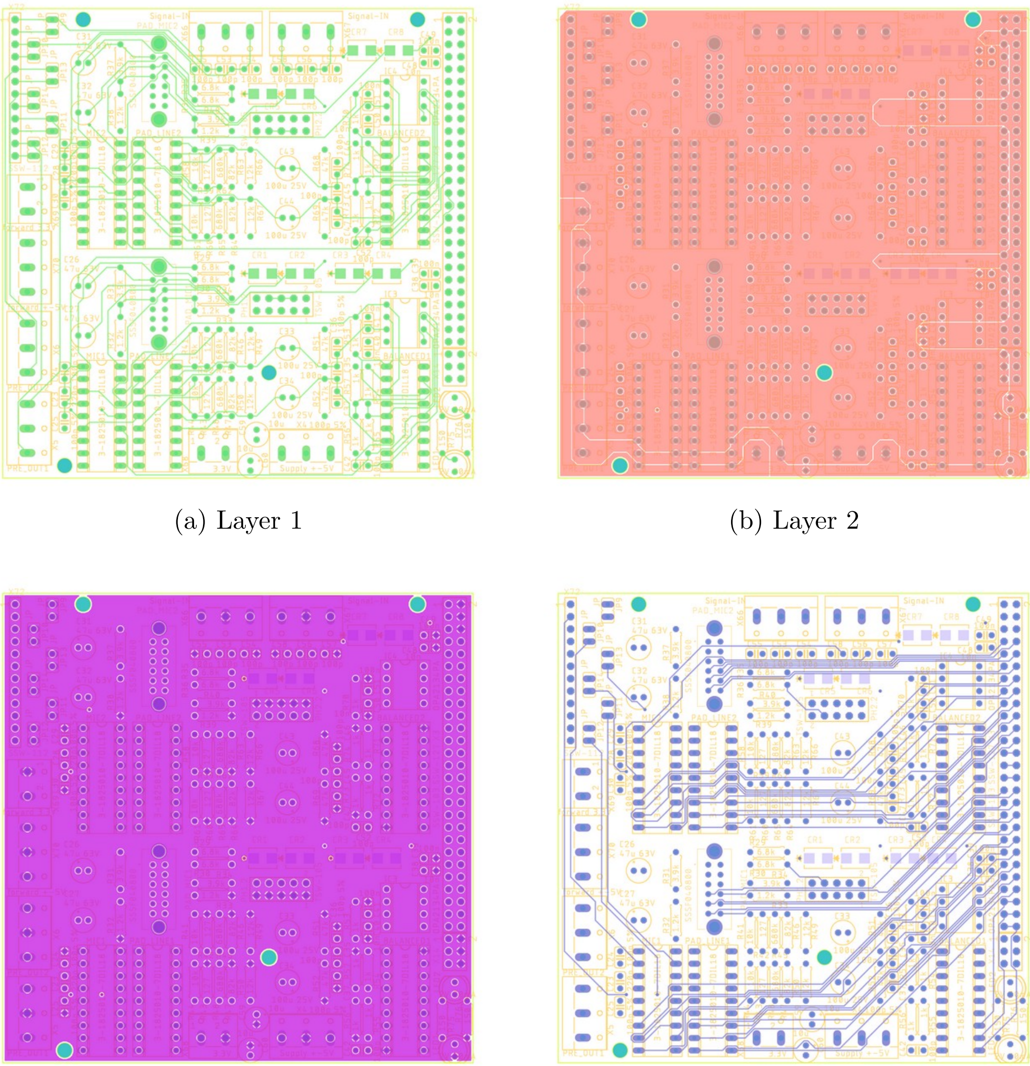

(a) Layer 1

(b) Layer 2

(c) Layer 3

(d) Layer 4

Figure 3.22: The layout of layers 1 to 4 of the prototype main audio input board.

The most important thing for this layout is to keep the signal traces as short as possible and the components as close to each other as possible. Especially the layout of the active components needs to be arranged carefully: ceramic bypass capacitors should be placed as close as possible to the supply pins of the OPA2134. Other external components should also be placed close to the corresponding pins [28, p. 18]. Fortunately, there is no digital part on this circuit and layers two and three could be used as supply and ground planes.

3.7.2 Stereo Input Board

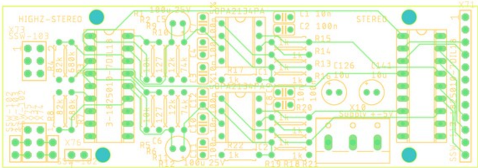

(a) Layer 1

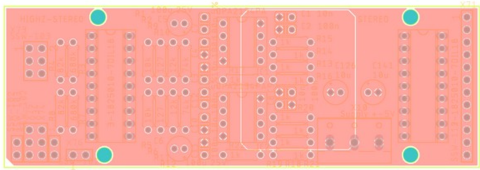

(b) Layer 2

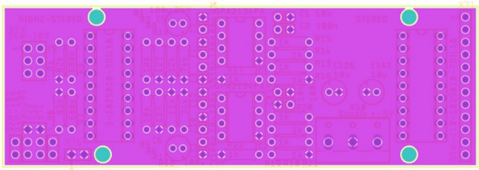

(c) Layer 3

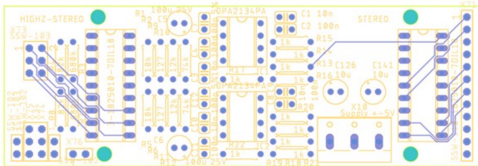

(d) Layer 4

Figure 3.23: The layout of layers 1 to 4 of the prototype stereo input board.

The stereo input board should have been included in the main audio input board, but due to size limitations an extra board has been created. The layout criteria is the same as in subsection 3.7.1. Because of this, the switches are placed differently than in the concept in figure 3.9.

3.7.3 Phantom Power Board

This board is very limited in size, as it should be no longer than $100mm$ and the width is also limited, as the board should be placed on top of the main audio input board and at the same time not cover the switches. The main objective is to place all components on the board and to keep the traces as short as possible. Decoupling caps are used for all active components and are placed as close to their supply pins as possible.

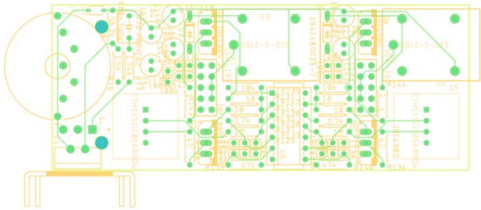

(a) Layer 1

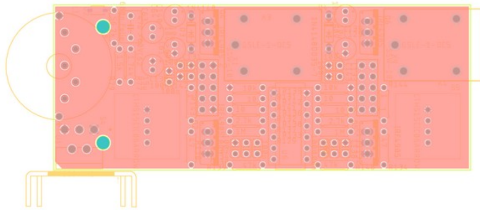

(b) Layer 2

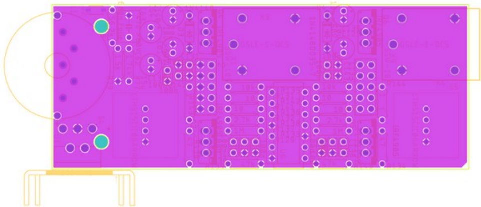

(c) Layer 3

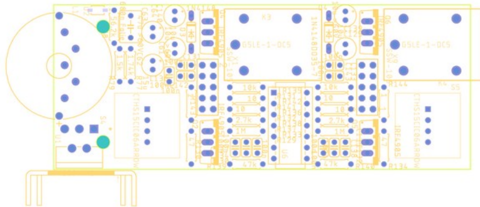

(d) Layer 4

Figure 3.24: The layout of layers 1 to 4 of the prototype phantom power board.

3.8 Usage

3.8.1 Main Audio Input Board

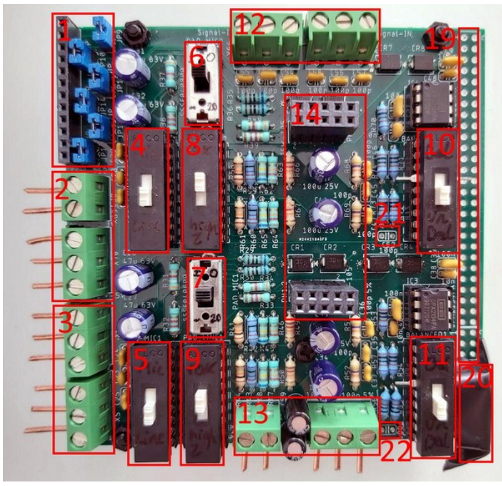

(a) Top view

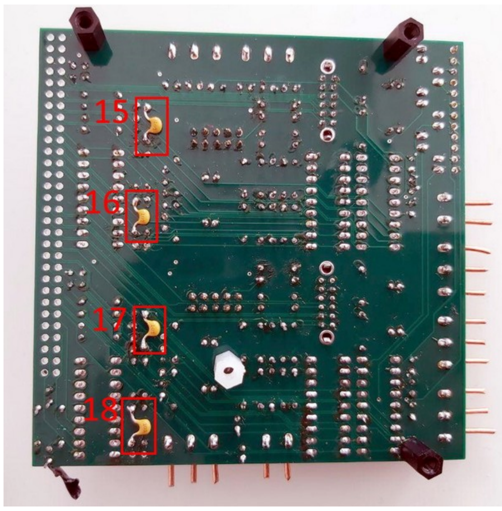

(b) Bottom view

Figure 3.25: These photos of the main input board illustrate all the switches and connectors. They also show some fixes, that have been applied to the prototype board. In the text a # symbol is used to refer to the red numbers in the picture.

The following descriptions refer to figure 3.25. The power for this board is applied at #13. From left to right the connectors are $+3.3v$, GND, $+5V$, GND and $-5V$. The board aligns perfectly with the power connectors of the DAC board but it can also be used with the supply from another source. The voltage is then forwarded through #2 to the preamp board. From top to bottom the order there is GND, $+3.3V$, $-5V$, GND and $+5V$. When the board is powered, this is indicated by the LEDs marked as #20. #12 is the signal input. Channel one is on the left-hand side. The connecters on both channels from left to right are cold-in, GND and hot-in. The output is labelled #3. Here, channel one is on the bottom. From top to bottom the connectors for each channel are hot-out, GND and cold-out. #1 can be used to connect to the stereo input board. If this is the case, the six jumpers have to be removed/open. #14 provides the socket for the phantom power board. All switches are connected to #19. This connector can be used to read the switch positions, or indicate them with LEDs. A board that would allow this is described in section 10.2. At #5 the input for channel one can be selected between microphone and line-in. #4 performs the same task for channel two. When the switch is in top position, microphone in is selected. #7 is used to turn on the $-20dB$ PAD for the microphone on channel one, while this can be done with #6 for channel two. When microphone input is selected for channel one, #9 can be used to select the input impedance. When the switch is in top position, $10k\Omega$ is selected, when it is in bottom position, high impedance is selected. #11 can then be used to select between balanced input (top) or un-balanced input (bottom). For channel two #8 has the same function as #9 while #10 provides the same function as #11 for channel one. If un-balanced input is selected, the cold-input for the corresponding channel is left floating. In order to fix some problems with the prototype board, C42 is moved from #22 to #18 and C52 from #21 to #16. C214 is added at #17 and C215 at #15. It is also important to not plug in Pin4 and Pin15 of #10 and #11, as this would result in shorting R55 or R72 when differential input is selected.

3.8.2 Stereo Input Board

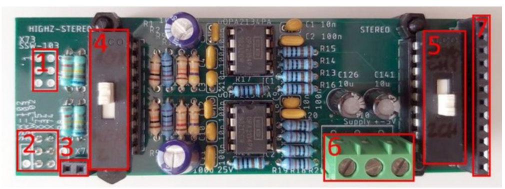

(a) Top view

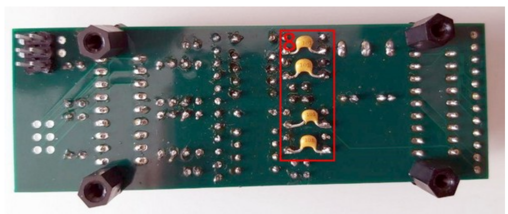

(b) Bottom view

Figure 3.26: These photos of the stereo input board illustrate all the switches and connectors. They also show some fixes, that have been applied to the prototype board. In the text a # symbol is used to refer to the red numbers in the picture.

This paragraph describes figure 3.26. If this board is connected to the main input board through #7, it can be used to split stereo input on channel one into left/right mono input signals. Then those signals are provided to the two separate channels of the preamp and ADC. To do so #5 has to be in top position, otherwise the signals flow right back to the main input board. If the signal is split, #4 can be used to select the input impedance. Top position of the switches selects $10k\Omega$, bottom position selects high impedance. The position of the switch can be indicated through #1. This board needs to be powered by #6. The connectors are $+5V$, GND and $-5V$ from left to right. They align perfectly with the power forwarded by the preamp board. #2 connects the board to ground. The top left pin should be placed on the top left pin (pin 1) of P2 of the dspSoM carrier board in figure 9.6. #3 is used to connect the ground from the preamp to the carrier board. The capacitors in #8 are C217, C216, C219 and C218 from top to bottom. They are used to prevent instability of the circuits.

3.8.3 Phantom Power Board

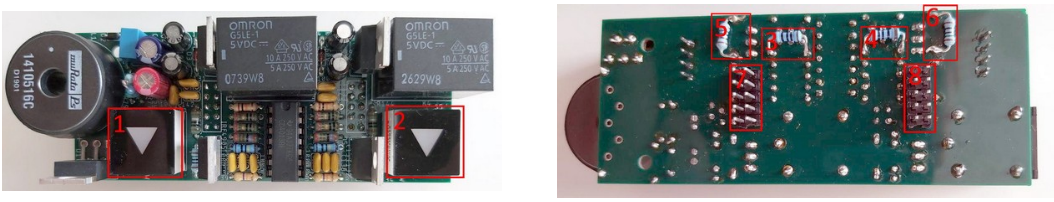

(a) Top view

(b) Bottom view

Figure 3.27: These photos of the phantom power board illustrate all the switches and connectors. They also show some fixes, that have been applied to the prototype board. In the text a # symbol is used to refer to the red numbers in the picture.

This is the description of figure 3.27. The board can be placed on top of the main audio input board, using the connectors #7 and #8. The board is designed to fit and work either way, but generally #8 should be on top, so that the coil does not affect the input signals that much. The touch-switches #1 and #2 turn on the relays, which then switch the phantom power of $48V$ to the main input board. Whichever switch is on top, switches the voltage for channel two, while the one on the bottom switches channel one. #5 and #6 are R201 and R202, which are used to reduce the resistance for the LED to 75Ω. #3 and #4 reduce the value of R129 and R133 to 100Ω. In the prototype this value was too high, consequently, the rise time was to long for the flip-flop.

4 Preamplifier

The preamplifier is supposed to adjust the signal so that the dynamic range of the ADC can be used optimally. This means that the signal should just be low enough to avoid clipping but still high enough to make good use of the resolution of the ADC.

4.1 Gain Control

Microphone signal levels can be very low, when recording lute music or very high, when the mic is inside a kick-drum. Thus, a very wide variable amplification range, typically $70dB$ or more, is required for the preamp [15, p. 725].

4.1.1 Manual

Gain can be adjusted through manual gain control, that can be active or passive and should be logarithmic or linear in dB [15, p. 342].

Passive

Passive amplifier is quiet a misleading therm, as they can only attenuate the signal [15, p. 341]. They usually consist of just a potentiometer, which works as voltage divider. In order to make it somewhat logarithmic, a fixed resistor can be put in parallel to the output. The ration between potentiometer and fixed resistor should be about 1 : 10 to provide a good result [29].

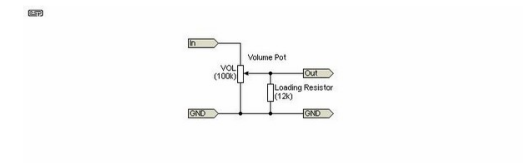

(a) passive gain control

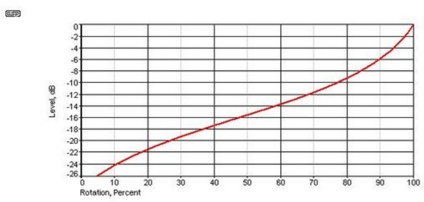

(b) passive gain control law

Figure 4.1: This gain control consists of a linear potentiometer and a resistor. The corresponding gain control law can be seen on the right-hand side.
Source: adapted from [29]

Active

The simplest form of an active gain control uses a potentiometer in the feedback-loop of an inverting amplifier.

Figure 4.2: This graphic shows two versions of an active gain control and the corresponding gain formula. Each of these two options are very simple and only use one op-amp. The first one (a) has linear gain, while the second one (b) has a somewhat logarithmic gain.
Source: adapted from [15, p. 357]

An example for a better active gain control is shown in figure 4.3.

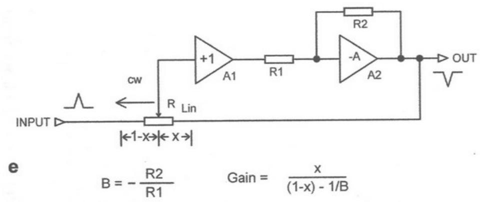

(a) Baxandall gain control

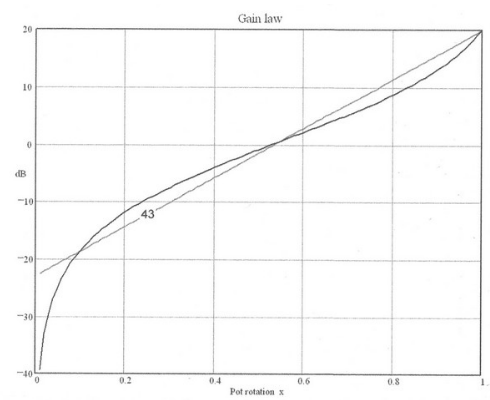

(b) Baxandall gain control law

Figure 4.3: This gain control was developed by Peter Baxandall. It is a logarithmic gain control, that can attenuate the signal as well. Figure (a) shows the circuit and the gain formula and figure (b) shows the corresponding gain in relation to the potentiometer rotation x.
Source: adapted from [15, p. 357] and [15, p. 360]

4.1.2 Digital

There are also digitally controlled preamps available, that can be programmed over common bus interfaces.

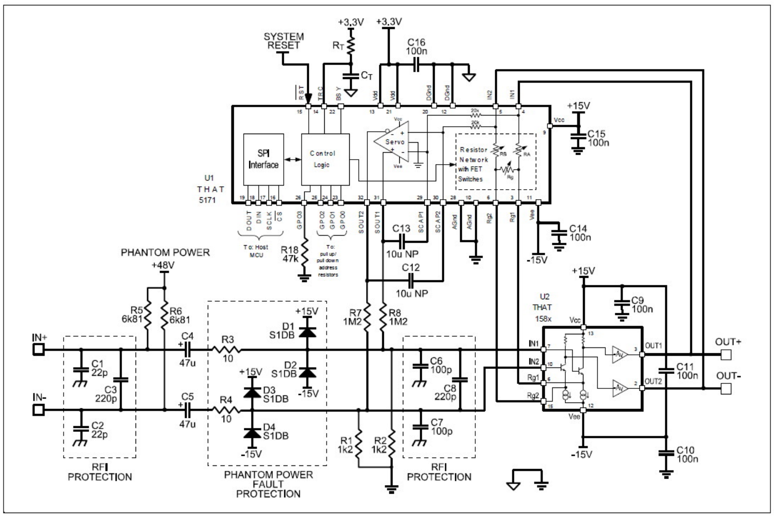

Figure 4.4: This is the basic application circuit for the THAT1580, controlled by the THAT5171, for microphone input. There is no PAD included, but phantom power and the protection circuit are included. The input impedance is $1.2k\Omega$. The THAT5171 can be programmed over SPI.
Source: adapted from [20, p. 8]

THAT Combo

The THAT 5171 and THAT 1580 combination, for example, has a minimum gain of $5.6dB$ and provides gains from $13.6dB$ to $68.6dB$ in $1dB$ steps [19, p. 8]. It can be programmed over a serial peripheral interface (SPI) bus.

4.2 Audio Operational Amplifiers

The selection of the right op-amp depends on the budget [15, p. 124], otherwise it would be an obvious choice to use a modern, expensive audio-op-amp. The package is also something that should be considered, as it affects the prize and size of the final board. The small-outline integrated circuit (SOIC) package is very common for a surface-mounted device (SMD). Devices that use through-hole technology (THT) often come in dual in-line (DIL) packages. It is easier and cheaper to get sockets for the latter ones. Another important factor is the input device type: BJTs tend to have higher current noise (in), while junction gate field-effect transistor (JFET) inputs have higher voltage noise (en) and are therefore better suited for high source resistances [15, p. 157]. Moreover, BJT inputs usually require a significantly higher input bias current (I_B) [15, p. 123]. The slew rate (SR) generally should be high enough to cover the audio band [15, p. 121]. The common-mode voltage range (CMVR) should be close to the supply rail voltages, which is rather common among audio op-amps [15, p. 122]. While the input offset voltage (V_{OS}) can be a problem, its effect can often be eliminated by using DC blocking caps in the signal path [15, p. 123].

4.2.1 Comparison

In table 4.1 the electrical characteristics of several audio-op-amps are compared. There are the old standard ones as the TL052, which uses a field-effect transistor (FET) input and the 5532a with a BJT input. Modern ones as the OPA2134 and OPA1611 are also included in the list as well as the LM741 as a budget op-amp and probably a negative example. The AD8674 is used for an active filter after the DAC, this is why it is listed here as well. Finally, the THAT1580, a controllable current feedback amplifier (CFA) is also included because it is used for the preamp.

	Input device	Package	en ($nV/\sqrt{Hz}$)	in($pA/\sqrt{Hz}$)	SR ($V/\mu s$)	CMVR (V)	V_{OS} (mV)	I_B (nA)	Price (€)
TL052	FET	DIL SOIC	18	0.01	13	(V-)+2.7 to (V+)+0.6 *	0.73	0.02	2.22 0.535
OPA 2134	FET	DIL SOIC	8	0.003	20	(V-)+2.5 to (V+)-2.5	0.5	0.005	4.22 0.483
5532a	BJT	DIL SOIC	5	0.7	9	(V-) to (V+)	0.5	200	2.21 1.014
LM741	BJT	DIL	20	??	0.5	(V-) to (V+)	0.8	80	0.71
THAT 1580	CFA	16PIN QFN	18.3 (0dB) to 1 (60dB)	1.5	53	(V-)+3.7 to (V+)-3.2	10 (0dB) 0.25 (60dB)	6800	5.32
OPA 1611	BJT	SOIC	1.1	1.7	27	(V-)-0.5 to (V+)+0.5	0.1	60	4.269
AD 8674	BJT	SOIC	2.8	0.3	4	(V-)+2.5 to (V+)-2.5	0.02	3	6.6

Table 4.1: It can be clearly seen, that the FET inputs have higher voltage noise but lower current noise and a lower input bias current. The LM741 is too slow for the whole audio band. Modern audio op-amps have excellent features, for example the OPA1611 can handle signals outside its supply rails, but they are rather expensive.
* when the TL072 hits negative limit, it inverts its phase. It then latches up or creates nightmare clipping behaviour.

The values are taken from Dougles Self's *Small Signal Audio Design* [15] and directly from the corresponding datasheet. Additional op-amps are listed in *Small Signal Audio Design* [15] and in *Handbuch der Audio-Schaltungstechnik* by Paul Skritek [16, p. 411]. Special focus should be on The LM741, as it is the only one with a slew rate, that does not cover the whole audio spectrum [15, p. 121]. The TL052 shows a very interesting behaviour as it inverts the phase when the input comes close to the negative rail, which causes either latch-up or nightmare clipping behaviour [15, p. 122].

4.3 Requirements

The preamp should have a wide gain range and it should be controllable by the DSP, which means it has to be digitally controllable. It is recommended to use the THAT1580, as it combines all of these aspects and has been successfully used on the previous design by Victor Palos [1].

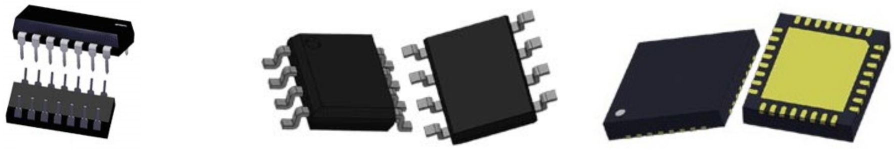

(a) DIL (b) SOIC (c) QFN

Figure 4.5: These are some IC packages from the op-amps used in the circuit. The most common package for THT is the DIL package, whereas for SMD the SOIC package is used frequently.
Source: Adapted from [30]

When using the THAT1580, $1.2k\Omega$ resistors are required on the input. They provide a low source impedance for the THAT1580 and a low load for microphone input. Additionally, they keep the generated noise due to the input current noise low. [31, p. 7]

The input board (chapter 3) ensures that other inputs than microphones are adjusted correctly. The preamp board connects the input board with the ADC board. Even tough the size is theoretically limited by the costs, this is not particularly an issue for this board. It is based on a microphone amplifier from the THAT coporation.

4.4 Circuit

The circuit has essentially been taken from the THAT5171 data-sheet, as shown in figure 4.7. The input conditioning, including the application of the phantom power and the corresponding protection circuit, are already on the input board. The capacitors C102, C103, C106 and C107 are typical decoupling capacitors with $100nF$ for the analog supply voltages. C108 decouples the positive from the negative supply. C104 does the same for digital supply and is connected to $3.3V$ and the digital ground. R112 and C105 set the timeout for zero-crossing detection that is typically set to $22ms$ [20, p. 11], which means C105 has a value of $1nF$ and R112, a value of $22M\Omega$. The input impedance for the THAT1580 should be at about $1k\Omega$, as higher values produce more noise [31, p. 7], therefore $1,2k\Omega$ has been chosen for R25 and R26. The servo resistors should have thousand times the value of these resistances, consequently, R110 and R111 have $1.2M\Omega$ each. A $47k\Omega$ pull-down resistor (R114) is placed at the GPO3 pin. GPO0 through GPO2 define the address, during reset. These pins are all pulled down, as each controller should be selected by the CS input. If other addresses are required, the board has to be modified. R115 to R117 all have $47k\Omega$.

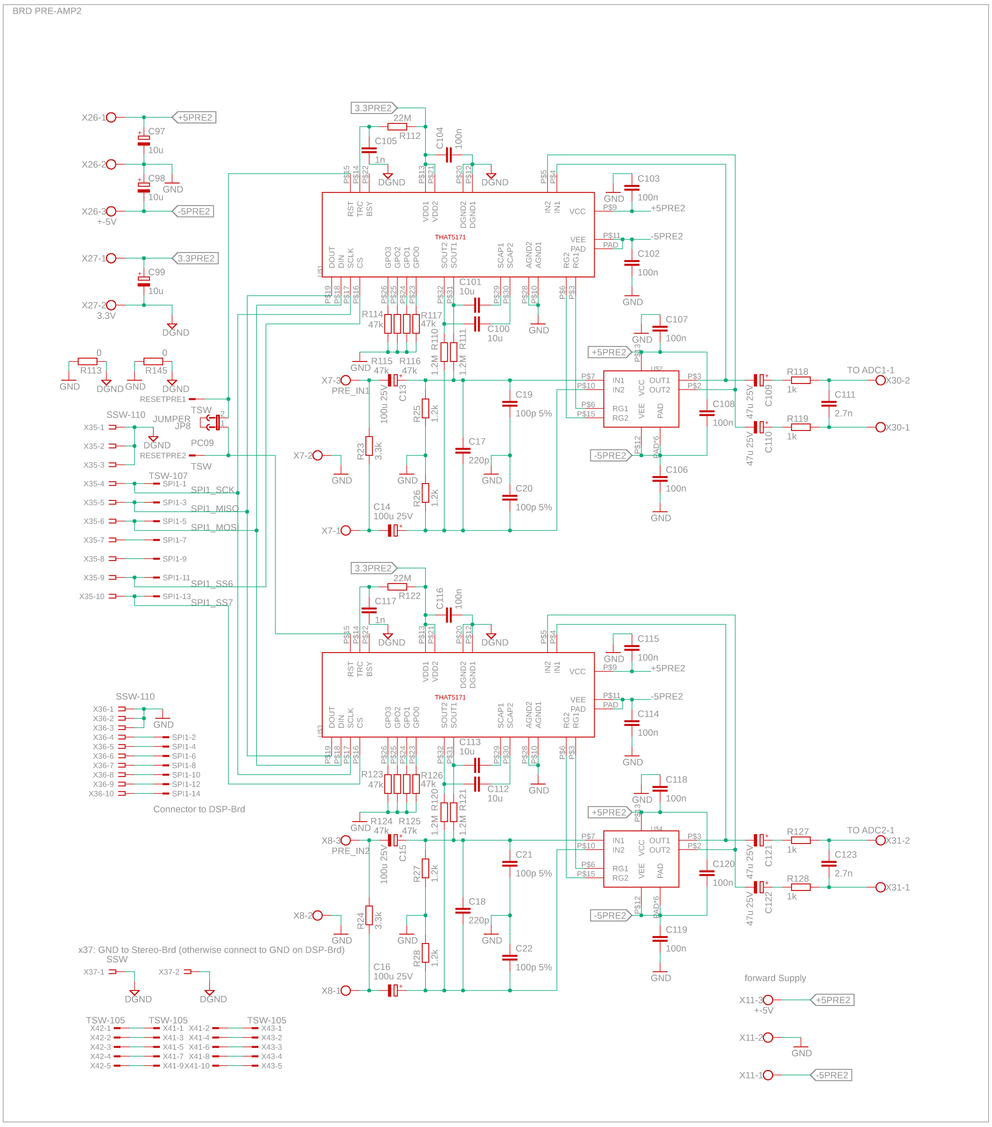

Figure 4.6: The combination of the THAT5171 and the THAT1580 form a controllable amplifier that can be programmed over SPI. Such a combination is used once per channel. On this board a RFI protection and the required $1.2k\Omega$ input resistors are included.

At the input is a $3.3k\Omega$ resistor (R23) that provides an input when switching on the input board. It also reduces the input resistance for differential input. This resistor might be removed or split into two smaller resistors connected to ground, if it has a negative effect. It should be kept in mind that doing so would effect the input impedance of the microphone input on the input board. The capacitors C13 and C14 are for DC blocking and C17, C19 and C20 provide RFI protection.

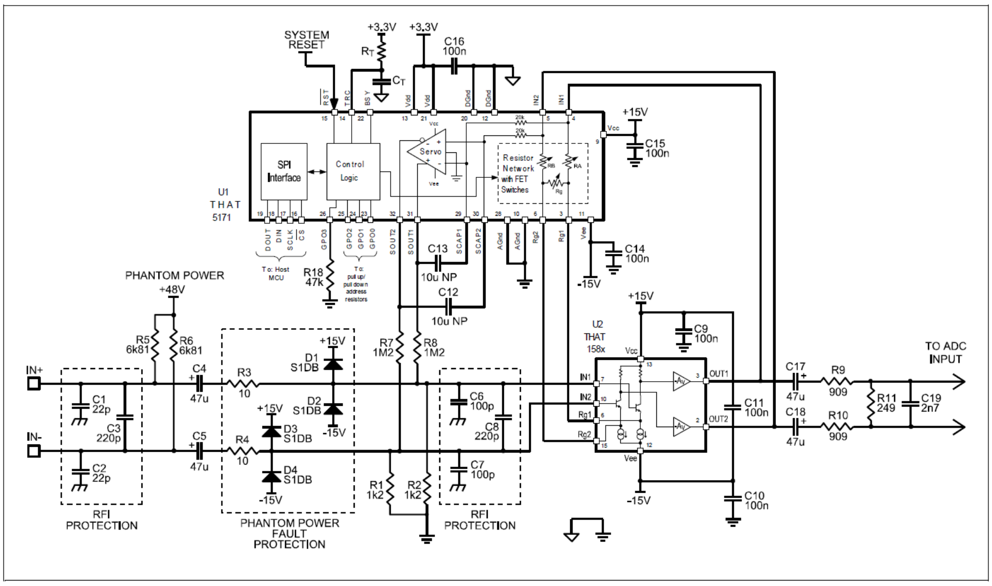

Figure 4.7: This is a low cost application of the THAT combo. Everything before and including the phantom power fault protection is incorporated in the input board and therefore not relevant for this chapter.
Source: adapted from [20, p. 9]

As the maximum single output of the THAT1580 equals $V_{+} - 1V$ [31, p. 2], which for this application means $4V$, the maximum differential output is $8V_{PP}$. The ADAU1979 can handle a typical input of $4.5V_{RMS}$ [22, p. 14], which would be $12.7V_{PP}$ with no further attenuation required. C110 and C109 are used for DC coupling, while R118 and R119 in combination with C111 form a low-pass anti-aliasing filter (AAF) with a cutoff frequency of about $30kHz$.

$$f_c = \frac{1}{2 \cdot \pi \cdot (R118 + R119) \cdot C111} = 29.473kHz \tag{4.1}$$

Through jumper JP8 both preamps can be reset with the same reset line, otherwise two different reset lines can be connected.

4.5 Layout

The most sensitive part of the circuit are both THAT ICs and their configuration. The connection between the Rg pins should not be above a ground or supply plane. The connections should be as short as possible and symmetrical [20, p. 17], an example for is shown in figure 4.9. This has been achieved by placing another plane, which is not connected to anything, below the connections. Analogue and digital ground should be treated as separate planes and the decoupling caps should be placed as close to the supply pins as possible, especially for the digital supply.

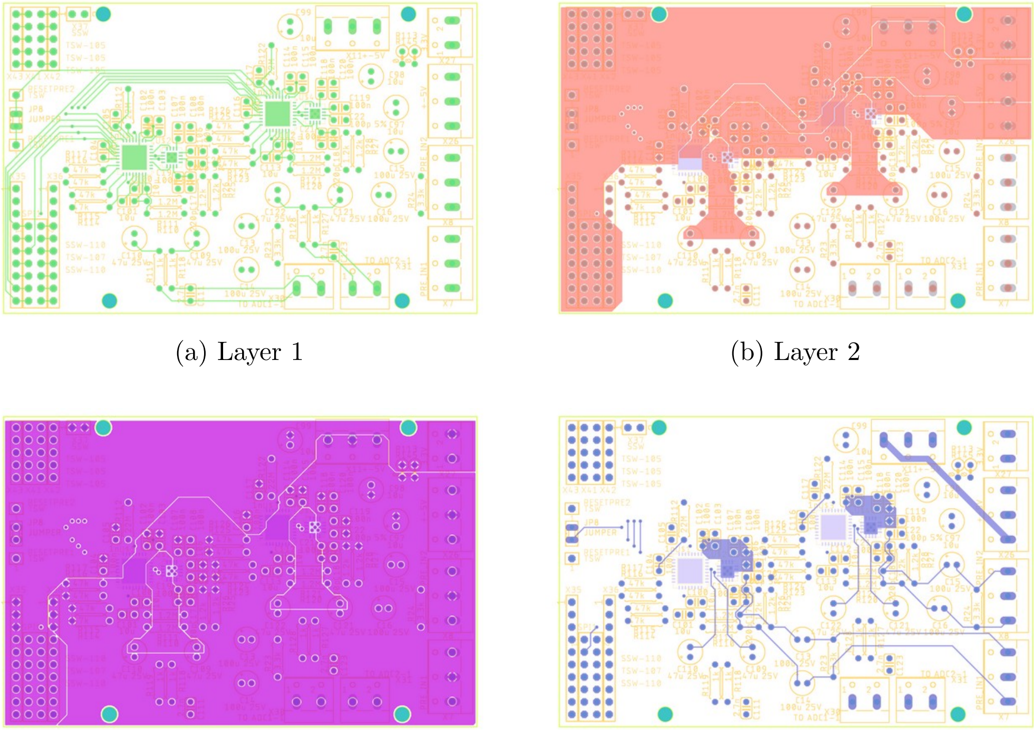

(a) Layer 1 (b) Layer 2

(c) Layer 3 (d) Layer 4

Figure 4.8: The layout of layers 1 to 4 of the prototype preamplifier board.

The RFI protection should be placed as close as possible to the input of the THAT1580 [31, p. 12]. Both grounds are connected with a ferrite bead.

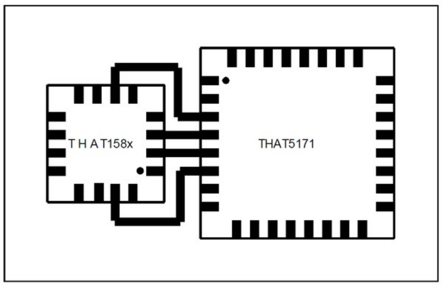

Figure 4.9: The recommended layout for the THAT1580 and the THAT5171.
Source: adapted from [20, p. 17]

4.6 Usage

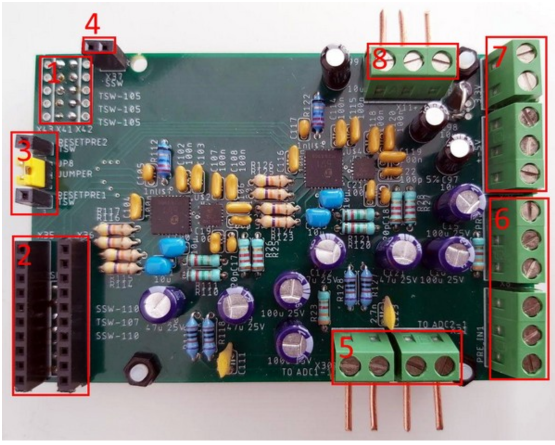

Figure 4.10: This photo of the preamplifier board illustrates all the switches and connectors. In the text a # symbol is used to refer to the red numbers in the picture.

The numbers in this text refer to figure 4.10. The top left pin of #1 should be connected to pin 9 of P2 from the adapter board (figure 9.6), while the top left pin of #2 connects to pin 41 of P2. The pull-up network can be plugged in the left-hand side of #2 on the lowest pins and then also needs to be connected to $+3.3V$. Each pin of #1 and #2 is either connected to the left or to the right. The jumper on #3 can be used to connect the reset lines of the two amplifiers, in this way only one of the plugs has to be connected to the preamp-reset of the DSP. The board is powered over #7, where the connectors from top to bottom are digital ground, $+3.3V$, $-5V$, analogue ground and $+5V$. The analogue voltage is forwarded to #8, where the connectors are $+5V$, ground and $-5V$ from left to right. #4 should be connected to the stereo input board or to pin 1 or pin 2 on P2 of the DSP adapter board, if the stereo board is not used. #6 is the signal input. The connectors on the top are for channel two and the ones on the bottom for channel one. From top to bottom they are hot, ground and cold, for each channel. The output is then provided on #5, where channel one is on the left and channel two is on the right. The hot output is on the right-hand side of each connector, however, at this point it should not matter anymore.

5 Analog-to-Digital Converter

Digital audio hugely increases the possibilities of audio signal processing. In order to digitise an audio signal, analog-to-digital converters are required. Modern ADCs are excellent for this purpose [15, p. 723]. When comparing ADC types, $\Sigma - \Delta$-converters become the obvious choice for audio applications because they provide a high resolution at a lower sampling rate compared to others [32, p. 505]. The fact that the frequency band of audio signals usually is considerably lower than the inherently low sampling rate of an $\Sigma - \Delta$-ADC, makes them perfect for audio applications.

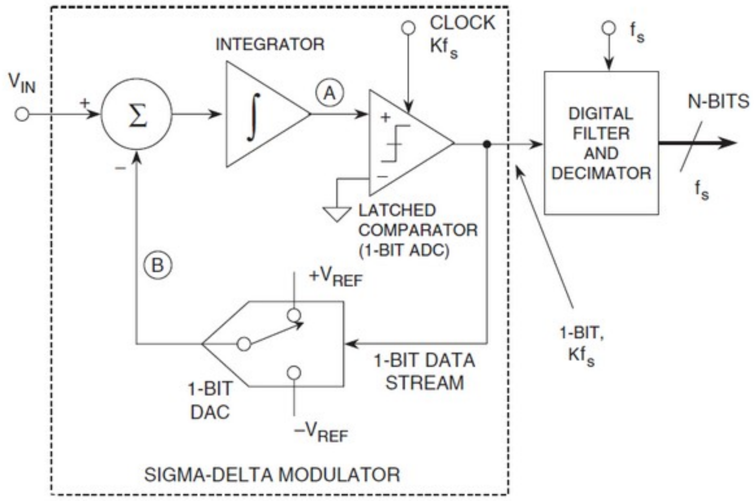

Figure 5.1: An example of a first order sigma-delta ADC. The average output equals the input voltage.
Source: adapted from [33, p. 72]

The principle of a sigma-delta ADC, as shown in figure 5.1, is the following: when a DC voltage is at the input, the integrator is either ramping up or ramping down. The comparator then outputs zeros or ones. In the feedback loop this output is then converted to either $+V_{REF}$ or $-V_{REF}$ in the 1-BIT DAC. The difference between the input voltage and the feedback voltage is the new input voltage of the integrator and the circle starts again. This means when the input voltage is close to $+V_{REF}$, the comparator will output more ones than zeros and if it is close to $-V_{REF}$, it will generate more zeros and less ones. Assuming the absolute value of $-V_{REF}$ equals $+V_{REF}$ and the input is at $0V$ (GND), the number of ones and zeros should be equal. The final data is then processed in a digital filter and a decimator process. [33, p. 72]

Independent of the type of ADC that is used, an AAF, which not only prevents aliasing but it also removes unwanted signals outside the bandwidth of interest, should be implemented. Oversampling can have the benefit of relaxing the requirements of this filter. For this application an AAF is implemented at the output of the preamplifier board by means of a differential $30kHz$ low-pass filter [33, p. 71].

5.1 Requirements

With regards to the ADC, the ADAU1979 has already proven its worth in the previous design. It should be used in this design as well because in this way the code to control the ADC is compatible for both designs. The ADAU1979 is a 24-Bit ADC [22, p. 3] that uses sigma-delta ($\Sigma - \Delta$) architecture [22, p. 1]. It can be controlled over SPI and I2C [22, p. 1]. This design uses the I2C BUS to control the ADC and DAC.

5.2 Circuit

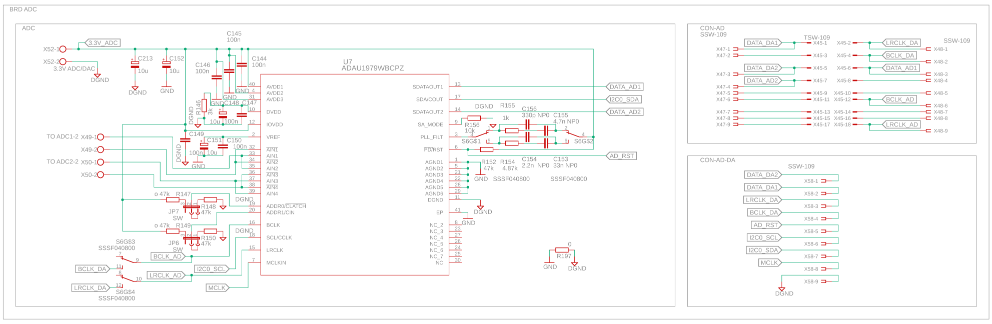

Figure 5.2: Two of the four ADCs provided on the ADAU1979 are connected to use the 2-channel summing mode. The special feature of this design is that the PLL filter can be selected by a switch. The address can also be changed by switches.

The supply is decoupled with the two $10\mu F$ capacitors C213 and C152. As described in the data-sheet, all AVDD pins are decoupled with a $100nF$ to the nearest AGND pin using the capacitors C144, C145 and C146. The voltage on DVDD is generated internally, but needs the external decoupling capacitors C148 with $10\mu F$ and C147 with a capacitance of $100nF$ as well as R146, a $3k\Omega$ Resistor. The same is true for the reference voltage (VREF) and the capacitors C151 and C150. The IOVDD pin needs a decoupling capacitor (C149) with $100nF$. [22, p. 12]

As the output of the preamp is not followed by an active attenuation, the reference voltage is not needed anywhere else, which is why the pin has no wiring besides the capacitors. R147 through R150 are either pull-up or pull-down resistors with $47k\Omega$. The reason why two resistors are used after the switch and not only one before the switch is to avoid a short circuit during switching. It requires more space, but is less sensitive to errors. The standalone mode is disabled by the $47k\Omega$ pull-down resistor R156 and the reset line uses a pull-up resistor R152 with the same value.

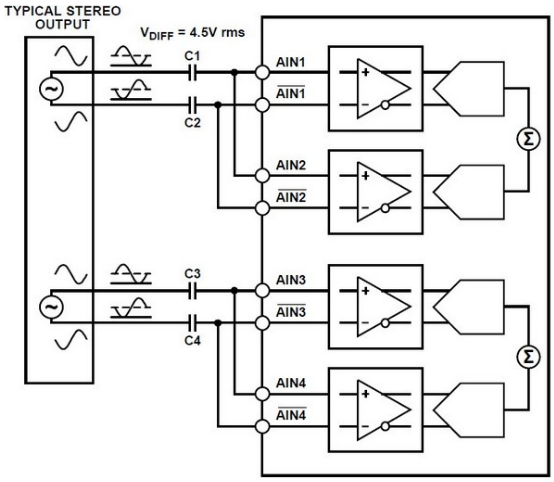

Figure 5.3: Two of the four inputs of the ADAU1979 can be connected for the 2-channel summing mode. This improves the SNR by $3dB$.
Source: adapted from [22, p. 16]

As the whole design provides two input channels, it is logical to use the four inputs of the ADAU1979 in the 2-channel summing mode. This is why the inputs AIN1 and AIN2 are connected in figure 5.2. The same applies to AIN3 and AIN4 and the corresponding inverted inputs.

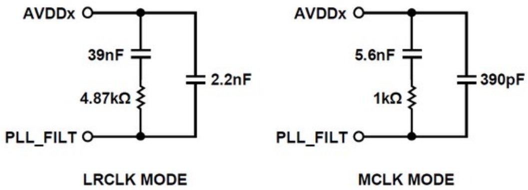

Figure 5.4: The ADAU1979 can either generate its own clock signal from a master clock (MCLK MODE) or use an already provided external clock (LRCLK MODE). Each mode requires a different filter for the phase-locked loop (PLL).
Source: adapted from [22, p. 13]

On this board a switch allows the selection of the PLL-filter. When LRCLK MODE is selected, the also switch connects the DCLK and LRCLOCK pins to the clock signals coming from the DAC-board. The filter components are basically the same as in figure 5.4, but as $39nF$, $390pF$ and $2.6nF$ were not available as THT components, C135 has $33nF$, C156, $330pF$ and C155, $4,7nF$. So far no complications have been detected.

The I2C connections are wired to the DAC-board and then forwarded to the DSP.

The required $2k\Omega$ pull-up resistors for the I2C BUS is also on the DAC-board.

5.3 Layout

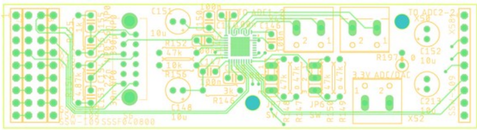

(a) Layer 1

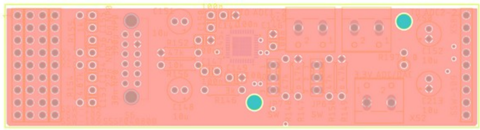

(b) Layer 2

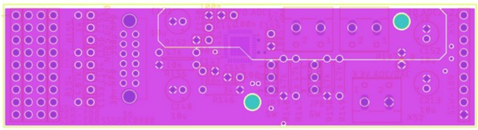

(c) Layer 3

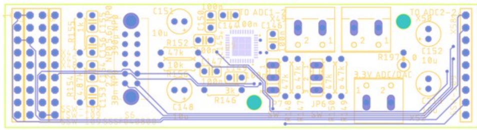

(d) Layer 4

Figure 5.5: The layout of layers 1 to 4 of the prototype ADC board.

The layout of the ADC board is rather simple: the ground plane is separated into digital and analogue ground which are connected by a ferrite bead. The analogue ground covers everything from the signal input the the ADCas well as some of the ADCs wiring. The decoupling capacitors are placed as close to the supply pins as possible.

5.4 Usage

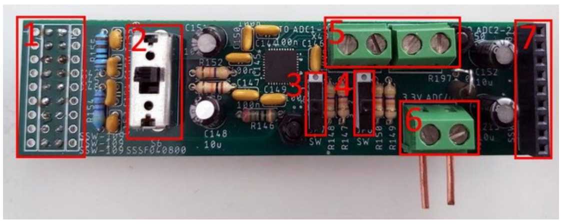

Figure 5.6: This photo of the ADC board illustrates all the switches and connectors. In the text a # symbol is used to refer to the red numbers in the picture.

The following paragraph explains figure 5.6. The top left pin of #1 should be connected to pin 57 on P2 of the DSP adapter board (figure 9.6). All pins are connected to either the left ore the right. This additional connections can be used for measurement and to connect unused pins on P2. #2 can be used to select if the clock of the ADC is in master or slave mode. The default (mastermode) is active when switched to the top. Using this switch connects the correct PLL-filter to the ADC. In mastermode the DCLK and LRCLK are generated on the ADC, while in slave mode the DCLK and LRCLK are taken from the DAC. Switch #3 can be used to set ADDR0 and switch #4 sets ADDR1. By default both are set to zero, which is the bottom switch position. The top position sets them to one. #7 is used to connect the board to the DAC board. This is necessary because both boards need to be used together in order to operate correctly. The board is supplied by #6, which connects exactly to the supply board. $+3.3V$ is on the right-hand side and ground on the left-hand side. Finally, #5 is used for signal input, where channel one is on the left and channel two is on the right.

6 Digital-to-Analog Converter

Digital-to-analog converters assign a discrete voltage or current value to a digital input value [32, p. 455]. Common devices are capable of 24bit operations [15, p. 729]. Regarding ADCs, using multibit sigma-delta architectures is common practice for audio DACs.

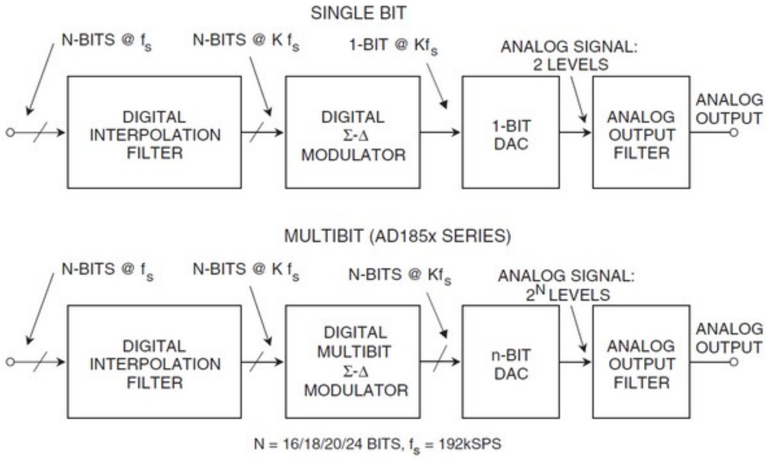

Figure 6.1: An example of 1-bit and multibit sigma-delta ADCs.
Source: adapted from [33, p. 109]

Unlike sigma-delta ADCs, DACs are mostly digital. Typically, an interpolation filter is first, which inserts zeros to a low rate signal and then applies a digital filter algorithm. This is followed by a delta-sigma modulator, that converts the resulting data into a high speed bit stream. At the end a 1-bit DAC switches between the positive and negative reference values. Using more than one bit in the DAC leads to the multibit architecture, but the basic concept is the same. The output is then filtered by an external reconstruction filter. Oversampling can reduce the requirements for this filter. [33, p. 109]

6.1 Requirements

To increase the compatibility with the previously developed board, the same DAC should be used. In this way program code is easier to use for both. The ADAU1962A is a high performance, $192kHz$ and 24-Bit ADC. It has twelve channels and uses a multibit sigma-delta ($\Sigma - \Delta$) architecture [34, p. 1]. The master clock should provide a frequency of $24.576 MHz$, as the ADC and the DAC can use most of their available sampling frequencies with this master clock input frequency.

6.2 Circuit

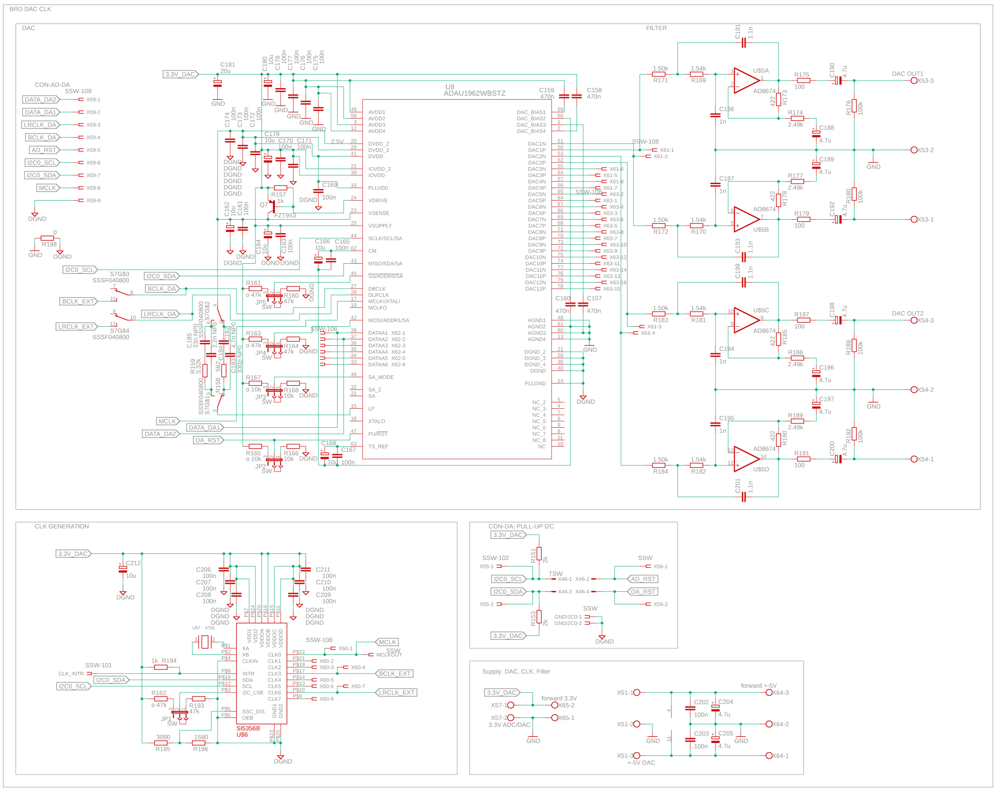

Figure 6.2: On the DAC board are the DAC configuration, the output filter, the clock generator and the pull-up resistors for the I2C BUS. The circuit is mostly wired as described in the corresponding data-sheet.

The circuit on the DAC board consists of three main parts. The DAC configuration circuit, the output filter and the clock generator. Additionally, the I2C pull-up resistors R151 and R153 have been placed on this board.

6.2.1 Main DAC Circuit

At the supply input C181, a $20 \mu F$ capacitor, and C180 with $10 \mu F$ are placed on the board for decoupling. AVDD1 to AVDD4 are decoupled with C175 to C175, each of which are $100 nF$ capacitors, to the corresponding AGND1 to AGND4. VSUPPLY is decoupled with the $10 \mu F$ capacitor C164 and the $100 nF$ capacitor C163. Capacitors with equal values are used to decouple the TS_REF pin (C168 and C167) and the CM pin (C165 and C166). [34, p. 20]

C157 is used to AC couple DAC_BIAS3 with a $470nF$ capacitor to AGND3 and C158 does the same for DAC_BIAS3 and AVDD3. VSENCE has to be bypassed with the $10\mu F$ capacitor C162 in parallel to the $100nF$ capacitor C161. [34, p. 9]

DAC_BIAS1 is AC coupled to AVDD2 by C159 to AVDD2 and DAC_BIAS1 is AC coupled by C160 to AGND2. Each of the two capacitors have a value of $470nF$. [34, p. 10]

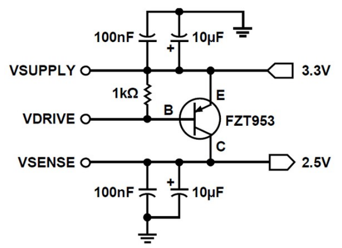

Figure 6.3: This circuit is recommended for the 2.5V regulation for VSENSE.
Source: adapted from [34, p. 13]

Figure 6.3 shows the recommended $2.5V$ regulator circuit from the data-sheet. This circuit is realized by Q7 and the $1k\Omega$ resistor R157. The decoupling capacitors C162 and C161 have already been explained before. $The 100nF$ capacitors C172, C173 and C174 are used to decouple the DVDD pins and C169 for the PLLVDD. The digital supply IOVDD and IOVDD_2 are decoupled with the $10\mu F$ capacitor C179 and with a $100nF$ capacitor on each input (C170 and C171).

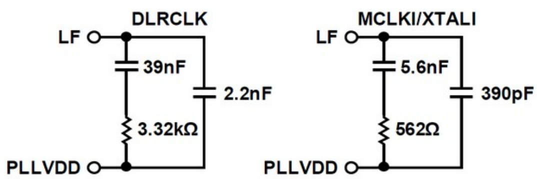

Figure 6.4: The ADAU1962A can generate the DCLOCK and LRCLOCK signal by itself from a master clock or use an external clock. Depending on which mode is used, the PLL-filter uses different values.
Source: adapted from [34, p. 13]

Just as the ADAU1979, the ADAU1962A can either generate the DCLOCK and LR-CLOCK from a master clock signal or use clock signals from an external source. The required filters for each configuration can be seen in figure 6.4. Both versions are implemented on this board. Again, some capacitor values are not available in THT. This is why C185 has $33nF$, C183 has $330pF$ and C182 has $4.7nF$. The other values in the filters are the same as in figure 6.4. It is possible to select the configuration with a switch. If the switch is set to use an external clock, it is taken from the clock generator also placed on this board. With the four switches JP2, JP3, JP4 and JP5 pull-up or pull-down configuration can be selected for the corresponding pin. The resistors for setting the dress (R160, R161, R163, R164) all have $47k\Omega$, while the resistors R165 to R168 have $10k\Omega$ each. Their corresponding switches JP3 and JP2 can be used to activate the stand alone mode and for reset. Just as for the ADC, this configuration with two resistors instead of one, avoids a short circuit while switching.

6.2.2 Output Filter

The output filter is the one recommended in the data-sheet, as seen in figure 6.5

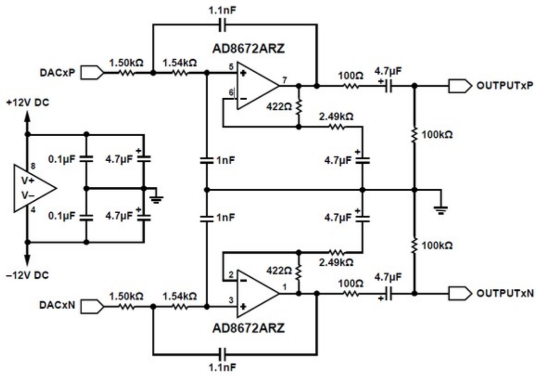

Figure 6.5: This circuit shows the typical active DAC output filter for differential signals, as it is presented in the data-sheet.
Source: adapted from [34, p. 13]

There are no further explanations in the data sheet, thus, the circuit was simulated in LTspice, as can be seen in figure 6.6 and figure 6.7.

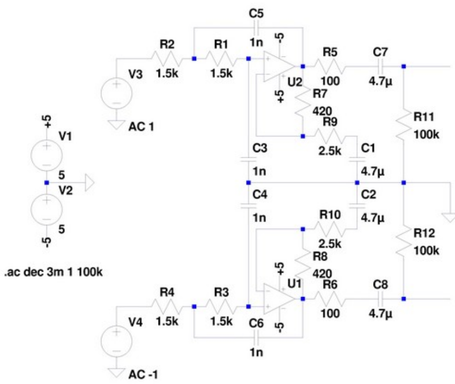

Figure 6.6: The filter was rebuilt in LTspice using the standard op-amp. Some values are rounded already, as they have been used in the actual design.

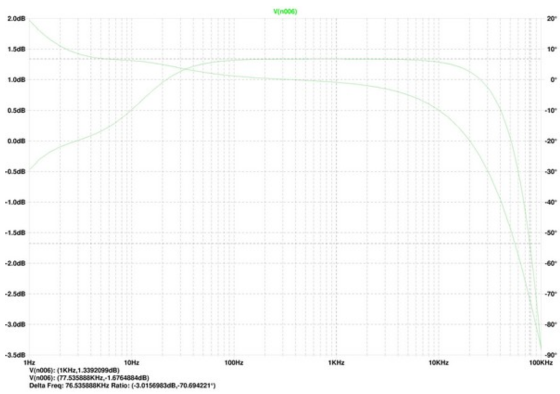

Figure 6.7: Here, the phase response of the filter can be observed.

Using the cursor, the $3dB$ corner frequency can be identified as about $77kHz$, as shown in figure 6.8. Even though the data-sheet recommends the AD8672, the four op-amp version AD8674 has been used, as each channel requires a filter. Furthermore, the four channel version needs less space and is usually less expensive than two AD8672 ICs.

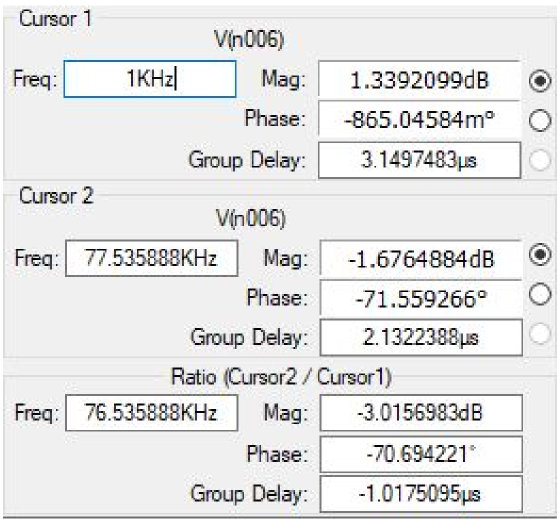

Figure 6.8: The $-3dB$ corner frequency seems to be about $77kHz$. It was measured by placing one cursor at $1kHz$ and moving the second one to the position where the ratio has a magnitude of $-3dB$.

6.2.3 Clock Generator

The master clock for the ADC and DAC is also generated on this board. For the clock generation the Si5356A has been selected. Up to eight clock signals can be generated by this clock generator and it can be programmed via I2C. The quartz used is an ECS-

250-20-3X-TR, which is a 25MHz 20pF quartz. It is connected across XA and XB. As a quartz is used, the CLKIN pin and the output enable pin OEB are tied to ground. Each of the six supply pins is bypassed by a $100nF$ capacitor (C206 to C2011). The voltage on the SSC_DIS pin must not exceed 1.2V [35, p. 21]. The data-sheet recommends 3090Ω for R_{SE} (R195) and 1580Ω for R_{SH} (R196) with a supply voltage of $3.3V$ [35, p. 10]. The open drain pin INTR requires the $1k\Omega$ pull-up resistor R194. With the switch JP1 the least significant bit (LSB) of the address can be selected. This is then done by either R162 or R193, each of which has $47k\Omega$. CLK0 is used to generate the master clock, while CLK3 and CLK6 can provide the BCLK and LRCLK when needed. Unused pins must be left floating [35, pp. 21–22], although all pins are provided on a multiway connector on the board. Figure 6.9 shows the possible clock configurations for the DAC and the ADC. For each configuration the PLL filter on the converters is also switched to the correct values, depending on whether they use master-clock mode or slave-clock mode. In each case, BCLK and LRCLK use the same source and can not be switched separately.

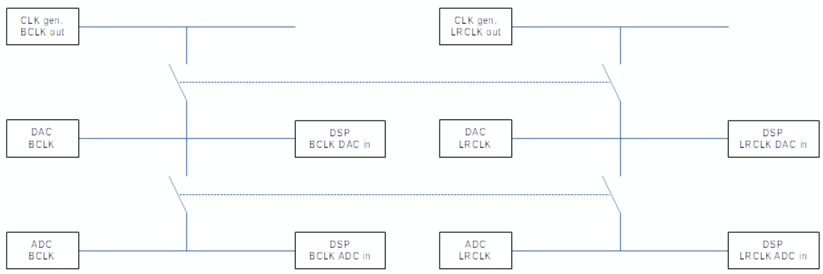

Figure 6.9: The BCLK and LRCLK from the clock generator can be used as BCLK and LRCLK for the DAC. The BCLK and LRCLK from the DAC can be used for the ADC, whether they come from the clock generator or the DAC itself.

6.3 Layout

The layout for the DAC board is separated in an analogue part covering the DAC output and the filter, and a digital part covering the DAC configuration and the clock generator. This can be seen by the split ground in layer three of figure 6.10. Decoupling capacitors are placed as close as possible to the supply pins of each IC. Generally, the objective was to keep all connections as short as possible. Some signal paths of the filter are placed on the bottom layer, where an extra shield is used between the analogue and the digital part.

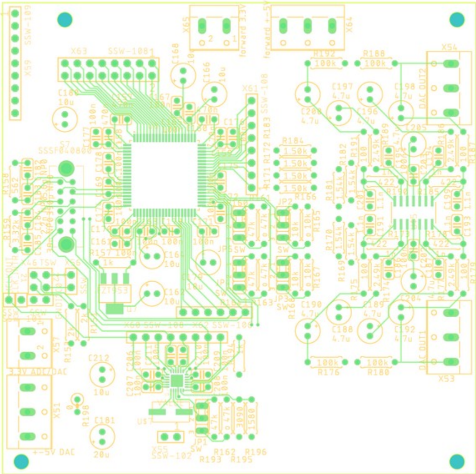

(a) Layer 1

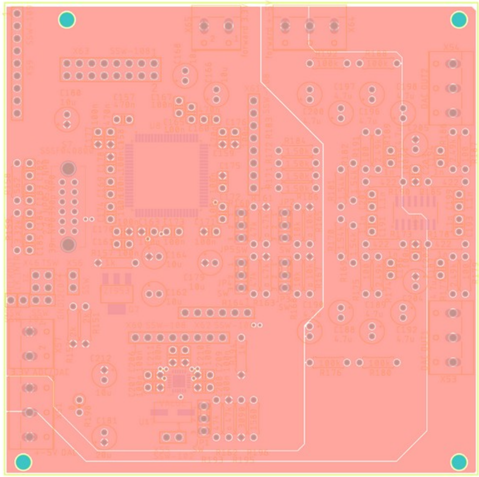

(b) Layer 2

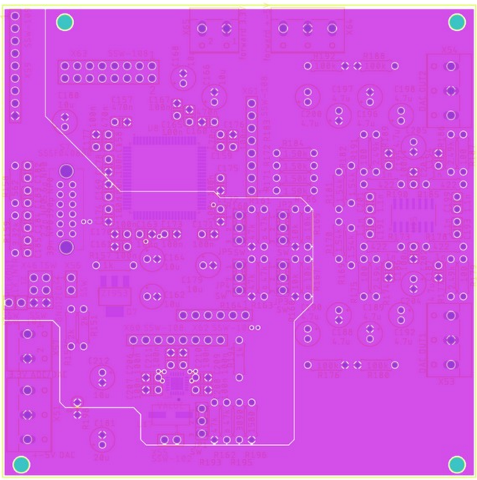

(c) Layer 3

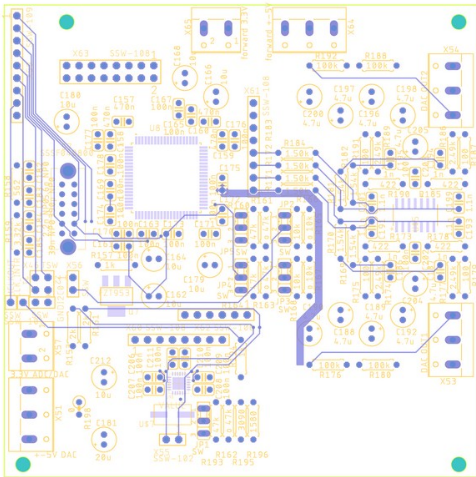

(d) Layer 4

Figure 6.10: The layout of layers 1 to 4 of the prototype DAC board.

6.4 Usage

The following text describes figure 6.11. The DAC board should be connected to the ADC board by using #1, and to P1 of the DSP adapter board shown in figure 9.6, using #2. Which signals is on which pin can be seen in figure 6.12. The board is supplied by #3, where the connectors are $+3.3V$, digital ground, $+5V$, analogue ground and $-5V$ from top to bottom. The voltage is forwarded to #6 with $+5V$, analogue ground and $-5V$ from left to right, and to #7, where $+3.3V$ are on the left-hand side. #8 provides unused DAC output pins. Each pair of pins provides one output, from right to left the

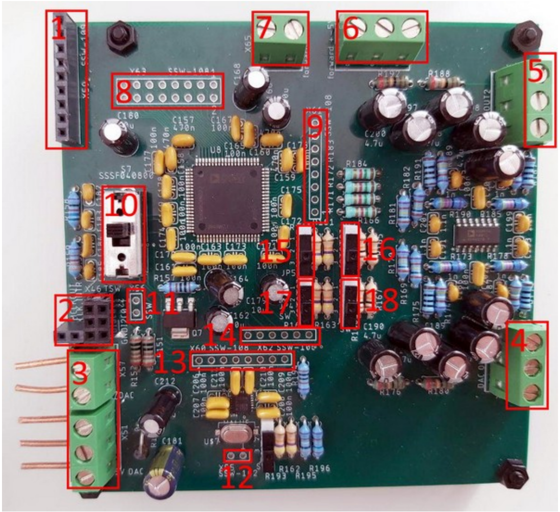

Figure 6.11: This photo of the ADC board illustrates all the switches and connectors. In the text a # symbol is used to refer to the red numbers in the picture.

outputs start at output 5 and ends at output 12. #9 provides the used outputs one and two as well as the unused outputs 3 and 4 (bottom to top). Each output has two pins. To switch between master-clock mode and slave-clock mode #10 can be used. It applies the correct filter for each mode. In slave mode the outputs 3 and 6 from the clock generator are used as BCLK and LRCLOCK. By default the switch is up, which is the master-clock mode. Whether the clock is created on the DAC or the clock generator, the used clock is forwarded to the ADC board. #11 provides additional AD reset (top) and DA reset connectors (bottom). #12 can be used for additional I2C components, as it provides connection to the I2C SDA (left) and the I2C SCL (right). #13 provides all clock outputs from 1 to 8, whether they are used or not. #14 provides all data inputs for the DAC, where the first one is on the right. In this application the first two data lines are used. #15 defines ADDR0, which is zero by default if the switch is down. The same goes for #17 and ADDR1. #16 connects to the reset pin. If the switch is down, reset is not active. It should be this way for normal operation. #18 can be used to enable the stand-alone mode. The default position (bottom) sets the pin to low.

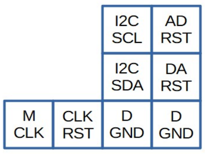

Figure 6.12: This graphic shows the pin configuration of #2.

7 Power Supply

7.1 Requirements

The previous design uses a $12V$ power supply, but the DSP requires $5V$. In order to reduce the amount of different supply voltages and therefore the number of DC/DC regulators, the supply voltage used throughout all boards should be $\pm 5V$ for most analog circuits and $3.3V$ for the digital part. This can be somewhat limiting to the gain control, for example, but as switching regulators tend to emit some kind of electromagnetic interference, in this way it is easier to keep the signals clean. Furthermore, $5V$ provide compatibility to USB voltage.

7.2 Circuit

The input voltage of $5V$ is supplied by an external power supply. The Z-diode D5 keeps this voltage at $5V$ and provides reverse polarity protection in combination with a fast fuse F1. The $1000\mu F$ capacitor C94 is supposed to decouple this supply. A LED indicates if the supply is connected and allows the capacitor to discharge when disconnected and turned off. The switch S3 disconnects both the supply and the ground, when switched off. C72 is used for decoupling after the switch and LED5 shows if the circuit is turned on. Both the $-5V$ and the $3.3V$ generation are provided by the WEBENCH®Power Designer [24] by Texas Instruments. They were selected because of the simplicity of the circuits and the package of the regulator to keep the soldering process simple. But the most important factor was, that the same regulator could be used for both voltages. Both designs should be capable of providing at least $500mA$, as the total power consumption is unknown. The LM43601 can handle up to $1A$ [36, p. 1], which should not only provide enough power for all circuits, but also allow to add more in the future. The data-sheet refers to the WEBENCH®Power Designer [24] for custom designs [36, p. 1].

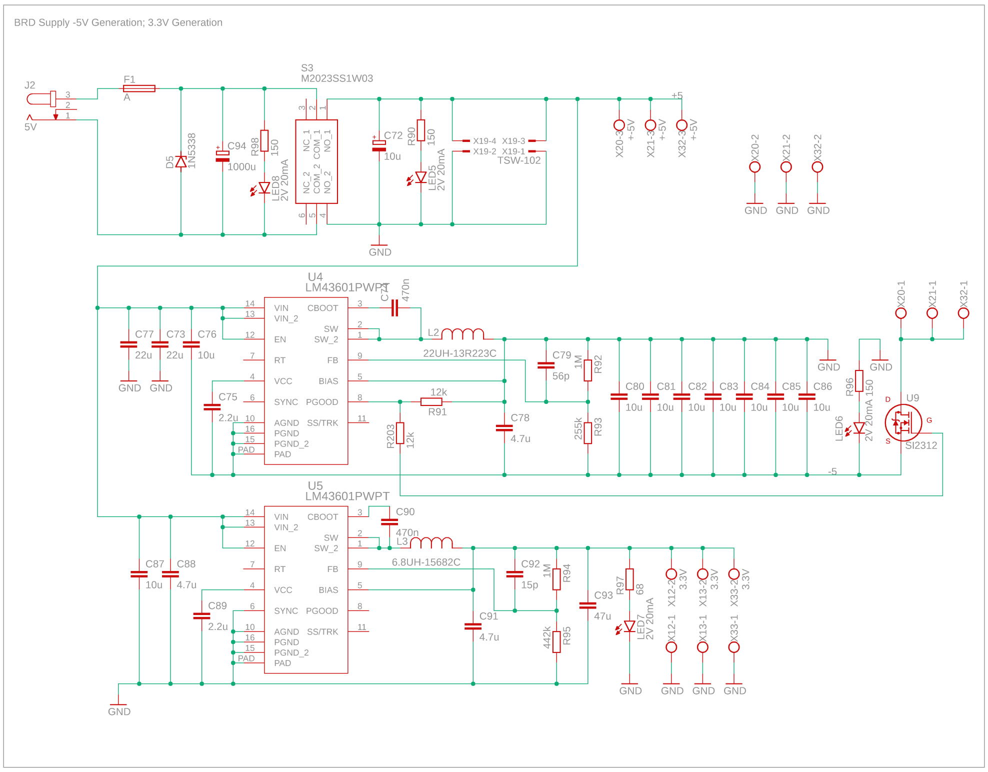

Figure 7.1: This is the circuit diagram of the supply board. The board forwards the $5V$ input voltage and provides $-5V$ as well as $3.3V$. Both voltages are generated by a LM43601.

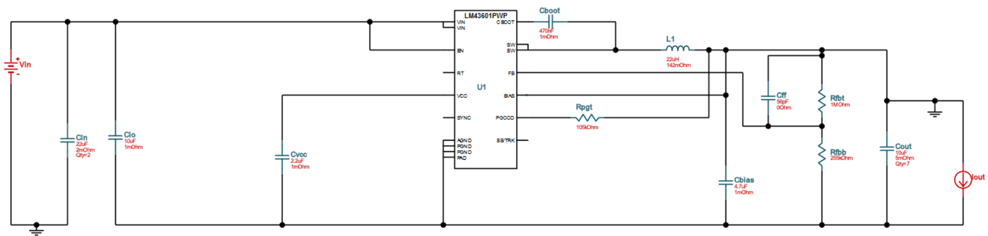

Figure 7.2: This figure shows the circuit for the $-5V$ switching regulator as provided by the WEBENCH®Power Designer [24] as. It should be noted that at Cin and Cout a quantity is given. This reduces the equivalent series resistance (ESR) and equivalent series inductance (ESL), compared to a larger single capacitor. All capacitors should be ceramic caps, when available.

Source: adapted from [24]

The design for the $-5V$ generator is available under the link: `https://webench.ti.com/appinfo/webench/scripts/SDP.cgi?ID=8015E88F60FA62A2`. As this circuit has had problems with supplying active components, that also require a positive supply, the resistor R91 on the PGOOD pin has been changed to $12k\Omega$ and R203 has been added. The MOSFET U9 only switches the output voltage to the connectors when it is ready.

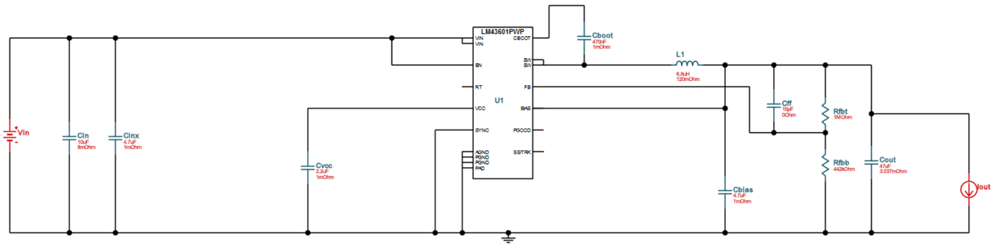

Figure 7.3: This circuit has been designed using the WEBENCH®Power Designer [24]. This application requires no alterations of the circuit.
Source: adapted from [24]

The design shown in figure 7.3, generates the voltage for the digital parts. It can be found under `https://webench.ti.com/appinfo/webench/scripts/SDP.cgi?ID=6BD271881B9EA322` and has been incorporated into the schematic unmodified.

7.3 Layout

The critical components of this layout are both LM43061 ICs. As the layout effects their performance and EMC. Bypass capacitors are placed as close as possible to the VCC and BIAS pins. The length of the FB pins should be as short as possible [36, p. 43], this is achieved by placing the voltage dividers and the corresponding capacitors as close to the pins as possible. The connection to the inductor should be short and as wide as possible. The connection to V_{IN} and V_{OUT} should, equally, be as wide as possible [36, p. 43]. The letter is easily achieved as each voltage level has its own plane, which is unique among all four-layer boards. Another unique feature of this particular layout is that the ground plane has been moved to the top plane for the $+3.3V$ generation in order to provide a good heat-sink for both ICs.

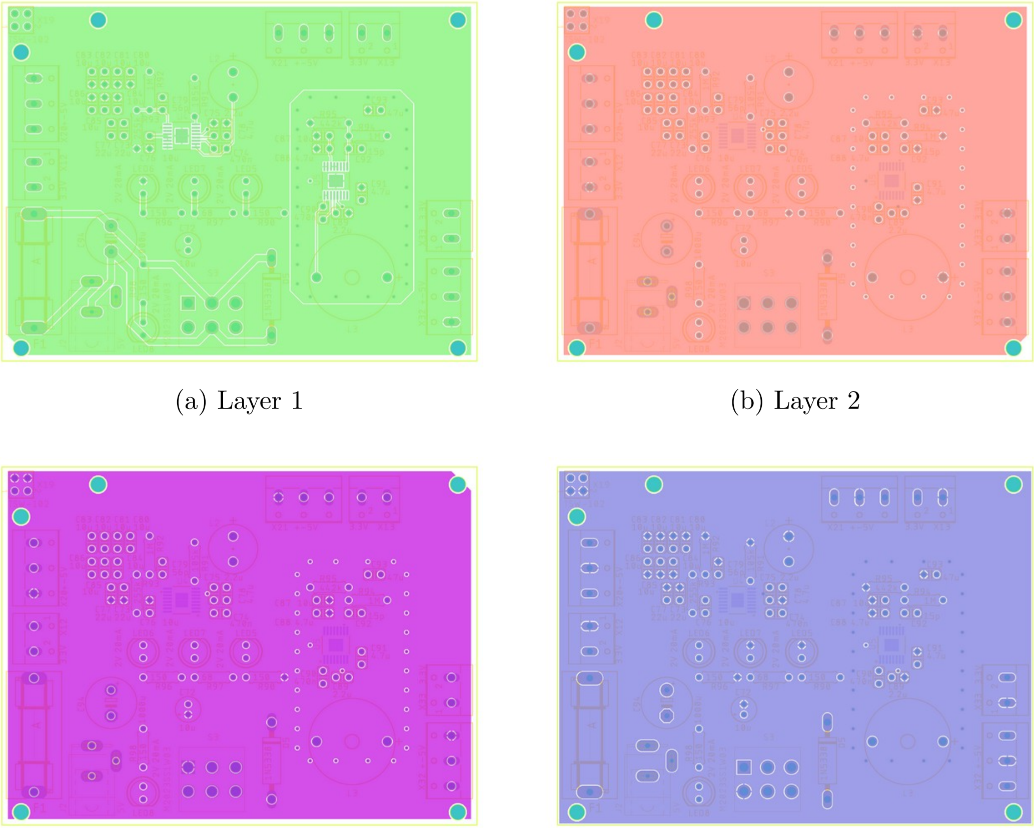

(a) Layer 1

(b) Layer 2

(c) Layer 3

(d) Layer 4

Figure 7.4: The layout of layers 1 to 4 of the prototype supply board.

7.4 Usage

This paragraph describes figure 7.5. #1 is the connector to the external $+5V$ power supply. The fast fuse #2 should protect the following circuit from too much current and from applying the wrong polarity together with a diode. #3 is the main switch, it connects both supply and ground to the circuit when switched to the right. Middle and left position disconnect the supply and the ground. The LED #4 indicates the external power supply even when the board is switched off. The LEDs #5 to #7 indicate the three voltages when the board is turned on. #5 shows that the $-5V$ generation is working and #6 that the $+3.3V$ is working. #7 indicates that the switch is on the "ON" position. The output voltage is provided on #8, #9 and #10. The connectors with three outputs always provide $-5V$, ground and $+5V$ (from left to right, seen from the outside). The two output connectors provide ground and $+3.3V$ (from left to right, seen from the outside). The top left pin of #14 must be plugged into pin 75 of P2 of the DSP adapter board shown in figure 9.6, otherwise the DSP will not be powered.

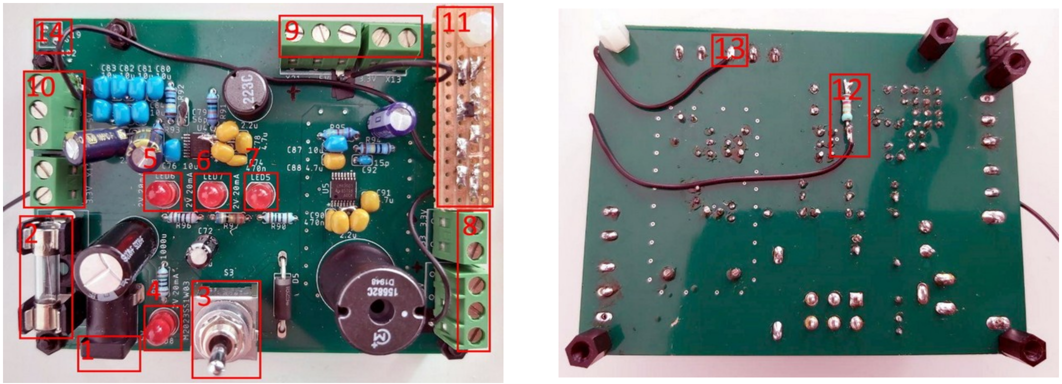

(a) Top view (b) Bottom view

Figure 7.5: These photos of the power supply board illustrate all the switches and connectors. It also shows some fixes applied to the prototype board. In the text a # symbol is used to refer to the red numbers in the picture.

As the $-5V$ has had problems with starting up when used with active components that require positive and negative supply, some corrections have been made on the prototype board. This has been accomplished by adding the MOSFET U9 before the output. It is turned on when the PGOOD pin indicates that the correct output voltage is reached. R91 needed to be reduced to $12k\Omega$, this has been achieved by putting the $12k\Omega$ resistor #12 in parallel to the existing resistor. A second $12k\Omega$ resistor is used to connect the PGOOD pin to the gate of the MOSFET. This resistor and the transistor are placed on the stripeboard #11. The $-5V$ outputs are now connected to the drain of the MOSFET. At #13 the source of the MOSFET is connected to the generated $-5V$. All three outputs can be used, as the SI2312 can sustain more drain current than the LM43061 can supply.

8 JTAG

The DSP has an implemented JTAG interface, through which it can be programmed. The interface is named after the Joint Test Action Group that has standardised it in the IEEE 1149.1 [32, p. 579]. The ICE-1000 emulator from Analog Devices provides USB connection and can be used to program the DSP through JTAG.

8.1 Requirements

The pinouts for the ICE-1000 can be seen in figure 8.1. These pins have to be connected to the corresponding pins on the DSP.

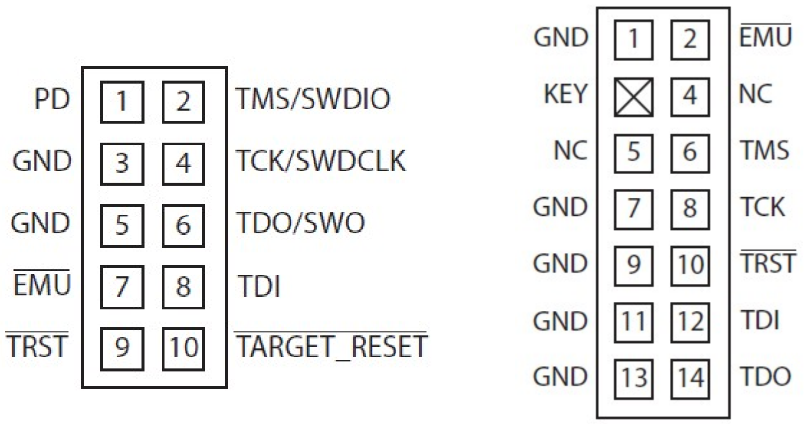

(a) 10 pin JTAG connector pinout

(b) 14 pin JTAG connector pinout

Figure 8.1: The ICE-1000 provides two connectors: a 10 pin connector with a 1.27mm grid and a 14 pin connector with a 2.54mm grid. Although the 2.54mm connector has more pins, it has actually less pins with a function.
Source: adapted from [37, p. 6] and [37, p. 7]

8.2 Circuit

The difficulty with this circuit is to correctly cross-out the wires and to connect the right pins. In figure 8.2 the wire is named after the pin it connects to on the DSP board. For the 10 pin connector, for example, PD (1) is connected to the 3.3V supply on pin 25

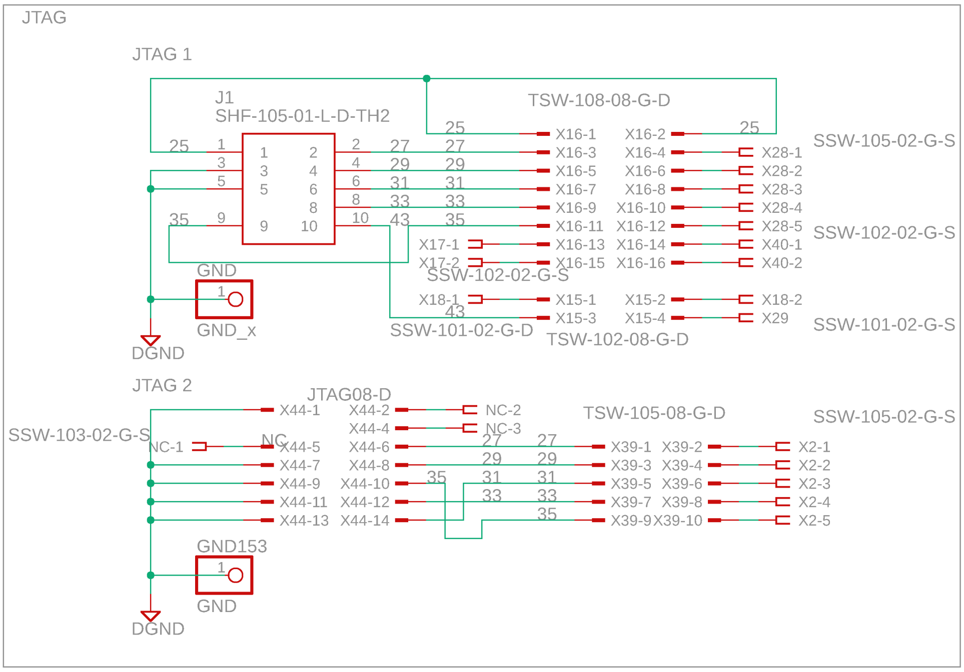

Figure 8.2: This circuit creates an interface between the ICE-1000 and the DSP.

and 26 of the DSP. The EMU pin (7) is used as KEY and therefore has to be removed. Pin 2 from J1 on the ICE-1000 connects to pin 27 on the DSP board, and so forth.

8.3 Layout

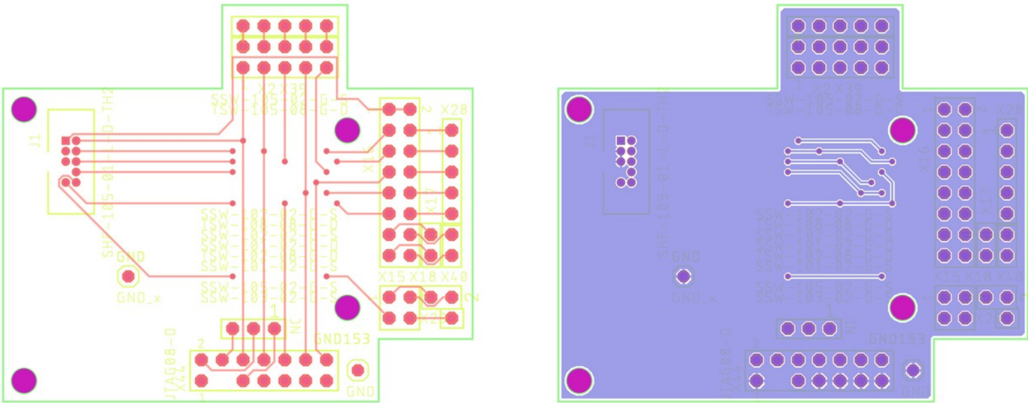

(a) Layer 1

(b) Layer 2

Figure 8.3: The layout of layers 1 and 2 of the prototype JTAG board.

The layout of the JTAG board only consists of interconnections between connectors. It requires only two layers and the free space on the second layer is filled with a ground plane. The geometry on this board is quite unique, as it should be possible to plug this board onto the DSP adapter board in two different ways. Both ways are designed to cover as few unused pins as possible. Moreover, it should be possible to plug the ICE-1000 onto this board in two ways. This explains the distances used for the bottom and the left connectors.

8.4 Usage

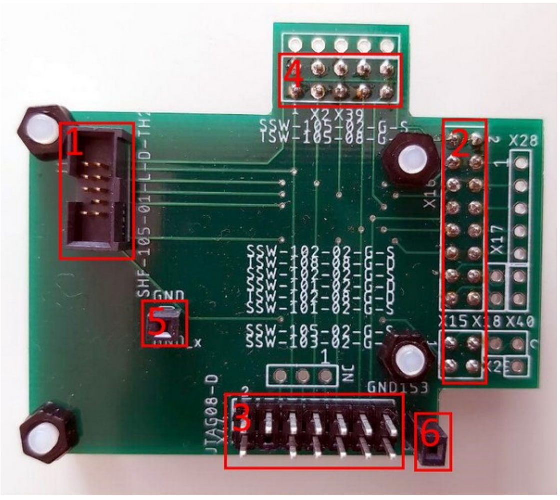

Figure 8.4: This photo of the JTAG board illustrates the connectors. In the text a # symbol is used to refer to the red numbers in the picture.

The following paragraph refers to figure 8.4. When using the 10pin connector of the ICE-1000 (#1), the top left pin of #2 should be plugged into pin 25 of P1 on the DSP adapter board (figure 9.6). #1 provides a key pin in order to avoid wrong connection. #2 also provides some sort of key pins, as there is a gap where P1 has a gap. If the 14pin connector (#3) is used, the board can be rotated ninety degrees clockwise. Consequently, the top left pin of #4 can be plugged to pin 27 of P1, which would reduce the pins covered up by this board. #3 can also be used when #2 is plugged in P1. Either way, one of the ground pins #5 or #6 must be connected to ground on P1, which would be pin 79 or pin 80. Without the grounding, the board might not work correctly.

9 DSP Adapter Board

The dspSoM 589 has three connectors, that do not allow connection to single pins. Therefore, for each new connection a new board would be required. In order to reduce costs and increase usability, an adapter board with standard pin headers was created. Single pins are easy accessible and the board is freely expandable.

9.1 Requirements

The DSP adapter board connects the dspSoM 589, as seen in figure 9.1, to $2,54mm$ socket strips with two rows.

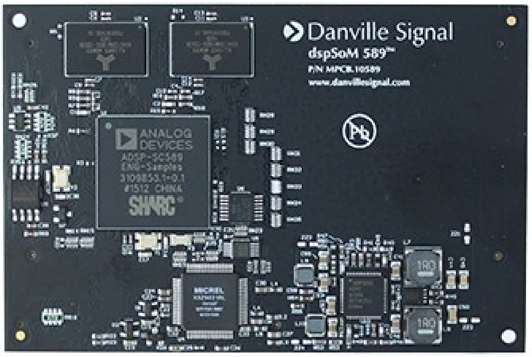

Figure 9.1: The top view of the dspSoM 589.
Source: adapted from [38]

The sockets to the connectors of the dspSoM 589 are the 5177983-3 and the 5177983-4 from TE Connectivity. The position of the connectors can only be measured and should fit to the dspSoM 589 as good as possible.

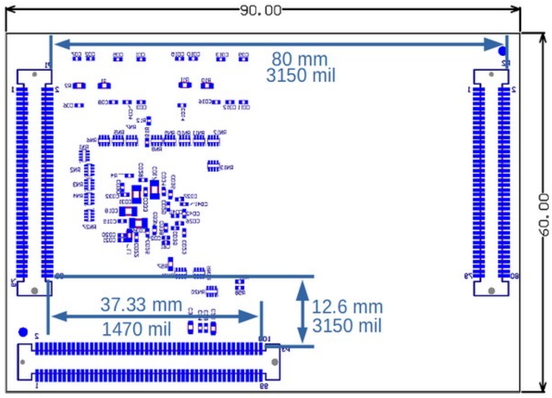

Figure 9.2: This graphic shows the estimated position of the connectors. It seems to work, although it is not perfectly aligned with the original.
Source: adapted from [39, p. 10]

9.2 Circuit

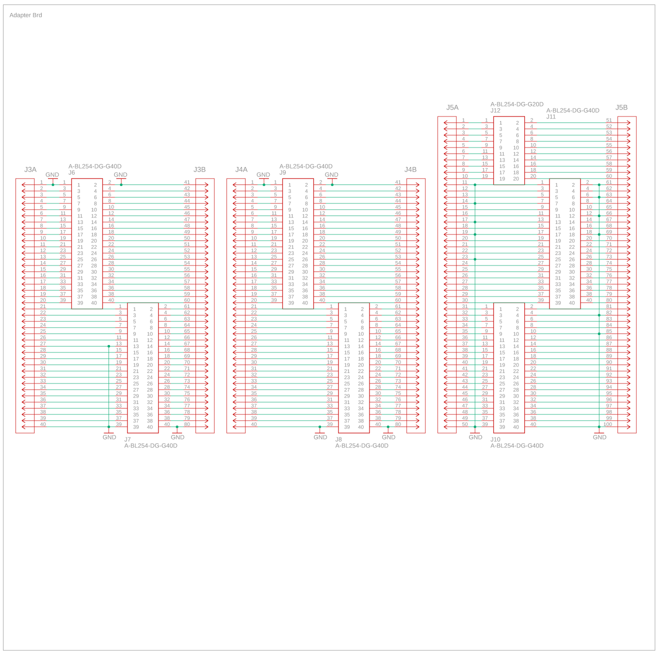

Figure 9.3: The connectors of the dspSoM 589 are wired to 2.45mm socket strips.

The pinout can be seen on pages two, six and seven in the dspSoM 589 circuit diagram [39, p. 2, 6, 7].

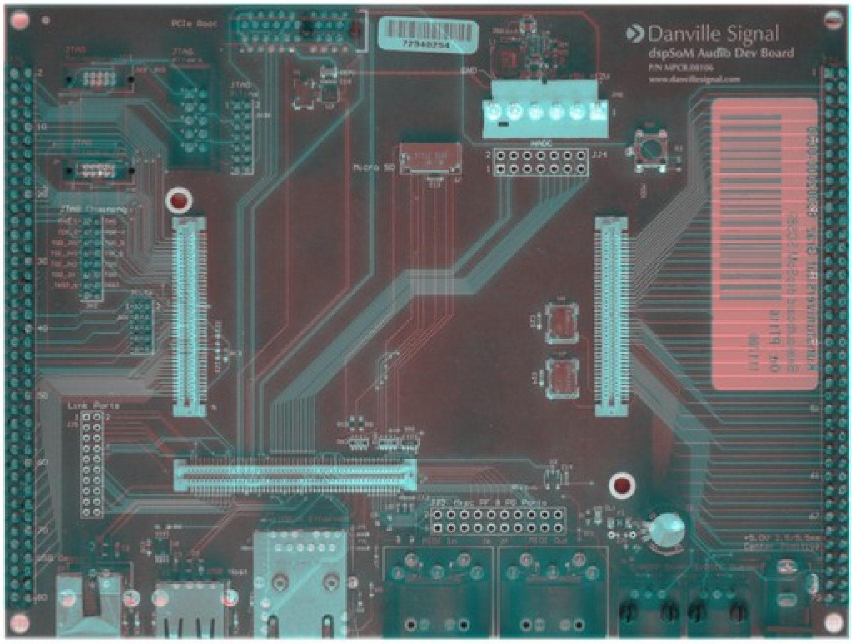

Figure 9.4: In order to analyse and reverse engineer the original carrier board of the dspSoM 589, pictures of both sides were taken, colored differently and overlayed. This is very useful for tracking wires wires to a pin, which later can be verified by measuring.

9.3 Layout

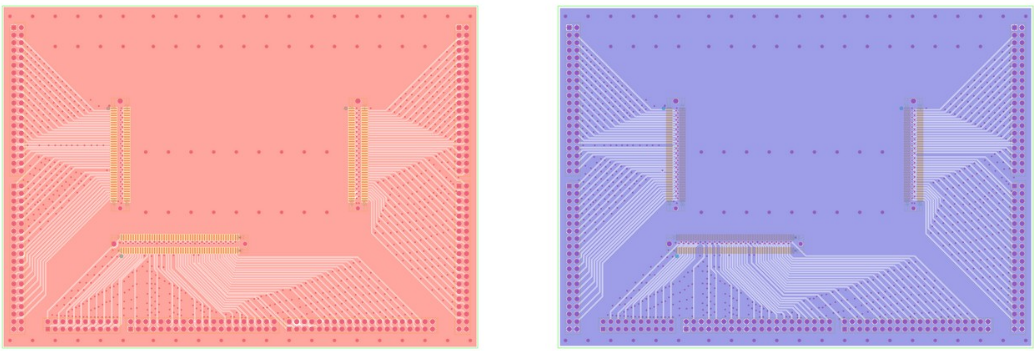

(a) Layer 1 (b) Layer 2

Figure 9.5: The layout of layers 1 and 2 of the prototype DSP adapter board.

The board is designed as a two-layer board and connects the connectors of the dspSoM 589 with more common $2,54mm$ socket strips with two rows. All in all six 40 pin socket strips and one 20 pin socket strip were used.

9.4 Usage

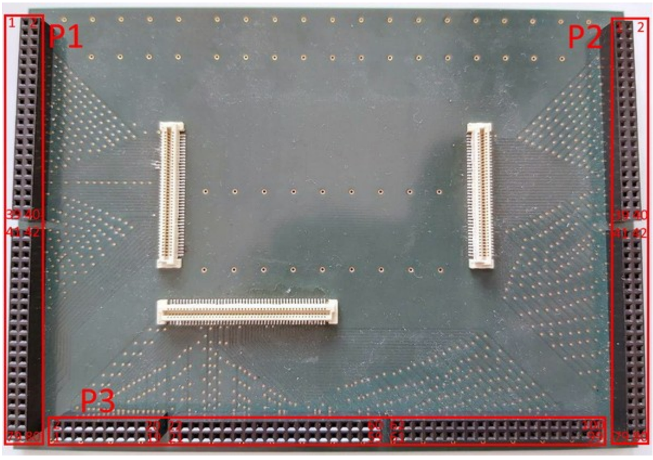

(a) adapter board

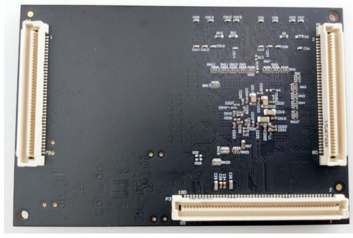

(b) dspSoM 589 bottom view

Figure 9.6: The dspSoM589 can be plugged onto the adapter board. Now its outputs P1, P2 and P3 can be used more conveniently.

As the output connectors P1, P2 and P3 now consist of multiple socket strips, some gaps are in between the connectors. This should be considered, when designing a board that connects to one of them. However, the advantage is, that it is easier to figure out the pin numbers.

For the prototype design the power supply must be plugged into pin 75 to pin 80 of P2 in order to supply the DSP. The pins 57 to 74 are used to connect to the ADC board. The top pins of the preamp connect to the pins 9 to 18 in order to ensure stability, while the bottom pins connect to the pins 41 to 54. The stereo input board is connected to the pins 1 to 6.

P1 is used for the JTAG interface board, which connects to the pins 25 to 44. Pin 17 is used to reset the preamp and must be connected to this board. Pin 21 is used for SCL of the I2C bus, while pin 23 is used for SDA. Pin 22 provides the AD reset and pin 24 provides the DA reset. All of them need to be connected to the DAC board correctly. The ground of the DAC board should be connected to pin 1 or 2, while the ground on the JTAG board must either be connected to pin 79 or pin 80. It is also important to connect pin 52 with pin 54 and pin 56 to pin 58 because in this way, the DSP will use the integrated clock [39, p. 4]. For this purpose, a stripboard circuit has been created.

10 Other Circuits

10.1 Stripboard Circuits

Some circuits are manufactured on stripboards because of their simplicity. This also helps to keep the costs low.

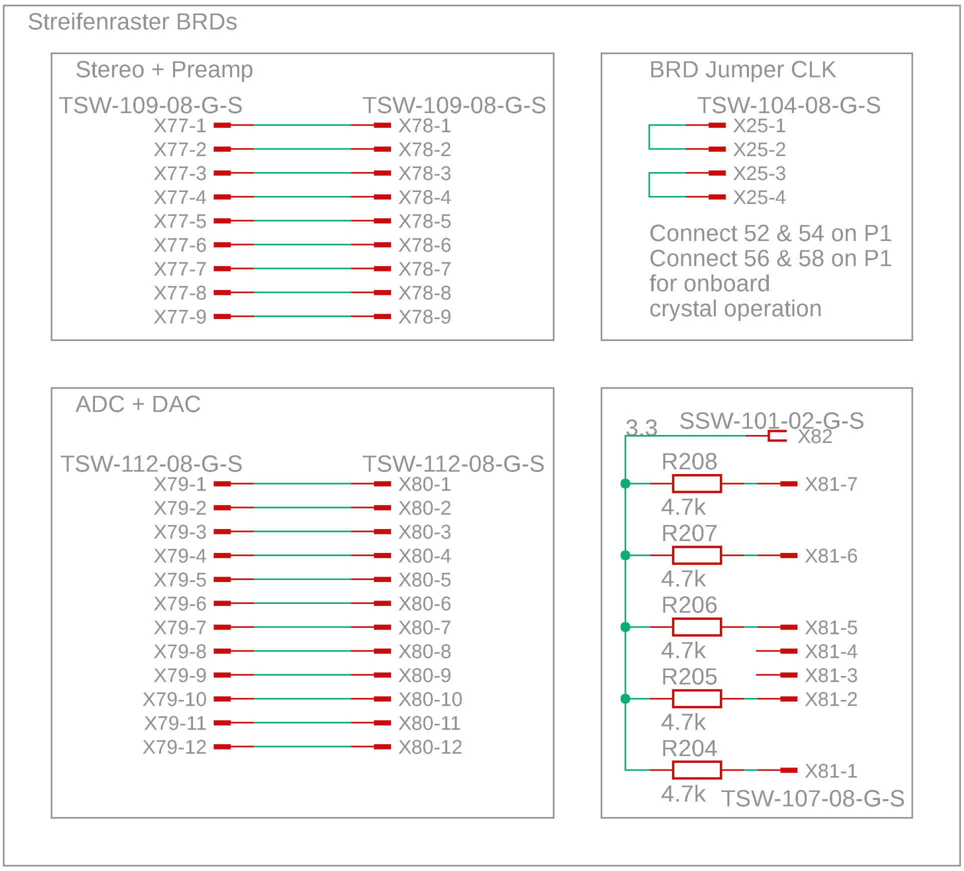

Figure 10.1: These schematics are manufactured on stripboards. They are used for interconnecting circuits, setting the DSP to use the internal clock and providing a pull-up network for the SPI-BUS.

Some boards require interconnection through $2,45mm$ terminal strips. The circuit boards of this connection adapters are depicted on (a) and (b) of figure 10.1. #1 is used to connect the ground of the preamp board to the ground of the stereo input board. #2 connects the input stereo board with the main input board and #3 connects the ADC with the DAC. Circuit #4 is a pull-up network for the SPI-BUS as this bus can be configurated to use an open-drain mode [40, p. 16]. The circuit board shown in (c) is labelled as #5 in (a) and (b). It is used for interconnecting pins 42 and 54 and pins 56 and 58 on P1 of the dspSoM 589, in order to use its internal clock [39, p. 4].

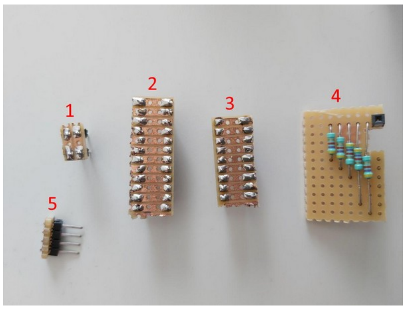

(a) top view

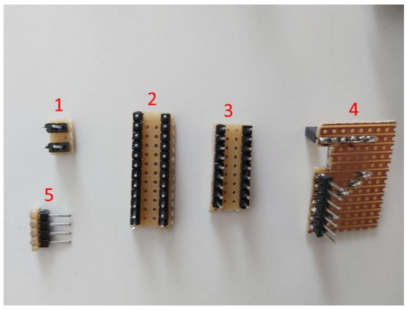

(b) bottom view

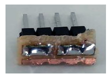

(c) CLK jumper top view

Figure 10.2

10.2 Not Manufactured Circuits

These circuits had already been designed but were not manufactured, either because of the cost, or because they were scrapped.

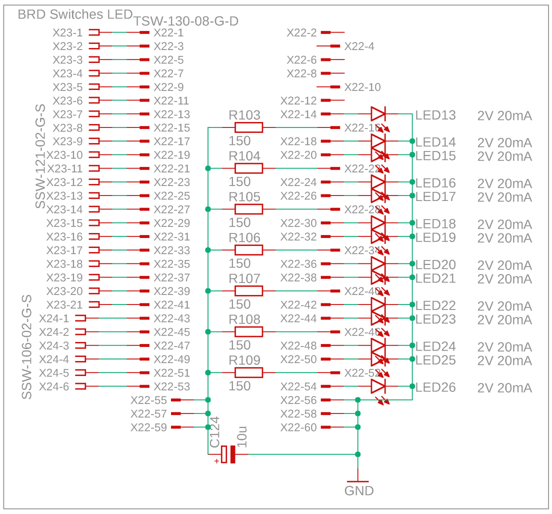

Figure 10.3: This board is compatible with the audio input board. It would indicate the position of the switches, by turning on the corresponding LED.

The LED switch indication, as seen in figure 10.3, can be used to indicate which switch of the audio input board is turned on. This would highlight possible errors from the user, although it would probably it would possible be better to use less bright LEDs.

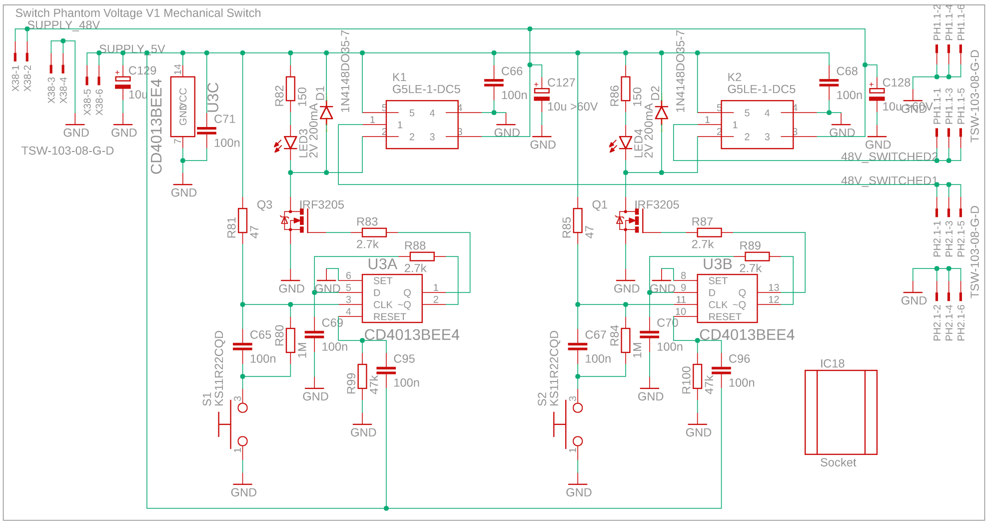

Figure 10.4: This was the first design of the phantom power switches. Instead of using touch-witches it uses push-buttons. This allows low-side switches, which are easier to design, as n-channel MOSFETs can be used. The $48V$ have to be generated on a different board.

The circuit shown in figure 10.4 was replaced by the phantom power generating and switching circuit shown in figure 3.3. However, a lot of the features from the final design were also used in the first design. As this circuit has not been tested, it may contain some errors and might not work in its current form.

11 Measurement

The first measured results of the two parallel working channels can be seen in figure 11.1.

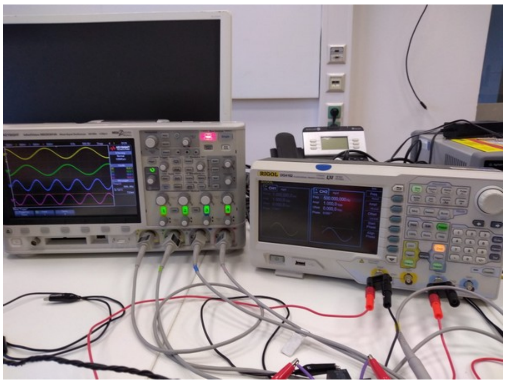

(a) measuring both channels at the same time

(b) different frequencies for each channel

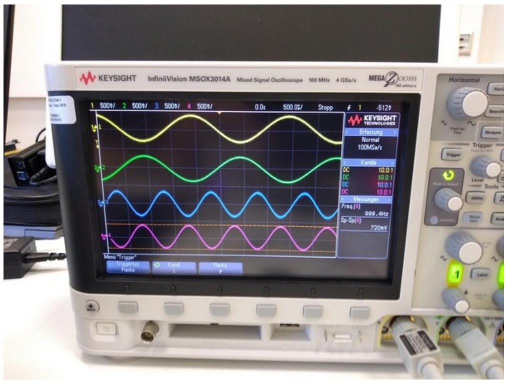

(c) differential output of both outputs

Figure 11.1: A single-ended signal with a peak-to-peak value of $1V$ is applied at each channel. The frequencies are different to display the different inputs. The un-balanced configuration for line-in is used to generate the differential signal from the single-ended input.

To analyse the quality of the circuit the *Rohde & Schwarz UPL 16* AUDIO ANAYZER is used. When directly connecting the input and output of the device, a total harmonic distortion plus noise (THD+N) value of about $-106dB$ can be measured. The signal-to-noise-and-distortion ratio (SINAD) is equal to THD+N, if the bandwidths used for both measurements equal the Nyquist bandwidth [41, p. 5]. The following calculations are based on an ideal ADC where no distortion occurs. This means that for this consideration the SNR equals the SINAD. The signal-to-noise ratio can be calculated from the effective value of the signal and the effective value of the noise.

$$SNR = 20 \cdot log_{10}\left(\frac{u_{eff,signal}}{u_{eff,noise}}\right) \tag{11.1}$$

For the quantisation noise of an N-bit ADC this means:

$$SNR = 20 \cdot log_{10}\left(\frac{RMS\ value\ of\ the\ full - scale\ input}{RMS\ value\ of\ quantisation\ noise}\right) \tag{11.2}$$

This RMS values can be calculated with the following equations:

$$RMS\ value\ of\ quantisation\ noise = \frac{q}{\sqrt{12}} \tag{11.3}$$

$$RMS\ value\ of\ the\ full - scale\ input = \frac{q \cdot 2^N}{2 \cdot \sqrt{2}} \tag{11.4}$$

where q equals the value of the LSB [42, p. 1]. Therefore, the SNR of the N-bit convert can be calculated as:

$$SNR = 20 \cdot log_{10}\left(\frac{\frac{q \cdot 2^N}{2 \cdot \sqrt{2}}}{\frac{q}{\sqrt{12}}}\right) = 20 \cdot log_{10}\left(2^N\right) + 20 \cdot log_{10}\left(\sqrt{\frac{3}{2}}\right) \tag{11.5}$$

This can be approximated with:

$$SNR = 6.02 \cdot N + 1.76dB \tag{11.6}$$

The formula seen in equation 11.6 is generally used to calculate the quantisation noise and is valid from DC to $f_s/2$ [42, p. 3].

As audio CDs usually have a resolution of 16 bit, they should have a quantisation noise of $-98.08dB$ when using equation 11.6. This is below the measured THD+N value from the audio analyser, which means that ideal 16-bit ADCs should be measurable with it. In this project a 24-bit ADC is used. The expected SNR would be $-146.24dB$. Assuming that the value for THD+N is far below this, this analyser is still used for testing.

Limited by the available equipment, it was only possible to use unbalanced input, which means only the unbalanced input configuration for line-in could be tested. The measurement was done for both channels. Because of the assumption, that the $48V$ generation for the phantom voltage would effect the signal, the first measurement has been carried out without the phantom power board.

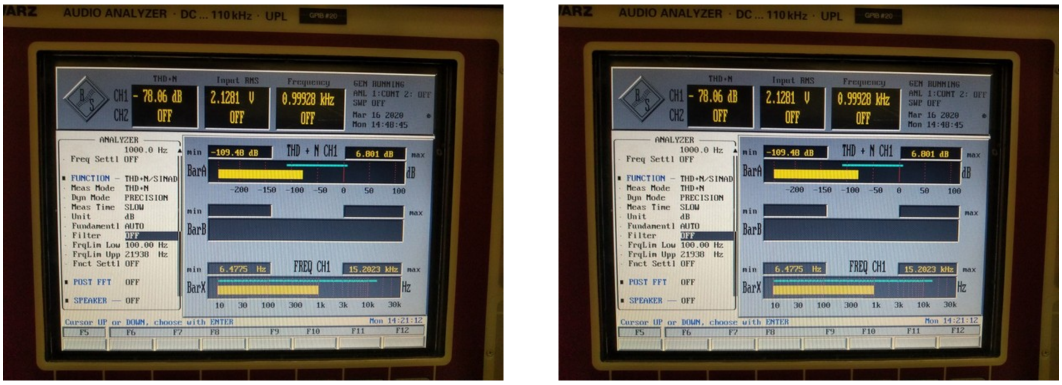

(a) channel 1　　　　(b) channel 2

Figure 11.2: The measurement for channel 1 can be seen on the left-hand side, while the measurement for channel 2 is on the right-hand side. Both measurements show a THD+N of below $-78dB$.

The numbers of the THD+N were changing rapidly for both channels because of a glitch that occurs with low frequency possibly below $20Hz$. Most certainly, this glitches have been caused by a software error. Therefore, it was assumed that the highest values showed the behaviour of the hardware. Those values were at about $-78dB$ THD+N. Afterwards, the measurement was repeated with the phantom power board added, with the expectation that the second measurement would produce worse results.

(a) channel 1　　　　(b) channel 2

Figure 11.3: Again, the measurement for channel 1 can be seen on the left-hand side and for channel 2 on the right-hand side. These measurements also show a THD+N of below $-78dB$.

Fortunately, the measured values did not change. This means the whole design can be used as planned and the coil from the $48V$ generation needs no extra shielding. It was possible to undercut the commonly requested value for THD+N of 0.03%, which equals

$-70dB$. Finally, the frequency response was examined. A bode plot was created by the audio analyser, which can be seen in figure 11.4

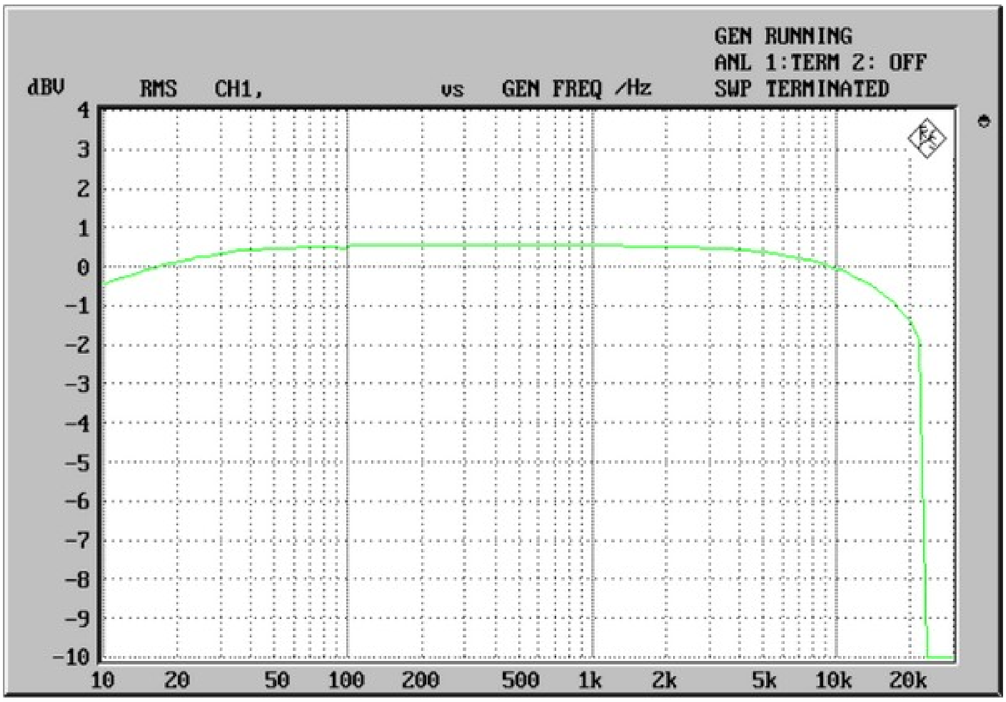

Figure 11.4: At about $50Hz$, the frequency response remains fairly constant until it slowly starts to decrease at $3kHz$. The $-3dB$ corner frequency is higher than $20kHz$.

For this measurement the amplification of the preamplifier was set to $+30dB$. Therefore, there was a slight total amplification, which can be seen in figure 11.4. Therefore, the y-axis is displayed from $+4dBV$ to $-10dBV$. The sampling frequency is set to $48kHz$, which sets the maximum output frequency to $24kHz$. This explains the quick decrease past $20kHz$. The x-axis covers the whole audio band as it ranges from $10Hz$ to $30kHz$.

12 Conclusion

The goal of this thesis was to create an affordable audio signal processor evaluation board, that can be recreated by students in order to develop their own signal processing algorithms. The costs for this project are divided into the costs for the printed circuit board (PCB), which are about 440 € for five copies, and the costs for the components, which amount to about 560 €. Therefore, the total costs for the board are about 1000 €. Usually, prototypes are rather expensive compared to the final product, so these costs could be greatly reduced. For example, ordering a single board with the same size as all the boards combined from the same distributor would cut the price by half to 220 € for five copies. If all five copies can be used, the price per PCB would be 44 €. Since the function of each circuit has been verified, this could be easily accomplished by creating a new layout.

Creating one large board would mean losing variability in terms of exchange or modification of the single modules, but offer two advantages. Firstly, the costs would further decrease because considerably less connectors would be required. As they are rather expensive, about 100 € could be saved. It would also improve the EMC, as the interconnection of the boards is especially susceptible to electromagnetic interference. The usability could further be enhanced by allowing the board to be placed on top of the DSP adapter board. This would greatly reduce the size of the combined product, and the external interconnection to P1 would not be needed.

Secondly, costs could also be reduced by replacing resistors and capacitors from a higher E-series with a combination of more common ones. The components from a higher E-series cost about four times the amount of the standard ones. This means, combining two standard resistors to create a rarer one could reduce the price by half. In this way, about 50 € could be saved. It should be noted that this could increase the board size and the effort required for soldering slightly. It is also important to know that using components from a higher E-series means less tolerance. Therefore, the $6.8k\Omega$ phantom power resistors should not be exchanged and for other resistors the correct value and matching could be checked by measuring before adding them. Assuming that five boards are manufactured, the total cost per board would amount to about 495 € or possibly less, as quantity discount, which varies from component to component, has not been taken into account. Finally, most components can only be ordered in higher quantities than are required for one board and therefore it is not necessary to order them for each board separately.

Unfortunately, the price of the processor (dpsSoM 589) and the ICE-1000 emulator required for programming are not included. At the time of writing this thesis, the ADZS-SC589-EZLITE evaluation board including the ICE-1000 emulator was available for about 600 €. As it provides a great range of functions for a good price, it is legitimate to ask why one should build his or her own board. The answer is short and simple, versatility. New functions can be easily developed, added and extended.

Even if the measuring results shown in chapter 11 are quite good, with a THD+N below 0.03%, it is still possible to improve the circuit. Most of the following suggestions apply to the layout, as for example the suggestion to create one single board, as mentioned beforehand. Firstly, some filters in the signal path could be placed closer to the input-pins of the ICs, especially on the input board they should be placed closer to the op-amps instead of the switches. It is generally a good idea to focus on the input lines, as they are more sensitive to interference. This is a lot easier with a single board compared to the modular design. Secondly, better suited inductors for phantom voltage, $+3.3V$ and $-5V$ generation could be used. Their maximum current is over-designed significantly. Furthermore, when inductors with ferrite sheathing are used, the electromagnetic emissions, and the effect on the rest of the board should be reduced. Moreover, the paths to the inductors could be made shorter and wider traces for them and the input and output could enhance the performance of the DC-DC converters. Finally, the DC blocking capacitors at the output of the preamp board should be placed after the filter because in combination with this filter, an undesired voltage divider that attenuates the signal is created. It should be placed on the ADC board instead, close to ADC input for better filtering of in-coupled interference.

In addition to all of these suggestions it should still be kept in mind that this thesis provides a well working and versatile design. It guides through the design process which enables others to recreate the board and hopefully encourages and inspires them to create their own design. Although it can be time consuming and occasionally challenging, it is an interesting and instructive task, that has granted me unexpected insights into many different areas. It has shown me the relations and connections between electronics and audio signal processing and has also strengthened them between the corresponding institutes, the Institute for Electronic Music and Acoustics (IEM) from the University of Music and Performing Arts Graz and the Institute of Electronics (IFE) from the Graz University of Technology.

Bibliography

[1] B. Victor Palos, “Analog and digital interface board for sound processing”, MASTER’S THESIS, Graz University of Technology, Graz, 2017. [Online]. Available: `https://www.analog.com/media/en/training-seminars/tutorials/MT-001.pdf`.

[2] T. Görne, *Mikrofone in Theorie und Praxis: Mit 23 Tabellen*, 9. Aufl. Aachen: Elektor-Verl., 2010, ISBN: 978-3-89576-189-8.

[3] S. Weinzierl, Ed., *Handbuch der Audiotechnik*, [Ausgabe in 2 Bänden]. Berlin and Heidelberg: Springer, 2008, ISBN: 978-3-540-34300-4.

[4] AlanM1, *File:Line levels.svg - Wikimedia Commons*, 23.01.2020. [Online]. Available: `https://commons.wikimedia.org/wiki/File:Line_levels.svg` (visited on 02/06/2020).

[5] OVE Österreichischer Verband für Elektrotechnik, *ÖVE/ÖNORM EN 61938:2013*.

[6] D. J. Dailey, *Electronics for Guitarists*, 2nd ed. 2013. New York, NY: Springer, 2013, ISBN: 978-1-4614-4086-4. DOI: `10.1007/978-1-4614-4087-1`. [Online]. Available: `http://site.ebrary.com/lib/alltitles/docDetail.action?docID=10656562`.

[7] closer.org, *Frequenztabellen Gitarre und Bass*. [Online]. Available: `https://www.cloeser.org/ext/Frequenztabellen_Gitarre_und_Bass.pdf` (visited on 02/06/2020).

[8] MACKIE., *Arcane Mysteries: Balanced Lines, Phantom Powering, Grounding, and Other Arcane Mysteries*, LOUD Technologies Inc., Ed.

[9] Bill Whitlock, *Balanced Lines in Audio Systems: Fact, Fiction, and Transformers**, J. Audio Eng. Soc., Ed., 1995.

[10] NElL A. MUNCY, *Noise Susceptibility in Analogand Digital Signal ProcessingSystems**, J. Audio Eng. Soc., Ed., 1995.

[11] Philip Giddings, *An Introduction to Electromagnetic Compatibility (EMC) and Electromagnetic Interference (EMI) for Audio System Designers**, J. Audio Eng. Soc., Ed., 1989.

[12] Bill Whitlock, *Jensen AN-003: INTERCONNECTION OF BALANCED AND UNBALANCED EQUIPMENT*, I. Jensen Transformers, Ed.

[13] Rainer Boettchers von www.justchords.com, *Thomann Online-Ratgeber Stecker & Kupplungen Kabel*, thomann.de, Ed. [Online]. Available: https://www.thomann.de/at/onlineexpert_page_kabel_stecker_kupplungen.html (visited on 02/06/2020).

[14] Sengpiel, *8 Ohm Output and 150 Ohm Input - What is that?*, UdK Berlin, Ed., 2013. [Online]. Available: http://www.sengpielaudio.com/8OhmOutputWhatIsThat.pdf.

[15] D. Self, *Small signal audio design*, Second edition. Burlington, Massachusetts and Oxfordshire, England: Focal Press, 2015, ISBN: 978-0-415-70973-6. [Online]. Available: http://site.ebrary.com/lib/alltitles/Doc?id=10941447.

[16] P. Skritek, *Handbuch der Audio-Schaltungstechnik: Berechnungsmethoden, Messverfahren, Schaltungsentwicklung, digitale Tonverarbeitung.* München: Franzis, 1988, ISBN: 3-7723-8731-4.

[17] Jörg Wuttke, *The feeble phantom*, Microphone Data Ltd., Ed., 2003. [Online]. Available: http://www.microphone-data.com/media/filestore/articles/Powering%20mics-10.pdf.

[18] Chris Woolf, *Powering Microphones*, Microphone Data Ltd., Ed. [Online]. Available: http://www.microphone-data.com/media/filestore/articles/Powering%20mics-10.pdf.

[19] THAT Corporation, Ed., *THAT Corporation Design Note 140: Input and Output Circuits for THAT Preamplifier ICs: Phantom Power, Mic-Input Pads, Line Inputs,Single-ended and Differential Outputs.* [Online]. Available: http://www.thatcorp.com/datashts/dn140.pdf.

[20] THAT Corporation, Ed., *THAT 5171: High-Performance Digital Preamplifier Controller IC.* [Online]. Available: http://www.thatcorp.com/datashts/THAT_1580_Datasheet.pdf (visited on 02/07/2020).

[21] John Ardizzoni and Jonathan Pearson, *"Rules of the Road" for High-Speed Differential ADC Drivers*, Analog Dialogue, Ed., 2009. [Online]. Available: https://www.analog.com/media/en/analog-dialogue/volume-43/number-2/articles/rules-for-high-speed-differential-adc-drivers.pdf.

[22] I. Analog Devices, *ADAU1979 (Rev. 0)*, 2013. [Online]. Available: https://www.analog.com/media/en/technical-documentation/data-sheets/ADAU1962A.pdf (visited on 02/07/2020).

[23] www.neutrik.com, Ed., *CIRCUITS - INSTRUCTION: Combined XLR Receptacle and Phone Jack*, 25.10.2009. [Online]. Available: https://www.neutrik.com/media/8030/download/combo-circuits.pdf?v=1 (visited on 02/07/2020).

[24] *Power Designer*, 2020-02-01. [Online]. Available: https://webench.ti.com/power-designer/ (visited on 03/04/2020).

[25] *Toggle Switch Number 1*, 2015-11-25. [Online]. Available: http://www.ti.com/lit/ds/symlink/cd4013b.pdf (visited on 03/04/2020).

[26] Texas Instruments, Incorporated [SCHS023, and E], *CD4013B CMOS Dual D-Type Flip-Flop datasheet (Rev. E)*. [Online]. Available: https://docs.rs-online.com/4b0c/0900766b815c249a.pdf (visited on 03/04/2020).

[27] VCC, "CTH Series: Capacitive Touch Sensor Display", [Online]. Available: https://docs.rs-online.com/ab22/0900766b8132a177.pdf (visited on 03/04/2020).

[28] Texas Instruments, Incorporated [SBOS058, and A], *OPAx134 SoundPlus^{TM} High Performance Audio Operational Amplifiers datasheet (Rev. A)*. [Online]. Available: http://www.ti.com/lit/ds/symlink/opa2134.pdf (visited on 03/11/2020).

[29] R. Elliott, *ESP - A Better Volume Control*, 19.09.2019. [Online]. Available: https://sound-au.com/project01.htm (visited on 02/18/2020).

[30] components101.com, Ed., *Different Types of IC Packages and Which One Should You Select?*, 7.02.2020. [Online]. Available: https://components101.com/articles/different-ic-package-types-and-which-one-should-you-select (visited on 02/07/2020).

[31] THAT Corporation, Ed., *THAT 1580: Low-Noise, Differential Audio Preamplifier IC*. [Online]. Available: http://www.thatcorp.com/datashts/THAT_1580_Datasheet.pdf (visited on 03/02/2020).

[32] H. Hartl, E. Krasser, W. Pribyl, P. Söser, and G. Winkler, *Elektronische Schaltungstechnik: Mit Beispielen in PSpice*, ser. ing elektrotechnik. München: Pearson Studium, 2008, ISBN: 9783827373212. [Online]. Available: http://ebookcentral.proquest.com/lib/gbv/detail.action?docID=5583745.

[33] W. Kester, Ed., *Mixed-signal and DSP design techniques*, ser. Analog Devices series. Amsterdam, Boston: Newnes, 2003, ISBN: 0750676116. [Online]. Available: http://proquest.tech.safaribooksonline.de/9780080511764.

[34] I. Analog Devices, *ADAU1962A (Rev. A)*. [Online]. Available: http://www.ti.com/lit/ds/symlink/lm43601.pdf (visited on 03/07/2020).

[35] Silicon Laboratories, Ed., *si5356a-datasheet*, 2014. (visited on 03/07/2020).

[36] Texas Instruments, Incorporated [SNVSA44, and B], *LM43601 3.5-V to 36-V, 1-A Synchronous Step-Down Voltage Converter datasheet (Rev. B)*. [Online]. Available: https://www.analog.com/media/en/dsp-documentation/evaluation-kit-manuals/ICE_emu_1000_2000_rev_manual.pdf (visited on 03/08/2020).

[37] A. Devices and Inc, *ICE-1000/ICE-2000 Emulator User's Guide, Revision 1.2, April 2015*, 2015. (visited on 03/10/2020).

[38] L. A. Clark, *Announcing the dspSoM 589 based on Analog Devices SHARC® ADSP-SC589 | dspblok | Products*, 2020-10-03. [Online]. Available: https://www.danvillesignal.com/dspblok/dspsom-589-based-on-analog-devices-sc589 (visited on 10/03/2020).

[39] I. Danville Signal Processing, *dspSoM 589*, 2016. [Online]. Available: http://www.ti.com/lit/ds/symlink/opa2134.pdf.

[40] Analog Devices, *SHARC+ Dual Core DSP with ARM Cortex-A5: ADSP-SC582/SC583/SC584/SC587/SC589/ADSP-21583/21584/21587*, 2016. [Online]. Available: `www.analog.com`.

[41] W. Kester, *MT-003:Understand SINAD, ENOB, SNR, THD, THD + N, and SFDR so You Don't Get Lost in the Noise Floor*. [Online]. Available: `https://www.analog.com/media/en/training-seminars/tutorials/MT-003.pdf` (visited on 03/16/2020).

[42] ——, *MT-001: Taking the Mystery out of the Infamous Formula,"SNR = 6.02N + 1.76dB," and Why You Should Care*. [Online]. Available: `https://www.analog.com/media/en/training-seminars/tutorials/MT-003.pdf` (visited on 03/16/2020).

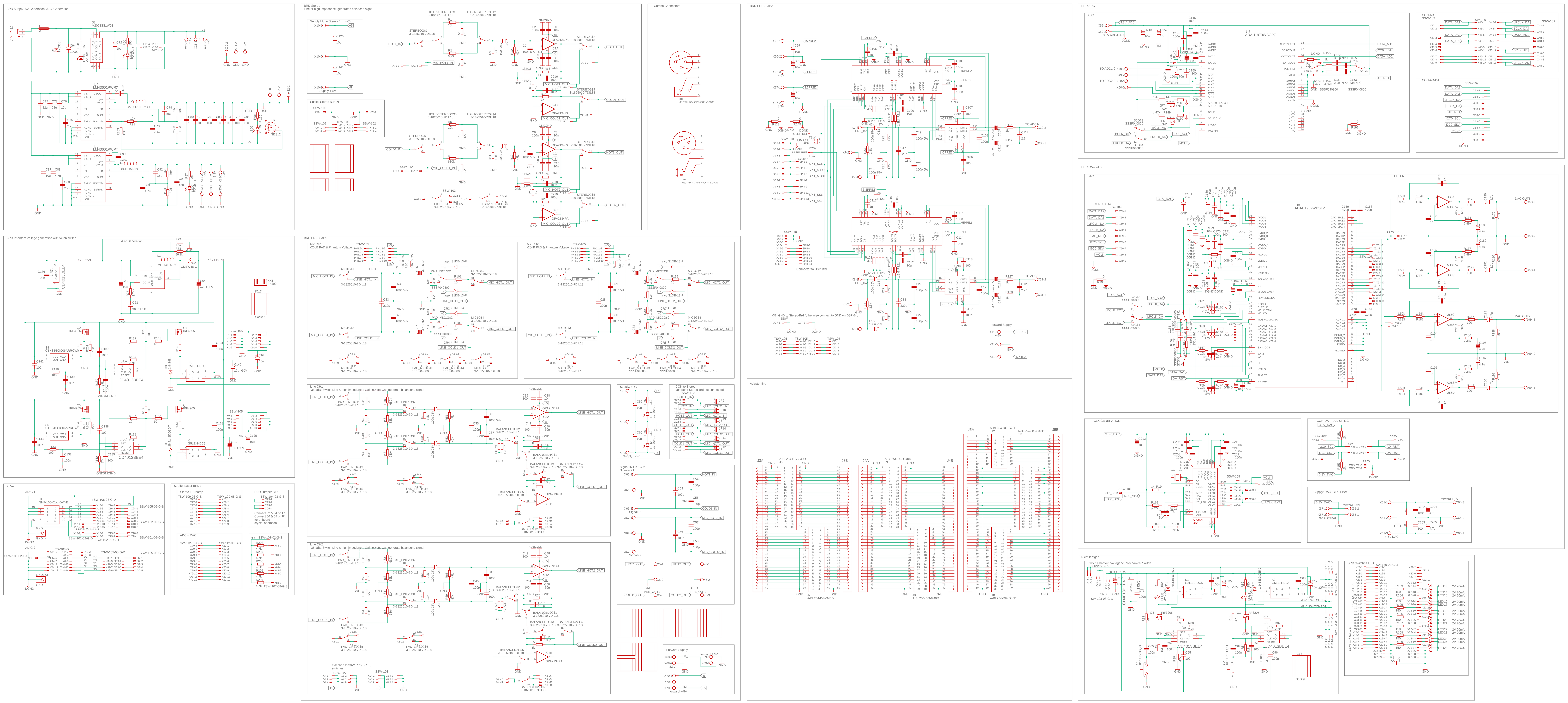

Part	Value	Device	Package	Description
BALANCED1	3-1825010-7DIL18	3-1825010-7DIL18	DIL18	PCB Slide Switch DPDT On-On 300 mA Top
BALANCED2	3-1825010-7DIL18	3-1825010-7DIL18	DIL18	PCB Slide Switch DPDT On-On 300 mA Top
C1	10n	C-EU025-024X044	C025-024X044	CAPACITOR, European symbol
C2	100n	C-EU025-024X044	C025-024X044	CAPACITOR, European symbol
C3	10n	C-EU025-024X044	C025-024X044	CAPACITOR, European symbol
C4	100n	C-EU025-024X044	C025-024X044	CAPACITOR, European symbol
C5	100u 25V	CPOL-EUE2-5	E2-5	POLARIZED CAPACITOR, European symbol
C6	100u 25V	CPOL-EUE2-5	E2-5	POLARIZED CAPACITOR, European symbol
C7	100p 5%	C-EU025-024X044	C025-024X044	CAPACITOR, European symbol
C8	10n	C-EU025-024X044	C025-024X044	CAPACITOR, European symbol
C9	100n	C-EU025-024X044	C025-024X044	CAPACITOR, European symbol
C10	10n	C-EU025-024X044	C025-024X044	CAPACITOR, European symbol
C11	100n	C-EU025-024X044	C025-024X044	CAPACITOR, European symbol
C12	100p 5%	C-EU025-024X044	C025-024X044	CAPACITOR, European symbol
C13	100u 25V	CPOL-EUE2-5	E2-5	POLARIZED CAPACITOR, European symbol
C14	100u 25V	CPOL-EUE2-5	E2-5	POLARIZED CAPACITOR, European symbol
C15	100u 25V	CPOL-EUE2-5	E2-5	POLARIZED CAPACITOR, European symbol
C16	100u 25V	CPOL-EUE2-5	E2-5	POLARIZED CAPACITOR, European symbol
C17	220p	C-EU025-024X044	C025-024X044	CAPACITOR, European symbol
C18	220p	C-EU025-024X044	C025-024X044	CAPACITOR, European symbol
C19	100p 5%	C-EU025-024X044	C025-024X044	CAPACITOR, European symbol
C20	100p 5%	C-EU025-024X044	C025-024X044	CAPACITOR, European symbol
C21	100p 5%	C-EU025-024X044	C025-024X044	CAPACITOR, European symbol
C22	100p 5%	C-EU025-024X044	C025-024X044	CAPACITOR, European symbol
C23	220p	C-EU025-024X044	C025-024X044	CAPACITOR, European symbol
C24	100p 5%	C-EU025-024X044	C025-024X044	CAPACITOR, European symbol
C25	100p 5%	C-EU025-024X044	C025-024X044	CAPACITOR, European symbol
C26	47u 63V	CPOL-EUE2-5	E2-5	POLARIZED CAPACITOR, European symbol
C27	47u 63V	CPOL-EUE2-5	E2-5	POLARIZED CAPACITOR, European symbol
C28	220p	C-EU025-024X044	C025-024X044	CAPACITOR, European symbol
C29	100p 5%	C-EU025-024X044	C025-024X044	CAPACITOR, European symbol
C30	100p 5%	C-EU025-024X044	C025-024X044	CAPACITOR, European symbol
C31	47u 63V	CPOL-EUE2-5	E2-5	POLARIZED CAPACITOR, European symbol
C32	47u 63V	CPOL-EUE2-5	E2-5	POLARIZED CAPACITOR, European symbol
C33	100u 25V	CPOL-EUE2-5	E2-5	POLARIZED CAPACITOR, European symbol
C34	100u 25V	CPOL-EUE2-5	E2-5	POLARIZED CAPACITOR, European symbol
C35	100p	C-EU025-024X044	C025-024X044	CAPACITOR, European symbol
C36	100p 5%	C-EU025-024X044	C025-024X044	CAPACITOR, European symbol
C37	100p 5%	C-EU025-024X044	C025-024X044	CAPACITOR, European symbol
C38	10n	C-EU025-024X044	C025-024X044	CAPACITOR, European symbol
C39	100n	C-EU025-024X044	C025-024X044	CAPACITOR, European symbol
C40	10n	C-EU025-024X044	C025-024X044	CAPACITOR, European symbol
C41	100n	C-EU025-024X044	C025-024X044	CAPACITOR, European symbol
C42	100p	C-EU025-024X044	C025-024X044	CAPACITOR, European symbol
C43	100u 25V	CPOL-EUE2-5	E2-5	POLARIZED CAPACITOR, European symbol
C44	100u 25V	CPOL-EUE2-5	E2-5	POLARIZED CAPACITOR, European symbol
C45	100p	C-EU025-024X044	C025-024X044	CAPACITOR, European symbol
C46	100p	C-EU025-024X044	C025-024X044	CAPACITOR, European symbol
C47	100p	C-EU025-024X044	C025-024X044	CAPACITOR, European symbol
C48	10n	C-EU025-024X044	C025-024X044	CAPACITOR, European symbol
C49	100n	C-EU025-024X044	C025-024X044	CAPACITOR, European symbol
C50	10n	C-EU025-024X044	C025-024X044	CAPACITOR, European symbol
C51	100n	C-EU025-024X044	C025-024X044	CAPACITOR, European symbol
C52	100p	C-EU025-024X044	C025-024X044	CAPACITOR, European symbol
C53	100p	C-EU025-024X044	C025-024X044	CAPACITOR, European symbol
C54	100p	C-EU025-024X044	C025-024X044	CAPACITOR, European symbol
C55	100p	C-EU025-024X044	C025-024X044	CAPACITOR, European symbol
C56	100p	C-EU025-024X044	C025-024X044	CAPACITOR, European symbol
C57	100p	C-EU025-024X044	C025-024X044	CAPACITOR, European symbol
C58	100p	C-EU025-024X044	C025-024X044	CAPACITOR, European symbol
C59	10u	CPOL-EUE2-5	E2-5	POLARIZED CAPACITOR, European symbol
C60	10u	CPOL-EUE2-5	E2-5	POLARIZED CAPACITOR, European symbol
C61	10u	CPOL-EUE2-5	E2-5	POLARIZED CAPACITOR, European symbol
C62	15u	CPOL-EUE2-5	E2-5	POLARIZED CAPACITOR, European symbol

Part	Value	Device	Package	Description
C63	680n Folie	C-EU050-050X075	C050-050X075	CAPACITOR, European symbol
C64	47u >60V	CPOL-EUE2-5	E2-5	POLARIZED CAPACITOR, European symbol
C65	100n	C-EU025-024X044	C025-024X044	CAPACITOR, European symbol
C66	100n	C-EU025-024X044	C025-024X044	CAPACITOR, European symbol
C67	100n	C-EU025-024X044	C025-024X044	CAPACITOR, European symbol
C68	100n	C-EU025-024X044	C025-024X044	CAPACITOR, European symbol
C69	100n	C-EU025-024X044	C025-024X044	CAPACITOR, European symbol
C70	100n	C-EU025-024X044	C025-024X044	CAPACITOR, European symbol
C71	100n	C-EU025-024X044	C025-024X044	CAPACITOR, European symbol
C72	10u	CPOL-EUE2-5	E2-5	POLARIZED CAPACITOR, European symbol
C73	22u	C-EU025-024X044	C025-024X044	CAPACITOR, European symbol
C74	470n	C-EU025-024X044	C025-024X044	CAPACITOR, European symbol
C75	2.2u	C-EU025-024X044	C025-024X044	CAPACITOR, European symbol
C76	10u	C-EU025-024X044	C025-024X044	CAPACITOR, European symbol
C77	22u	C-EU025-024X044	C025-024X044	CAPACITOR, European symbol
C78	4.7u	C-EU025-024X044	C025-024X044	CAPACITOR, European symbol
C79	56p	C-EU025-024X044	C025-024X044	CAPACITOR, European symbol
C80	10u	C-EU025-024X044	C025-024X044	CAPACITOR, European symbol
C81	10u	C-EU025-024X044	C025-024X044	CAPACITOR, European symbol
C82	10u	C-EU025-024X044	C025-024X044	CAPACITOR, European symbol
C83	10u	C-EU025-024X044	C025-024X044	CAPACITOR, European symbol
C84	10u	C-EU025-024X044	C025-024X044	CAPACITOR, European symbol
C85	10u	C-EU025-024X044	C025-024X044	CAPACITOR, European symbol
C86	10u	C-EU025-024X044	C025-024X044	CAPACITOR, European symbol
C87	10u	C-EU025-024X044	C025-024X044	CAPACITOR, European symbol
C88	4.7u	C-EU025-024X044	C025-024X044	CAPACITOR, European symbol
C89	2.2u	C-EU025-024X044	C025-024X044	CAPACITOR, European symbol
C90	470n	C-EU025-024X044	C025-024X044	CAPACITOR, European symbol
C91	4.7u	C-EU025-024X044	C025-024X044	CAPACITOR, European symbol
C92	15p	C-EU025-024X044	C025-024X044	CAPACITOR, European symbol
C93	47u	C-EU025-024X044	C025-024X044	CAPACITOR, European symbol
C94	1000u	CPOL-EUE5-10.5	E5-10,5	POLARIZED CAPACITOR, European symbol
C95	100n	C-EU025-024X044	C025-024X044	CAPACITOR, European symbol
C96	100n	C-EU025-024X044	C025-024X044	CAPACITOR, European symbol
C97	10u	CPOL-EUE2-5	E2-5	POLARIZED CAPACITOR, European symbol
C98	10u	CPOL-EUE2-5	E2-5	POLARIZED CAPACITOR, European symbol
C99	10u	CPOL-EUE2-5	E2-5	POLARIZED CAPACITOR, European symbol
C100	10u	C-EU025-024X044	C025-024X044	CAPACITOR, European symbol
C101	10u	C-EU025-024X044	C025-024X044	CAPACITOR, European symbol
C102	100n	C-EU025-024X044	C025-024X044	CAPACITOR, European symbol
C103	100n	C-EU025-024X044	C025-024X044	CAPACITOR, European symbol
C104	100n	C-EU025-024X044	C025-024X044	CAPACITOR, European symbol
C105	1n	C-EU025-024X044	C025-024X044	CAPACITOR, European symbol
C106	100n	C-EU025-024X044	C025-024X044	CAPACITOR, European symbol
C107	100n	C-EU025-024X044	C025-024X044	CAPACITOR, European symbol
C108	100n	C-EU025-024X044	C025-024X044	CAPACITOR, European symbol
C109	47u 25V	CPOL-EUE2-5	E2-5	POLARIZED CAPACITOR, European symbol
C110	47u 25V	CPOL-EUE2-5	E2-5	POLARIZED CAPACITOR, European symbol
C111	2.7n	C-EU025-024X044	C025-024X044	CAPACITOR, European symbol
C112	10u	C-EU025-024X044	C025-024X044	CAPACITOR, European symbol
C113	10u	C-EU025-024X044	C025-024X044	CAPACITOR, European symbol
C114	100n	C-EU025-024X044	C025-024X044	CAPACITOR, European symbol
C115	100n	C-EU025-024X044	C025-024X044	CAPACITOR, European symbol
C116	100n	C-EU025-024X044	C025-024X044	CAPACITOR, European symbol
C117	1n	C-EU025-024X044	C025-024X044	CAPACITOR, European symbol
C118	100n	C-EU025-024X044	C025-024X044	CAPACITOR, European symbol
C119	100n	C-EU025-024X044	C025-024X044	CAPACITOR, European symbol
C120	100n	C-EU025-024X044	C025-024X044	CAPACITOR, European symbol
C121	47u 25V	CPOL-EUE2-5	E2-5	POLARIZED CAPACITOR, European symbol
C122	47u 25V	CPOL-EUE2-5	E2-5	POLARIZED CAPACITOR, European symbol
C123	2.7n	C-EU025-024X044	C025-024X044	CAPACITOR, European symbol
C124	10u	CPOL-EUE2-5	E2-5	POLARIZED CAPACITOR, European symbol
C125	10u	CPOL-EUE2-5	E2-5	POLARIZED CAPACITOR, European symbol
C126	10u	CPOL-EUE2-5	E2-5	POLARIZED CAPACITOR, European symbol

Part	Value	Device	Package	Description
C127	10u >60V	CPOL-EUE2-5	E2-5	POLARIZED CAPACITOR, European symbol
C128	10u >60V	CPOL-EUE2-5	E2-5	POLARIZED CAPACITOR, European symbol
C129	10u	CPOL-EUE2-5	E2-5	POLARIZED CAPACITOR, European symbol
C130	100n	C-EU025-024X044	C025-024X044	CAPACITOR, European symbol
C131	100n	C-EU025-024X044	C025-024X044	CAPACITOR, European symbol
C132	100n	C-EU025-024X044	C025-024X044	CAPACITOR, European symbol
C133	100n	C-EU025-024X044	C025-024X044	CAPACITOR, European symbol
C134	100n	C-EU025-024X044	C025-024X044	CAPACITOR, European symbol
C135	100n	C-EU025-024X044	C025-024X044	CAPACITOR, European symbol
C136	100n	C-EU025-024X044	C025-024X044	CAPACITOR, European symbol
C137	100n	C-EU025-024X044	C025-024X044	CAPACITOR, European symbol
C138	100n	C-EU025-024X044	C025-024X044	CAPACITOR, European symbol
C139	10u >60V	CPOL-EUE2-5	E2-5	POLARIZED CAPACITOR, European symbol
C140	10u >60V	CPOL-EUE2-5	E2-5	POLARIZED CAPACITOR, European symbol
C141	10u	CPOL-EUE2-5	E2-5	POLARIZED CAPACITOR, European symbol
C142	100n	C-EU025-024X044	C025-024X044	CAPACITOR, European symbol
C143	100n	C-EU025-024X044	C025-024X044	CAPACITOR, European symbol
C144	100n	C-EU025-024X044	C025-024X044	CAPACITOR, European symbol
C145	100n	C-EU025-024X044	C025-024X044	CAPACITOR, European symbol
C146	100n	C-EU025-024X044	C025-024X044	CAPACITOR, European symbol
C147	100n	C-EU025-024X044	C025-024X044	CAPACITOR, European symbol
C148	10u	CPOL-EUE2-5	E2-5	POLARIZED CAPACITOR, European symbol
C149	100n	C-EU025-024X044	C025-024X044	CAPACITOR, European symbol
C150	100n	C-EU025-024X044	C025-024X044	CAPACITOR, European symbol
C151	10u	CPOL-EUE2-5	E2-5	POLARIZED CAPACITOR, European symbol
C152	10u	CPOL-EUE2-5	E2-5	POLARIZED CAPACITOR, European symbol
C153	33n NP0	C-EU025-024X044	C025-024X044	CAPACITOR, European symbol
C154	2.2n NP0	C-EU025-024X044	C025-024X044	CAPACITOR, European symbol
C155	4.7n NP0	C-EU025-024X044	C025-024X044	CAPACITOR, European symbol
C156	330p NP0	C-EU025-024X044	C025-024X044	CAPACITOR, European symbol
C157	470n	C-EU025-024X044	C025-024X044	CAPACITOR, European symbol
C158	470n	C-EU025-024X044	C025-024X044	CAPACITOR, European symbol
C159	470n	C-EU025-024X044	C025-024X044	CAPACITOR, European symbol
C160	470n	C-EU025-024X044	C025-024X044	CAPACITOR, European symbol
C161	100n	C-EU025-024X044	C025-024X044	CAPACITOR, European symbol
C162	10u	CPOL-EUE2-5	E2-5	POLARIZED CAPACITOR, European symbol
C163	100n	C-EU025-024X044	C025-024X044	CAPACITOR, European symbol
C164	10u	CPOL-EUE2-5	E2-5	POLARIZED CAPACITOR, European symbol
C165	100n	C-EU025-024X044	C025-024X044	CAPACITOR, European symbol
C166	10u	CPOL-EUE2-5	E2-5	POLARIZED CAPACITOR, European symbol
C167	100n	C-EU025-024X044	C025-024X044	CAPACITOR, European symbol
C168	10u	CPOL-EUE2-5	E2-5	POLARIZED CAPACITOR, European symbol
C169	100n	C-EU025-024X044	C025-024X044	CAPACITOR, European symbol
C170	100n	C-EU025-024X044	C025-024X044	CAPACITOR, European symbol
C171	100n	C-EU025-024X044	C025-024X044	CAPACITOR, European symbol
C172	100n	C-EU025-024X044	C025-024X044	CAPACITOR, European symbol
C173	100n	C-EU025-024X044	C025-024X044	CAPACITOR, European symbol
C174	100n	C-EU025-024X044	C025-024X044	CAPACITOR, European symbol
C175	100n	C-EU025-024X044	C025-024X044	CAPACITOR, European symbol
C176	100n	C-EU025-024X044	C025-024X044	CAPACITOR, European symbol
C177	100n	C-EU025-024X044	C025-024X044	CAPACITOR, European symbol
C178	100n	C-EU025-024X044	C025-024X044	CAPACITOR, European symbol
C179	10u	CPOL-EUE2-5	E2-5	POLARIZED CAPACITOR, European symbol
C180	10u	CPOL-EUE2-5	E2-5	POLARIZED CAPACITOR, European symbol
C181	20u	CPOL-EUE2-5	E2-5	POLARIZED CAPACITOR, European symbol
C182	4.7n NP0	C-EU025-024X044	C025-024X044	CAPACITOR, European symbol
C183	330p NP0	C-EU025-024X044	C025-024X044	CAPACITOR, European symbol
C184	2.2n NP0	C-EU025-024X044	C025-024X044	CAPACITOR, European symbol
C185	33n NP0	C-EU025-024X044	C025-024X044	CAPACITOR, European symbol
C186	1n	C-EU025-024X044	C025-024X044	CAPACITOR, European symbol
C187	1n	C-EU025-024X044	C025-024X044	CAPACITOR, European symbol
C188	4.7u	CPOL-EUE2-5	E2-5	POLARIZED CAPACITOR, European symbol
C189	4.7u	CPOL-EUE2-5	E2-5	POLARIZED CAPACITOR, European symbol
C190	4.7u	CPOL-EUE2-5	E2-5	POLARIZED CAPACITOR, European symbol

Part	Value	Device	Package	Description
C191	1.1n	C-EU025-024X044	C025-024X044	CAPACITOR, European symbol
C192	4.7u	CPOL-EUE2-5	E2-5	POLARIZED CAPACITOR, European symbol
C193	1.1n	C-EU025-024X044	C025-024X044	CAPACITOR, European symbol
C194	1n	C-EU025-024X044	C025-024X044	CAPACITOR, European symbol
C195	1n	C-EU025-024X044	C025-024X044	CAPACITOR, European symbol
C196	4.7u	CPOL-EUE2-5	E2-5	POLARIZED CAPACITOR, European symbol
C197	4.7u	CPOL-EUE2-5	E2-5	POLARIZED CAPACITOR, European symbol
C198	4.7u	CPOL-EUE2-5	E2-5	POLARIZED CAPACITOR, European symbol
C199	1.1n	C-EU025-024X044	C025-024X044	CAPACITOR, European symbol
C200	4.7u	CPOL-EUE2-5	E2-5	POLARIZED CAPACITOR, European symbol
C201	1.1n	C-EU025-024X044	C025-024X044	CAPACITOR, European symbol
C202	100n	C-EU025-024X044	C025-024X044	CAPACITOR, European symbol
C203	100n	C-EU025-024X044	C025-024X044	CAPACITOR, European symbol
C204	4.7u	CPOL-EUE2-5	E2-5	POLARIZED CAPACITOR, European symbol
C205	4.7u	CPOL-EUE2-5	E2-5	POLARIZED CAPACITOR, European symbol
C206	100n	C-EU025-024X044	C025-024X044	CAPACITOR, European symbol
C207	100n	C-EU025-024X044	C025-024X044	CAPACITOR, European symbol
C208	100n	C-EU025-024X044	C025-024X044	CAPACITOR, European symbol
C209	100n	C-EU025-024X044	C025-024X044	CAPACITOR, European symbol
C210	100n	C-EU025-024X044	C025-024X044	CAPACITOR, European symbol
C211	100n	C-EU025-024X044	C025-024X044	CAPACITOR, European symbol
C212	10u	CPOL-EUE2-5	E2-5	POLARIZED CAPACITOR, European symbol
C213	10u	CPOL-EUE2-5	E2-5	POLARIZED CAPACITOR, European symbol
C214	100p	C-EU025-024X044	C025-024X044	CAPACITOR, European symbol
C215	100p	C-EU025-024X044	C025-024X044	CAPACITOR, European symbol
C216	100p	C-EU025-024X044	C025-024X044	CAPACITOR, European symbol
C217	100p	C-EU025-024X044	C025-024X044	CAPACITOR, European symbol
C218	100p	C-EU025-024X044	C025-024X044	CAPACITOR, European symbol
C219	100p	C-EU025-024X044	C025-024X044	CAPACITOR, European symbol
CH1	NEUTRIK_NCJ5FI-V-0	NEUTRIK_NCJ5FI-V-0	NEUTRIK_NCJ5FI-V-0	Neutrik Combo Series NCJ5FI-V-0
CH2	NEUTRIK_NCJ5FI-V-0	NEUTRIK_NCJ5FI-V-0	NEUTRIK_NCJ5FI-V-0	Neutrik Combo Series NCJ5FI-V-0
CLK_INTR	SSW-101	SSW-101-02-G-S	SSW-101-02-G-S	THROUGH-HOLE .025 SQ POST SOCKET"
CR1	S1DB-13-F	S1DB-13-F	SMB	
CR2	S1DB-13-F	S1DB-13-F	SMB	
CR3	S1DB-13-F	S1DB-13-F	SMB	
CR4	S1DB-13-F	S1DB-13-F	SMB	
CR5	S1DB-13-F	S1DB-13-F	SMB	
CR6	S1DB-13-F	S1DB-13-F	SMB	
CR7	S1DB-13-F	S1DB-13-F	SMB	
CR8	S1DB-13-F	S1DB-13-F	SMB	
D1	1N4148DO35-7	1N4148DO35-7	DO35-7	DIODE
D2	1N4148DO35-7	1N4148DO35-7	DO35-7	DIODE
D3	1N4148	1N4148DO35-7	DO35-7	DIODE
D4	1N4148DO35-7	1N4148DO35-7	DO35-7	DIODE
D5	1N5338	1N5333	C1702-15	Z DIODE
F1	A	SH22,5A	SH22,5A	FUSE HOLDER grid 22,5mm
GND	GND_x	PINHD-1X1	1X01	PIN HEADER
GND153	GND	PINHD-1X1	1X01	PIN HEADER
GNDI2C0	SSW	SSW-102-02-G-S	SSW-102-02-G-S	THROUGH-HOLE .025 SQ POST SOCKET"
HIGHZ-STEREO	3-1825010-7DIL18	3-1825010-7DIL18	DIL18	PCB Slide Switch DPDT On-On 300 mA Top
IC1	OPA2134PA	OPA2134PA	DIL08	Dual Operational Amplifier
IC2	OPA2134PA	OPA2134PA	DIL08	Dual Operational Amplifier
IC3	OPA2134PA	OPA2134PA	DIL08	Dual Operational Amplifier
IC4	OPA2134PA	OPA2134PA	DIL08	Dual Operational Amplifier
IC5	Socket	SOCKET-DIL8S	SOCKET-08	Dual In Line Socket
IC6	Socket	SOCKET-DIL8S	SOCKET-08	Dual In Line Socket
IC7	Socket	SOCKET-DIL8S	SOCKET-08	Dual In Line Socket
IC8	Socket	SOCKET-DIL8S	SOCKET-08	Dual In Line Socket
IC9	Socket	SOCKET-DIL18S	SOCKET-18	Dual In Line Socket
IC10	Socket	SOCKET-DIL18S	SOCKET-18	Dual In Line Socket
IC11	Socket	SOCKET-DIL18S	SOCKET-18	Dual In Line Socket
IC12	Socket	SOCKET-DIL18S	SOCKET-18	Dual In Line Socket
IC13	Socket	SOCKET-DIL18S	SOCKET-18	Dual In Line Socket
IC14	Socket	SOCKET-DIL18S	SOCKET-18	Dual In Line Socket

Part	Value	Device	Package	Description
IC15	Socket	SOCKET-DIL18S	SOCKET-18	Dual In Line Socket
IC16	Socket	SOCKET-DIL18S	SOCKET-18	Dual In Line Socket
IC17	Socket	SOCKET-DIL14S	SOCKET-14	Dual In Line / Socket
IC18	Socket	SOCKET-DIL14S	SOCKET-14	Dual In Line / Socket
J1	SHF-105-01-L-D-TH2	SHF-105-01-L-D-TH2	SHDR10W40P127_2X5	SHF-105-01-L-D-TH, 1.27MM, 10WAY
J2	5V	JACK-PLUG1	SPC4078	DC POWER JACK
J3	5177983-3	5177983-3	CONN_5177983-3	
J4	5177983-3	5177983-3	CONN_5177983-3	
J5	5177983-4	5177983-4	CONN_5177983-4	
J6	A-BL254-DG-G40D	A-BL254-DG-G40D	SHDR40W87P254_2X20	female Socket Strip 2.54mm 40Way 2Row
J7	A-BL254-DG-G40D	A-BL254-DG-G40D	SHDR40W87P254_2X20	female Socket Strip 2.54mm 40Way 2Row
J8	A-BL254-DG-G40D	A-BL254-DG-G40D	SHDR40W87P254_2X20	female Socket Strip 2.54mm 40Way 2Row
J9	A-BL254-DG-G40D	A-BL254-DG-G40D	SHDR40W87P254_2X20	female Socket Strip 2.54mm 40Way 2Row
J10	A-BL254-DG-G40D	A-BL254-DG-G40D	SHDR40W87P254_2X20	female Socket Strip 2.54mm 40Way 2Row
J11	A-BL254-DG-G40D	A-BL254-DG-G40D	SHDR40W87P254_2X20	female Socket Strip 2.54mm 40Way 2Row
J12	A-BL254-DG-G20D	A-BL254-DG-G20D	SHDR20W82P254_2X10	2.54mm Pitch 20 Way 2 Row
J13	JUMPER	JUMPER	JUMP	JUMPER header
J14	JUMPER	JUMPER	JUMP	JUMPER header
J15	JUMPER	JUMPER	JUMP	JUMPER header
J16	JUMPER	JUMPER	JUMP	JUMPER header
J17	JUMPER	JUMPER	JUMP	JUMPER header
J18	JUMPER	JUMPER	JUMP	JUMPER header
J19	JUMPER	JUMPER	JUMP	JUMPER header
J20	JUMPER	JUMPER	JUMP	JUMPER header
JP1	SW	JP2E	JP2	JUMPER
JP2	SW	JP2E	JP2	JUMPER
JP3	SW	JP2E	JP2	JUMPER
JP4	SW	JP2E	JP2	JUMPER
JP5	SW	JP2E	JP2	JUMPER
JP6	SW	JP2E	JP2	JUMPER
JP7	SW	JP2E	JP2	JUMPER
JP8	JUMPER	JP1E	JP1	JUMPER
JP9	JP	JP1E	JP1	JUMPER
JP10	JP	JP1E	JP1	JUMPER
JP11	JP	JP1E	JP1	JUMPER
JP12	JP	JP1E	JP1	JUMPER
JP13	JP	JP1E	JP1	JUMPER
JP14	JP	JP1E	JP1	JUMPER
K1	G5LE-1-DC5	G5LE-1-DC5	G5LE-1	SPDT Non-Latching Relay, 8 A, 5V dc
K2	G5LE-1-DC5	G5LE-1-DC5	G5LE-1	SPDT Non-Latching Relay, 8 A, 5V dc
K3	G5LE-1-DC5	G5LE-1-DC5	G5LE-1	SPDT Non-Latching Relay, 8 A, 5V dc
K4	G5LE-1-DC5	G5LE-1-DC5	G5LE-1	SPDT Non-Latching Relay, 8 A, 5V dc
KK1	FK209	FK209	FK209	HEATSINK
L1	1mH-1410516C	1mH-1410516C	1410516C	Murata Induktivität, 1 mH, 1.6A dc
L2	22uH-13R223C	22uH-13R223C	1300R	Murata Induktivität, 22 uH, 2A dc
L3	6.8uH-15682C	6.8uH-15682C	15682C	Murata Induktivität, 6,8uH, 10.2A dc
LED1	2V 20mA	LED5MM	LED5MM	LED
LED2	2V 20mA	LED5MM	LED5MM	LED
LED3	2V 200mA	LED5MM	LED5MM	LED
LED4	2V 200mA	LED5MM	LED5MM	LED
LED5	2V 20mA	LED5MM	LED5MM	LED
LED6	2V 20mA	LED5MM	LED5MM	LED
LED7	2V 20mA	LED5MM	LED5MM	LED
LED8	2V 20mA	LED5MM	LED5MM	LED
LED13	2V 20mA	LED5MM	LED5MM	LED
LED14	2V 20mA	LED5MM	LED5MM	LED
LED15	2V 20mA	LED5MM	LED5MM	LED
LED16	2V 20mA	LED5MM	LED5MM	LED
LED17	2V 20mA	LED5MM	LED5MM	LED
LED18	2V 20mA	LED5MM	LED5MM	LED
LED19	2V 20mA	LED5MM	LED5MM	LED
LED20	2V 20mA	LED5MM	LED5MM	LED
LED21	2V 20mA	LED5MM	LED5MM	LED
LED22	2V 20mA	LED5MM	LED5MM	LED

Part	Value	Device	Package	Description
LED23	2V 20mA	LED5MM	LED5MM	LED
LED24	2V 20mA	LED5MM	LED5MM	LED
LED25	2V 20mA	LED5MM	LED5MM	LED
LED26	2V 20mA	LED5MM	LED5MM	LED
MCLKOUT	SSW	SSW-101-02-G-S	SSW-101-02-G-S	THROUGH-HOLE .025 SQ POST SOCKET"
MIC1	3-1825010-7DIL18	3-1825010-7DIL18	DIL18	PCB Slide Switch DPDT On-On 300 mA Top
MIC2	3-1825010-7DIL18	3-1825010-7DIL18	DIL18	PCB Slide Switch DPDT On-On 300 mA Top
NC	SSW-103-02-G-S	SSW-103-02-G-S	SSW-103-02-G-S	THROUGH-HOLE .025 SQ POST SOCKET"
PAD_LINE1	3-1825010-7DIL18	3-1825010-7DIL18	DIL18	PCB Slide Switch DPDT On-On 300 mA Top
PAD_LINE2	3-1825010-7DIL18	3-1825010-7DIL18	DIL18	PCB Slide Switch DPDT On-On 300 mA Top
PAD_MIC1	SSSF040800	SSSF040800	SSSF040800	Slide Switch 4PDT Maintained 100 mA
PAD_MIC2	SSSF040800	SSSF040800	SSSF040800	Slide Switch 4PDT Maintained 100 mA
PH1.1	TSW-103-08-G-D	TSW-103-08-G-D	TSW-103-XX-G-D	THROUGH-HOLE .025 SQ POST HEADER"
PH1.2	TSW-105	TSW-105-08-G-D	TSW-105-XX-G-D	THROUGH-HOLE .025 SQ POST HEADER"
PH2.1	TSW-103-08-G-D	TSW-103-08-G-D	TSW-103-XX-G-D	THROUGH-HOLE .025 SQ POST HEADER"
PH2.2	TSW-105	TSW-105-08-G-D	TSW-105-XX-G-D	THROUGH-HOLE .025 SQ POST HEADER"
Q1	IRF3205	IRF3205	TO220BV	HEXFET Power MOSFET
Q2	IRF4905	IRF4905	TO220BV	P-Channel HEXFETÂ® Power MOSFET
Q3	IRF3205	IRF3205	TO220BV	HEXFET Power MOSFET
Q4	IRF4905	IRF4905	TO220BV	P-Channel HEXFETÂ® Power MOSFET
Q5	IRF4905	IRF4905	TO220BV	P-Channel HEXFETÂ® Power MOSFET
Q6	IRF4905	IRF4905	TO220BV	P-Channel HEXFETÂ® Power MOSFET
Q7	FZT953	FZT753SMD	SOT223	PNP Transistor
R1	10k	R-EU_0207/7	0207/7	RESISTOR, European symbol
R2	127	R-EU_0207/7	0207/7	RESISTOR, European symbol
R3	680k	R-EU_0207/7	0207/7	RESISTOR, European symbol
R4	82k	R-EU_0207/7	0207/7	RESISTOR, European symbol
R5	10k	R-EU_0207/7	0207/7	RESISTOR, European symbol
R6	127	R-EU_0207/7	0207/7	RESISTOR, European symbol
R7	680k	R-EU_0207/7	0207/7	RESISTOR, European symbol
R8	82k	R-EU_0207/7	0207/7	RESISTOR, European symbol
R9	12k	R-EU_0207/7	0207/7	RESISTOR, European symbol
R10	47k	R-EU_0207/7	0207/7	RESISTOR, European symbol
R11	12k	R-EU_0207/7	0207/7	RESISTOR, European symbol
R12	47k	R-EU_0207/7	0207/7	RESISTOR, European symbol
R13	1k	R-EU_0207/7	0207/7	RESISTOR, European symbol
R14	1k	R-EU_0207/7	0207/7	RESISTOR, European symbol
R15	1k	R-EU_0207/7	0207/7	RESISTOR, European symbol
R16	1k	R-EU_0207/7	0207/7	RESISTOR, European symbol
R17	1k	R-EU_0207/7	0207/7	RESISTOR, European symbol
R18	1k	R-EU_0207/7	0207/7	RESISTOR, European symbol
R19	1k	R-EU_0207/7	0207/7	RESISTOR, European symbol
R20	1k	R-EU_0207/7	0207/7	RESISTOR, European symbol
R21	1k	R-EU_0207/7	0207/7	RESISTOR, European symbol
R22	1k	R-EU_0207/7	0207/7	RESISTOR, European symbol
R23	3.3k	R-EU_0207/7	0207/7	RESISTOR, European symbol
R24	3.3k	R-EU_0207/7	0207/7	RESISTOR, European symbol
R25	1.2k	R-EU_0207/7	0207/7	RESISTOR, European symbol
R26	1.2k	R-EU_0207/7	0207/7	RESISTOR, European symbol
R27	1.2k	R-EU_0207/7	0207/7	RESISTOR, European symbol
R28	1.2k	R-EU_0207/7	0207/7	RESISTOR, European symbol
R29	6.8k 0.5W	R-EU_0207/7	0207/7	RESISTOR, European symbol
R30	6.8k 0.5W	R-EU_0207/7	0207/7	RESISTOR, European symbol
R31	3.9k	R-EU_0207/7	0207/7	RESISTOR, European symbol
R32	1.2k	R-EU_0207/7	0207/7	RESISTOR, European symbol
R33	1.2k	R-EU_0207/7	0207/7	RESISTOR, European symbol
R34	3.9k	R-EU_0207/7	0207/7	RESISTOR, European symbol
R35	6.8k 0.5W	R-EU_0207/7	0207/7	RESISTOR, European symbol
R36	6.8k 0.5W	R-EU_0207/7	0207/7	RESISTOR, European symbol
R37	3.9k	R-EU_0207/7	0207/7	RESISTOR, European symbol
R38	1.2k	R-EU_0207/7	0207/7	RESISTOR, European symbol
R39	1.2k	R-EU_0207/7	0207/7	RESISTOR, European symbol
R40	3.9k	R-EU_0207/7	0207/7	RESISTOR, European symbol
R41	10k	R-EU_0207/7	0207/7	RESISTOR, European symbol

Part	Value	Device	Package	Description
R42	127	R-EU_0207/7	0207/7	RESISTOR, European symbol
R43	127	R-EU_0207/7	0207/7	RESISTOR, European symbol
R44	10k	R-EU_0207/7	0207/7	RESISTOR, European symbol
R45	680k	R-EU_0207/7	0207/7	RESISTOR, European symbol
R46	82k	R-EU_0207/7	0207/7	RESISTOR, European symbol
R47	82k	R-EU_0207/7	0207/7	RESISTOR, European symbol
R48	680k	R-EU_0207/7	0207/7	RESISTOR, European symbol
R49	12k	R-EU_0207/7	0207/7	RESISTOR, European symbol
R50	12k	R-EU_0207/7	0207/7	RESISTOR, European symbol
R51	47k	R-EU_0207/7	0207/7	RESISTOR, European symbol
R52	47k	R-EU_0207/7	0207/7	RESISTOR, European symbol
R53	1k	R-EU_0207/7	0207/7	RESISTOR, European symbol
R54	1k	R-EU_0207/7	0207/7	RESISTOR, European symbol
R55	1k	R-EU_0207/7	0207/7	RESISTOR, European symbol
R56	1k	R-EU_0207/7	0207/7	RESISTOR, European symbol
R57	1k	R-EU_0207/7	0207/7	RESISTOR, European symbol
R58	10k	R-EU_0207/7	0207/7	RESISTOR, European symbol
R59	127	R-EU_0207/7	0207/7	RESISTOR, European symbol
R60	127	R-EU_0207/7	0207/7	RESISTOR, European symbol
R61	10k	R-EU_0207/7	0207/7	RESISTOR, European symbol
R62	680k	R-EU_0207/7	0207/7	RESISTOR, European symbol
R63	82k	R-EU_0207/7	0207/7	RESISTOR, European symbol
R64	82k	R-EU_0207/7	0207/7	RESISTOR, European symbol
R65	680k	R-EU_0207/7	0207/7	RESISTOR, European symbol
R66	12k	R-EU_0207/7	0207/7	RESISTOR, European symbol
R67	12k	R-EU_0207/7	0207/7	RESISTOR, European symbol
R68	47k	R-EU_0207/7	0207/7	RESISTOR, European symbol
R69	47k	R-EU_0207/7	0207/7	RESISTOR, European symbol
R70	1k	R-EU_0207/7	0207/7	RESISTOR, European symbol
R71	1k	R-EU_0207/7	0207/7	RESISTOR, European symbol
R72	1k	R-EU_0207/7	0207/7	RESISTOR, European symbol
R73	1k	R-EU_0207/7	0207/7	RESISTOR, European symbol
R74	1k	R-EU_0207/7	0207/7	RESISTOR, European symbol
R75	150	R-EU_0207/7	0207/7	RESISTOR, European symbol
R76	150	R-EU_0207/7	0207/7	RESISTOR, European symbol
R77	1.74k	R-EU_0207/7	0207/7	RESISTOR, European symbol
R78	56.2k	R-EU_0207/7	0207/7	RESISTOR, European symbol
R79	1.5k	R-EU_0207/7	0207/7	RESISTOR, European symbol
R80	1M	R-EU_0207/7	0207/7	RESISTOR, European symbol
R81	47	R-EU_0207/7	0207/7	RESISTOR, European symbol
R82	150	R-EU_0207/7	0207/7	RESISTOR, European symbol
R83	2.7k	R-EU_0207/7	0207/7	RESISTOR, European symbol
R84	1M	R-EU_0207/7	0207/7	RESISTOR, European symbol
R85	47	R-EU_0207/7	0207/7	RESISTOR, European symbol
R86	150	R-EU_0207/7	0207/7	RESISTOR, European symbol
R87	2.7k	R-EU_0207/7	0207/7	RESISTOR, European symbol
R88	2.7k	R-EU_0207/7	0207/7	RESISTOR, European symbol
R89	2.7k	R-EU_0207/7	0207/7	RESISTOR, European symbol
R90	150	R-EU_0207/7	0207/7	RESISTOR, European symbol
R91	12k	R-EU_0207/7	0207/7	RESISTOR, European symbol
R92	1M	R-EU_0207/7	0207/7	RESISTOR, European symbol
R93	255k	R-EU_0207/7	0207/7	RESISTOR, European symbol
R94	1M	R-EU_0207/7	0207/7	RESISTOR, European symbol
R95	442k	R-EU_0207/7	0207/7	RESISTOR, European symbol
R96	150	R-EU_0207/7	0207/7	RESISTOR, European symbol
R97	68	R-EU_0207/7	0207/7	RESISTOR, European symbol
R98	150	R-EU_0207/7	0207/7	RESISTOR, European symbol
R99	47k	R-EU_0207/7	0207/7	RESISTOR, European symbol
R100	47k	R-EU_0207/7	0207/7	RESISTOR, European symbol
R101	10	R-EU_0207/7	0207/7	RESISTOR, European symbol
R102	10	R-EU_0207/7	0207/7	RESISTOR, European symbol
R103	150	R-EU_0207/7	0207/7	RESISTOR, European symbol
R104	150	R-EU_0207/7	0207/7	RESISTOR, European symbol
R105	150	R-EU_0207/7	0207/7	RESISTOR, European symbol

Part	Value	Device	Package	Description
R106	150	R-EU_0207/7	0207/7	RESISTOR, European symbol
R107	150	R-EU_0207/7	0207/7	RESISTOR, European symbol
R108	150	R-EU_0207/7	0207/7	RESISTOR, European symbol
R109	150	R-EU_0207/7	0207/7	RESISTOR, European symbol
R110	1.2M	R-EU_0207/7	0207/7	RESISTOR, European symbol
R111	1.2M	R-EU_0207/7	0207/7	RESISTOR, European symbol
R112	22M	R-EU_0207/7	0207/7	RESISTOR, European symbol
R113	0	R-EU_0207/2V	0207/2V	RESISTOR, European symbol
R114	47k	R-EU_0207/7	0207/7	RESISTOR, European symbol
R115	47k	R-EU_0207/7	0207/7	RESISTOR, European symbol
R116	47k	R-EU_0207/7	0207/7	RESISTOR, European symbol
R117	47k	R-EU_0207/7	0207/7	RESISTOR, European symbol
R118	1k	R-EU_0207/7	0207/7	RESISTOR, European symbol
R119	1k	R-EU_0207/7	0207/7	RESISTOR, European symbol
R120	1.2M	R-EU_0207/7	0207/7	RESISTOR, European symbol
R121	1.2M	R-EU_0207/7	0207/7	RESISTOR, European symbol
R122	22M	R-EU_0207/7	0207/7	RESISTOR, European symbol
R123	47k	R-EU_0207/7	0207/7	RESISTOR, European symbol
R124	47k	R-EU_0207/7	0207/7	RESISTOR, European symbol
R125	47k	R-EU_0207/7	0207/7	RESISTOR, European symbol
R126	47k	R-EU_0207/7	0207/7	RESISTOR, European symbol
R127	1k	R-EU_0207/7	0207/7	RESISTOR, European symbol
R128	1k	R-EU_0207/7	0207/7	RESISTOR, European symbol
R129	100	R-EU_0207/7	0207/7	RESISTOR, European symbol
R130	150	R-EU_0207/7	0207/7	RESISTOR, European symbol
R131	10k	R-EU_0207/7	0207/7	RESISTOR, European symbol
R132	10	R-EU_0207/7	0207/7	RESISTOR, European symbol
R133	100	R-EU_0207/7	0207/7	RESISTOR, European symbol
R134	150	R-EU_0207/7	0207/7	RESISTOR, European symbol
R135	10k	R-EU_0207/7	0207/7	RESISTOR, European symbol
R136	10	R-EU_0207/7	0207/7	RESISTOR, European symbol
R137	2.7k	R-EU_0207/7	0207/7	RESISTOR, European symbol
R138	2.7k	R-EU_0207/7	0207/7	RESISTOR, European symbol
R139	47k	R-EU_0207/7	0207/7	RESISTOR, European symbol
R140	47k	R-EU_0207/7	0207/7	RESISTOR, European symbol
R141	10	R-EU_0207/7	0207/7	RESISTOR, European symbol
R142	10	R-EU_0207/7	0207/7	RESISTOR, European symbol
R143	1	R-EU_0207/7	0207/7	RESISTOR, European symbol
R144	1	R-EU_0207/7	0207/7	RESISTOR, European symbol
R145	0	R-EU_0207/2V	0207/2V	RESISTOR, European symbol
R146	3k	R-EU_0207/7	0207/7	RESISTOR, European symbol
R147	o 47k	R-EU_0207/7	0207/7	RESISTOR, European symbol
R148	47k	R-EU_0207/7	0207/7	RESISTOR, European symbol
R149	o 47k	R-EU_0207/7	0207/7	RESISTOR, European symbol
R150	47k	R-EU_0207/7	0207/7	RESISTOR, European symbol
R151	2k	R-EU_0207/7	0207/7	RESISTOR, European symbol
R152	47k	R-EU_0207/7	0207/7	RESISTOR, European symbol
R153	2k	R-EU_0207/7	0207/7	RESISTOR, European symbol
R154	4.87k	R-EU_0207/7	0207/7	RESISTOR, European symbol
R155	1k	R-EU_0207/7	0207/7	RESISTOR, European symbol
R156	10k	R-EU_0207/7	0207/7	RESISTOR, European symbol
R157	1k	R-EU_0207/7	0207/7	RESISTOR, European symbol
R158	562	R-EU_0207/7	0207/7	RESISTOR, European symbol
R159	3.32k	R-EU_0207/7	0207/7	RESISTOR, European symbol
R160	47k	R-EU_0207/7	0207/7	RESISTOR, European symbol
R161	o 47k	R-EU_0207/7	0207/7	RESISTOR, European symbol
R162	o 47k	R-EU_0207/7	0207/7	RESISTOR, European symbol
R163	o 47k	R-EU_0207/7	0207/7	RESISTOR, European symbol
R164	47k	R-EU_0207/7	0207/7	RESISTOR, European symbol
R165	o 10k	R-EU_0207/7	0207/7	RESISTOR, European symbol
R166	10k	R-EU_0207/7	0207/7	RESISTOR, European symbol
R167	o 10k	R-EU_0207/7	0207/7	RESISTOR, European symbol
R168	10k	R-EU_0207/7	0207/7	RESISTOR, European symbol
R169	1.54k	R-EU_0207/7	0207/7	RESISTOR, European symbol

Part	Value	Device	Package	Description
R170	1.54k	R-EU_0207/7	0207/7	RESISTOR, European symbol
R171	1.50k	R-EU_0207/7	0207/7	RESISTOR, European symbol
R172	1.50k	R-EU_0207/7	0207/7	RESISTOR, European symbol
R173	422	R-EU_0207/7	0207/7	RESISTOR, European symbol
R174	2.49k	R-EU_0207/7	0207/7	RESISTOR, European symbol
R175	100	R-EU_0207/7	0207/7	RESISTOR, European symbol
R176	100k	R-EU_0207/7	0207/7	RESISTOR, European symbol
R177	2.49k	R-EU_0207/7	0207/7	RESISTOR, European symbol
R178	422	R-EU_0207/7	0207/7	RESISTOR, European symbol
R179	100	R-EU_0207/7	0207/7	RESISTOR, European symbol
R180	100k	R-EU_0207/7	0207/7	RESISTOR, European symbol
R181	1.54k	R-EU_0207/7	0207/7	RESISTOR, European symbol
R182	1.54k	R-EU_0207/7	0207/7	RESISTOR, European symbol
R183	1.50k	R-EU_0207/7	0207/7	RESISTOR, European symbol
R184	1.50k	R-EU_0207/7	0207/7	RESISTOR, European symbol
R185	422	R-EU_0207/7	0207/7	RESISTOR, European symbol
R186	2.49k	R-EU_0207/7	0207/7	RESISTOR, European symbol
R187	100	R-EU_0207/7	0207/7	RESISTOR, European symbol
R188	100k	R-EU_0207/7	0207/7	RESISTOR, European symbol
R189	2.49k	R-EU_0207/7	0207/7	RESISTOR, European symbol
R190	422	R-EU_0207/7	0207/7	RESISTOR, European symbol
R191	100	R-EU_0207/7	0207/7	RESISTOR, European symbol
R192	100k	R-EU_0207/7	0207/7	RESISTOR, European symbol
R193	47k	R-EU_0207/7	0207/7	RESISTOR, European symbol
R194	1k	R-EU_0207/7	0207/7	RESISTOR, European symbol
R195	3090	R-EU_0207/7	0207/7	RESISTOR, European symbol
R196	1580	R-EU_0207/7	0207/7	RESISTOR, European symbol
R197	0	R-EU_0207/2V	0207/2V	RESISTOR, European symbol
R198	0	R-EU_0207/2V	0207/2V	RESISTOR, European symbol
R199	10	R-EU_0207/7	0207/7	RESISTOR, European symbol
R200	10	R-EU_0207/7	0207/7	RESISTOR, European symbol
R201	150	R-EU_0207/7	0207/7	RESISTOR, European symbol
R202	150	R-EU_0207/7	0207/7	RESISTOR, European symbol
R203	12k	R-EU_0207/7	0207/7	RESISTOR, European symbol
R204	4.7k	R-EU_0207/7	0207/7	RESISTOR, European symbol
R205	4.7k	R-EU_0207/7	0207/7	RESISTOR, European symbol
R206	4.7k	R-EU_0207/7	0207/7	RESISTOR, European symbol
R207	4.7k	R-EU_0207/7	0207/7	RESISTOR, European symbol
R208	4.7k	R-EU_0207/7	0207/7	RESISTOR, European symbol
RESETPRE1	TSW	TSW-101-08-G-S	TSW-101-XX-G-S	THROUGH-HOLE .025 SQ POST HEADER"
RESETPRE2	TSW	TSW-101-08-G-S	TSW-101-XX-G-S	THROUGH-HOLE .025 SQ POST HEADER"
S1	KS11R22CQD	KS11R22CQD	KS11R23CQD	Momentary Push Button, 12.32 x 12.32mm
S2	KS11R22CQD	KS11R22CQD	KS11R23CQD	Momentary Push Button, 12.32 x 12.32mm
S3	M2023SS1W03	M2023SS1W03	M2023SS1W03	Switch Toggle ON OFF ON 6A 30VDC
S4	CTHS15CIC06ARROW	CTHS15CIC06ARROW	CTHS15CIC06ARROW	Touch Pushbutton CTH SQR 15mm
S5	CTHS15CIC06ARROW	CTHS15CIC06ARROW	CTHS15CIC06ARROW	Touch Pushbutton CTH SQR 15mm
S6	SSSF040800	SSSF040800	SSSF040800	Slide Switch 4PDT Maintained 100 mA
S7	SSSF040800	SSSF040800	SSSF040800	Slide Switch 4PDT Maintained 100 mA
SPI1	TSW-107	TSW-107-08-G-D	TSW-107-XX-G-D	THROUGH-HOLE .025 SQ POST HEADER"
STEREO	3-1825010-7DIL18	3-1825010-7DIL18	DIL18	PCB Slide Switch DPDT On-On 300 mA Top
U$1	THAT5171	THAT5171	THAT5171	THAT5171 Digital Preamplifier Controller
U$2	THAT1580_DRILL	THAT1580_DRILL	THAT1580_ADJ_DRILL	THAT 1580 Differential Audio Preamplifier
U$3	THAT5171	THAT5171	THAT5171	THAT5171 Digital Preamplifier Controller
U$4	THAT1580_DRILL	THAT1580_DRILL	THAT1580_ADJ_DRILL	THAT 1580 Differential Audio Preamplifier
U$5	AD8674	AD8674	R_14	
U$6	SI5356B	SI5356B	SI5356A	SI5356A - CLOCK GENERATOR
U$7	XTAL	XTAL	XTAL	
U1	LM2585T-ADJ/NOPB	LM2585T-ADJ/NOPB	T05D	
U2	CDBW46-G	CDBW46-G	CDBW	
U3	CD4013BEE4	CD4013BEE4	N14	
U4	LM43601PWPT	LM43601PWPT	PWP16	
U5	LM43601PWPT	LM43601PWPT	PWP16	
U6	CD4013BEE4	CD4013BEE4	N14	
U7	ADAU1979WBCPZ	ADAU1979WBCPZ	CP_40_14	

Part	Value	Device	Package	Description
U8	ADAU1962WBSTZ	ADAU1962WBSTZ	ST_80_2	
U9	SI2312	SI2312BDS-T1-GE3	TO-236	
X1	SSW-105	SSW-105-02-G-D	SSW-105-02-G-D	THROUGH-HOLE .025 SQ POST SOCKET"
X2	SSW-105-02-G-S	SSW-105-02-G-S	SSW-105-02-G-S	THROUGH-HOLE .025 SQ POST SOCKET"
X3	SSW-127	SSW-127-02-G-D	SSW-127-02-G-D	THROUGH-HOLE .025 SQ POST SOCKET"
X4	Supply +-5V	W237-103	W237-103	WAGO SCREW CLAMP
X5	PRE_OUT1	W237-103	W237-103	WAGO SCREW CLAMP
X6	PRE_OUT2	W237-103	W237-103	WAGO SCREW CLAMP
X7	PRE_IN1	W237-103	W237-103	WAGO SCREW CLAMP
X8	PRE_IN2	W237-103	W237-103	WAGO SCREW CLAMP
X9	SSW-105	SSW-105-02-G-D	SSW-105-02-G-D	THROUGH-HOLE .025 SQ POST SOCKET"
X10	Supply +-5V	W237-103	W237-103	WAGO SCREW CLAMP
X11	+-5V	W237-103	W237-103	WAGO SCREW CLAMP
X12	3.3V	W237-102	W237-102	WAGO SCREW CLAMP
X13	3.3V	W237-102	W237-102	WAGO SCREW CLAMP
X14	SSW-103	SSW-103-02-G-D	SSW-103-02-G-D	THROUGH-HOLE .025 SQ POST SOCKET"
X15	TSW-102-08-G-D	TSW-102-08-G-D	TSW-102-XX-G-D	THROUGH-HOLE .025 SQ POST HEADER"
X16	TSW-108-08-G-D	TSW-108-08-G-D	TSW-108-XX-G-D	THROUGH-HOLE .025 SQ POST HEADER"
X17	SSW-102-02-G-S	SSW-102-02-G-S	SSW-102-02-G-S	THROUGH-HOLE .025 SQ POST SOCKET"
X18	SSW-101-02-G-D	SSW-101-02-G-D	SSW-101-02-G-D	THROUGH-HOLE .025 SQ POST SOCKET"
X19	TSW-102	TSW-102-08-G-D	TSW-102-XX-G-D	THROUGH-HOLE .025 SQ POST HEADER"
X20	+-5V	W237-103	W237-103	WAGO SCREW CLAMP
X21	+-5V	W237-103	W237-103	WAGO SCREW CLAMP
X22	TSW-130-08-G-D	TSW-130-08-G-D	TSW-130-XX-G-D	THROUGH-HOLE .025 SQ POST HEADER"
X23	SSW-121-02-G-S	SSW-121-02-G-S	SSW-121-02-G-S	THROUGH-HOLE .025 SQ POST SOCKET"
X24	SSW-106-02-G-S	SSW-106-02-G-S	SSW-106-02-G-S	THROUGH-HOLE .025 SQ POST SOCKET"
X25	TSW-104-08-G-S	TSW-104-08-G-S	TSW-104-XX-G-S	THROUGH-HOLE .025 SQ POST HEADER"
X26	+-5V	W237-103	W237-103	WAGO SCREW CLAMP
X27	3.3V	W237-102	W237-102	WAGO SCREW CLAMP
X28	SSW-105-02-G-S	SSW-105-02-G-S	SSW-105-02-G-S	THROUGH-HOLE .025 SQ POST SOCKET"
X29	SSW-101-02-G-S	SSW-101-02-G-S	SSW-101-02-G-S	THROUGH-HOLE .025 SQ POST SOCKET"
X30	TO ADC1-1	W237-102	W237-102	WAGO SCREW CLAMP
X31	TO ADC2-1	W237-102	W237-102	WAGO SCREW CLAMP
X32	+-5V	W237-103	W237-103	WAGO SCREW CLAMP
X33	3.3V	W237-102	W237-102	WAGO SCREW CLAMP
X34	TSW-103	TSW-103-08-G-D	TSW-103-XX-G-D	THROUGH-HOLE .025 SQ POST HEADER"
X35	SSW-110	SSW-110-02-G-S	SSW-110-02-G-S	THROUGH-HOLE .025 SQ POST SOCKET"
X36	SSW-110	SSW-110-02-G-S	SSW-110-02-G-S	THROUGH-HOLE .025 SQ POST SOCKET"
X37	SSW	SSW-101-02-G-D	SSW-101-02-G-D	THROUGH-HOLE .025 SQ POST SOCKET"
X38	TSW-103-08-G-D	TSW-103-08-G-D	TSW-103-XX-G-D	THROUGH-HOLE .025 SQ POST HEADER"
X39	TSW-105-08-G-D	TSW-105-08-G-D	TSW-105-XX-G-D	THROUGH-HOLE .025 SQ POST HEADER"
X40	SSW-102-02-G-S	SSW-102-02-G-S	SSW-102-02-G-S	THROUGH-HOLE .025 SQ POST SOCKET"
X41	TSW-105	TSW-105-08-G-D	TSW-105-XX-G-D	THROUGH-HOLE .025 SQ POST HEADER"
X42	TSW-105	TSW-105-08-G-S	TSW-105-XX-G-S	THROUGH-HOLE .025 SQ POST HEADER"
X43	TSW-105	TSW-105-08-G-S	TSW-105-XX-G-S	THROUGH-HOLE .025 SQ POST HEADER"
X44	JTAG08-D	JTAG08-D	JTAG	THROUGH-HOLE .025 SQ POST HEADER"
X45	TSW-109	TSW-109-08-G-D	TSW-109-XX-G-D	THROUGH-HOLE .025 SQ POST HEADER"
X46	TSW	TSW-102-08-G-D	TSW-102-XX-G-D	THROUGH-HOLE .025 SQ POST HEADER"
X47	SSW-109	SSW-109-02-G-S	SSW-109-02-G-S	THROUGH-HOLE .025 SQ POST SOCKET"
X48	SSW-109	SSW-109-02-G-S	SSW-109-02-G-S	THROUGH-HOLE .025 SQ POST SOCKET"
X49	TO ADC1-2	W237-102	W237-102	WAGO SCREW CLAMP
X50	TO ADC2-2	W237-102	W237-102	WAGO SCREW CLAMP
X51	+-5V DAC	W237-103	W237-103	WAGO SCREW CLAMP
X52	3.3V ADC/DAC	W237-102	W237-102	WAGO SCREW CLAMP
X53	DAC OUT1	W237-103	W237-103	WAGO SCREW CLAMP
X54	DAC OUT2	W237-103	W237-103	WAGO SCREW CLAMP
X55	SSW-102	SSW-102-02-G-S	SSW-102-02-G-S	THROUGH-HOLE .025 SQ POST SOCKET"
X56	SSW	SSW-102-02-G-S	SSW-102-02-G-S	THROUGH-HOLE .025 SQ POST SOCKET"
X57	3.3V ADC/DAC	W237-102	W237-102	WAGO SCREW CLAMP
X58	SSW-109	SSW-109-02-G-S	SSW-109-02-G-S	THROUGH-HOLE .025 SQ POST SOCKET"
X59	SSW-109	SSW-109-02-G-S	SSW-109-02-G-S	THROUGH-HOLE .025 SQ POST SOCKET"
X60	SSW-108	SSW-108-02-G-S	SSW-108-02-G-S	THROUGH-HOLE .025 SQ POST SOCKET"
X61	SSW-108	SSW-108-02-G-S	SSW-108-02-G-S	THROUGH-HOLE .025 SQ POST SOCKET"
X62	SSW-106	SSW-106-02-G-S	SSW-106-02-G-S	THROUGH-HOLE .025 SQ POST SOCKET"

Part	Value	Device	Package	Description
X63	SSW-108	SSW-108-02-G-D	SSW-108-02-G-D	THROUGH-HOLE .025 SQ POST SOCKET"
X64	forward +-5V	W237-103	W237-103	WAGO SCREW CLAMP
X65	forward 3.3V	W237-102	W237-102	WAGO SCREW CLAMP
X66	Signal-IN	W237-103	W237-103	WAGO SCREW CLAMP
X67	Signal-IN	W237-103	W237-103	WAGO SCREW CLAMP
X68	3.3V	W237-102	W237-102	WAGO SCREW CLAMP
X69	forward 3.3V	W237-102	W237-102	WAGO SCREW CLAMP
X70	forward +-5V	W237-103	W237-103	WAGO SCREW CLAMP
X71	SSW-112	SSW-112-02-G-S	SSW-112-02-G-S	THROUGH-HOLE .025 SQ POST SOCKET"
X72	SSW-112	SSW-112-02-G-S	SSW-112-02-G-S	THROUGH-HOLE .025 SQ POST SOCKET"
X73	SSW-103	SSW-103-02-G-D	SSW-103-02-G-D	THROUGH-HOLE .025 SQ POST SOCKET"
X74	SSW-102	SSW-102-02-G-S	SSW-102-02-G-S	THROUGH-HOLE .025 SQ POST SOCKET"
X75	SSW-102	SSW-102-02-G-S	SSW-102-02-G-S	THROUGH-HOLE .025 SQ POST SOCKET"
X76	SSW-102	SSW-102-02-G-S	SSW-102-02-G-S	THROUGH-HOLE .025 SQ POST SOCKET"
X77	TSW-109-08-G-S	TSW-109-08-G-S	TSW-109-XX-G-S	THROUGH-HOLE .025 SQ POST HEADER"
X78	TSW-109-08-G-S	TSW-109-08-G-S	TSW-109-XX-G-S	THROUGH-HOLE .025 SQ POST HEADER"
X79	TSW-112-08-G-S	TSW-112-08-G-S	TSW-112-XX-G-S	THROUGH-HOLE .025 SQ POST HEADER"
X80	TSW-112-08-G-S	TSW-112-08-G-S	TSW-112-XX-G-S	THROUGH-HOLE .025 SQ POST HEADER"
X81	TSW-107-08-G-S	TSW-107-08-G-S	TSW-107-XX-G-S	THROUGH-HOLE .025 SQ POST HEADER"
X82	SSW-101-02-G-S	SSW-101-02-G-S	SSW-101-02-G-S	THROUGH-HOLE .025 SQ POST SOCKET"